Spring 12-31-1989

Correlation between particle velocities and conditions of abrasive waterjet formation

Wei-Long Chen
New Jersey Institute of Technology

Copyright Warning & Restrictions

The copyright law of the United States (Title 17, United States Code) governs the making of photocopies or other reproductions of copyrighted material.

Under certain conditions specified in the law, libraries and archives are authorized to furnish a photocopy or other reproduction. One of these specified conditions is that the photocopy or reproduction is not to be "used for any purpose other than private study, scholarship, or research." If a, user makes a request for, or later uses, a photocopy or reproduction for purposes in excess of "fair use" that user may be liable for copyright infringement,

This institution reserves the right to refuse to accept a copying order if, in its judgment, fulfillment of the order would involve violation of copyright law.

Please Note: The author retains the copyright while the New Jersey Institute of Technology reserves the right to distribute this thesis or dissertation

Printing note: If you do not wish to print this page, then select "Pages from: first page # to: last page #" on the print dialog screen

CORRELATION BETWEEN PARTICLES VELOCITIES AND CONDITIONS OF ABRASIVE WATERJET FORMATION

by

Wei-Long Chen

Dissertation submitted to the Faculty of the Graduate School of the New Jersey Institute of Technology in partial fulfillment of the requirement for the degree of Doctor of Engineering Science

1990

APPROVAL SHEET

Title of Thesis: Correlation between Particles Velocities and Conditions of Abrasive Waterjet Formation

Name of Candidate: Wei-Long Chen
Doctor of Engineering Science, 1990

Thesis and Abstract Approved:

E. S. Geskin — Date
Associate Professor
Mechanical Engineering Derpartment

VITA

Name: Wei-Long Chen

Degree to be conferred and date: Doctor of Engineering Science
December, 1989

Collegiate institution

attended	Dates	Degree	Date of Degree
Taitung Institute of Technology	9/76 - 5/80	B.S.M.E.	June, 1980
New Jersey Institute of Technology	9/84 - 5/86	M.S.M.E.	June, 1986

Position held:

Research Assistant
Department of Mechanical Engineering
N.J.I.T., June 1986 - Dec. 1989

Senior Research Engineer
Waterjet System
Ingersoll-Rand Company
Joining: Jan, 1990

ABSTRACT

Title of Dissertation: Correlation Between Particle Velocity and Conditions of Abrasive Waterjet Formation

Wei-Long Chen, Doctor of Engineering Science, 1990

Thesis directed by: Dr. E. S. Geskin
Associate Professor
Mechanical Engineering Department

The velocities of water and abrasive particles in abrasive waterjet(AWJ) were measured by the use of Laser Transit Anemometer(LTA). A setup for the velocity measurement was constructed and a statistical technique was used to improve the accuracy of the velocity determination. A comparison of the magnitude of velocities determined by LTA, Piezoelectric Force Transducer and Schlieren Photograph clearly indicates the feasibility of the use of LTA.

The velocities of water and particles were measured for different diameters of water and slurry nozzles, abrasive mass flow rates and particle sizes. The performed experiments enabled us to evaluate the effects of conditions of jet formation on the particles velocities. An empirical equation for the prediction of particles velocities was constructed by the use of obtained results. The coefficeint of correlation between experimental and computed results is equal to 0.93. The acquired information can be used to select the operational parameters in AWJ cutting. The obtained results also provide information on the acceleration mechanism of entrained particles, which may be used to improve the design of slurry nozzle.

ACKNOWLEDGEMENT

The author wishes to express his sincere gratitude to his advisor, Dr. Ernest Geskin, who provided many valuable suggestions, constant supervision, continuous guidance and encouragement throughout the course of investigation.

The author also wishes to express his sincere gratitute to Drs. Rong-Yaw Chen, R. Dave, A. Rosato and A.Harnoy who have kindly read through the original manuscript and provided valuable suggestions. Additionally, sincere thanks to Mr. Varadaraj V. Souda for his help in reviewing the manuscript and correcting the errors.

The author would also like to express his gratitude for the support from his family, especially his wife, Pei-Chih Hsu.

TABLE OF CONTENTS

LIST OF FIGURES

LIST OF TABLES

CHAPTER 1

INTRODUCTION

Waterjetting has been used as a cutting and cleaning tool in industrial applications for over twenty years. As shown in Fig. 1, water is pressurized up to 325 MPA and expelled through a sapphire orifice to form a coherent and high-velocity waterjet(WJ).

An abrasive waterjet cutting technology is an extension of waterjet cutting technology. As depicted in Fig. 2, waterjet is introduced into a carbide tube where the negative pressure is created and the abrasive particles are drawn into the tube. The turbulent processes in the tube cause the water and abrasive particles to mix together to form an abrasive waterjet. Here, part of the waterjet's momentum is transferred to the abrasives, whose velocities are abruptly increased. As a result of the momentum transfer between water and abrasives, a high-velocity stream of abrasives is formed which performs the cutting action. The cutting of material is a process in which material removal takes place due to the erosion action of such abrasive particles which strike upon the work surface with high impact velocity. [1].

As of today, the use of AWJ for material removal is

limited only to cutting applications. The main reason for this is our incapability to predict the exact nature of the erosion mechanism involved in its cutting process. The study of the erosion of the surface upon impingement by an AWJ may be divided into two major stages. The first stage is the determination from the fluid conditions of the number, the direction and the velocities of particles striking the surface. With the knowledge of such information , the second stage will be the calculation of the amount of surface material removed. Therefore, the determination of the particle velocities at different conditions of AWJ formation is essential to the establishment of the prediction model of the cutting results.

The conditions affecting AWJ formation can be categorized, in general, as follows:

* Water pressure(P_w).
* Sapphire nozzle diameter(d_n).
* Carbide tube(or slurry nozzle) diameter(d_c).
* Abrasive material.
* Size of the abrasive particle(d_a).
* Abrasive mass flow rate(m_a).
* Carbide tube length(l_c).

The purpose of this study is first to find one reliable experimental technique which allows us to measure the velocities of particles entrained in the AWJ under different diameters of sapphire and slurry nozzles and different

abrasive mass flow rates and particles. The selection of these parameters is based corresponding to the operating conditions prevailing in AWJ cutting in industry today, i.e., water pressure maintained at 325MPa, garnet sand was the abrasive used and the length of carbide tube was kept at 2"(50.8mm). An empirical equation expressing the correlation between particle velocities and selected parameters is thereafter to be constructed from the experimental results.

The velocities of particles in a stream of gas or liquid can be determined theoretically by solving the equation of motion of the particles based on the given initial and boundary conditions. For the abrasive waterjet which is our area of interest, theoretical determination of the velocities of entrained particles is not possible due to an insufficient knowledge of the particle acceleration mechanism, i.e., the nature of the mixture inside the carbide tube after the injection of abrasives is not clear. Also, the entry of air inside the mixture at the time of particle injection tends to make it a multiphase flow, thereby posing increasing difficulties to find a theoretical solution.

Pertaining to the measurement of the velocity of particle entrained in the AWJ, several problems are encountered due to the magnitude of jet diameter and impact pressure. Two experimental techniques have so far been

proposed. The use of a pair of current-carrying coils spaced 1.2" apart was first employed [2]. The particle velocity is determined by the measurement of the time elapsed between the signals induced by the magnetic particles passing the coils. This technique, however, allows us to measure only the mean velocity of a particle travelling through a considerably long distance compared to the jet diameter, which is only 0.05". Also, in this method, since the coil encloses the jet completely, the obtained velocity may represent the velocity of a particle at any point on the cross section of the jet and need not necessarily be at the center of the jet. Another technique to measure the average velocity of the abrasive particles at certain cross-section of the AWJ was based on counting the number of impact craters observed on an aluminum plate which was used as the test piece [3]. In addition to the shortcoming associated with the first experiment, the accuracy of the results of this measurement is strongly correlated to the counting method and can be used only for low abrasive flow rate.

Considerable efforts were made in this study to find one instrument which can be used to measure entrained particle velocities. The first technique was to take the photograph of the AWJ at 10,000 frames per second with the copper-vapor laser as the source of light [4]. The determination of the particle velocity is based on the trace of the trajectory of the particle from photograph. However, obtained photograph can not provide us such information due

to the difficulty in identifying the same particle in different frames. Another technique involves the use of Schlieren photography which is commonly used in supersonic flow measurement [5]. The determination of the velocity of the flow is based on the Mach number obtained from photograph. This technique, unfortunately, can not be employed for our purpose since the velocity of the particle can not be distinguished from obtained results. Finally, the use of Laser Transit Anemometer(LTA) was found to be applicable for the purpose of measurement of particle velocity due to the size of its measuring volume which is comparable with the diameter of the AWJ in question.

The LTA operates by detecting scattered light from small particles as they pass through two focal points formed by two highly focused laser beams. The velocity is determined by the measuring of the time taken for the movement of particles from one focal point to another and the known distance between these two focal points.

The application of LTA upto now was limited to the low turbulent single-phase or two-phase flows. Therefore, a special setup and measurement procedure was developed in this study in order to specifically measure the velocities of particles entrained in the desired region of high turbulent, multiphase AWJ. The developed setup enabled us to accurately align the laser beams emitted from the LTA and the axis of

the AWJ . And, the developed measurement procedure allowed us to distinctly identify the velocities of the driven fluid and entrained particles. A complete description of the setup and measurement procedure is given later in Chapter 3.

Despite the primary importance of the measurement of particle velocity, only two works out of several thousand studies concerned with the AWJ technology were devoted to the determination of this velocity. Our study is a complete work reporting the application of a reliable technique which enables us to measure directly particle velocity at different conditions of AWJ formation.

Due to the lack of the information related to the use of LTA for similar purpose, the reliability of the obtained measured results were validated by comparing the velocities of waterjet obtained from the computation using Bernoulli's equation and forces measured by Piezoelectrric Force Transducer. For the particle velocities, the comparison was performed by checking the range of the value of velocities obtained from Schlieren photography measurement.

A number of trials were performed to select the correct independent and dependent dimensionless variables which were necessary for the formation of an empirical equation. The foremost criteria for the selection of those variables was the correlation coefficient obtained by conducting the regression analysis of the variables. The obtained equation

is the first mathematical model describing the kinematics of particles entrained in the AWJ.

The description of the AWJ system is given in Chapter 2. The review of the previous work concerned with the study of the velocities of particles entrained in the AWJ and the use of LTA is given in Chapter 3. The description of experimental setup and measurement procedure is given in Chapter 4. Chapter 5 provides a review of the statistical technique which was used to identify the correlation in question. The validity of the use LTA for the determination of particle velocity is given in Chapter 6. The experimental results and the analysis of the obtained equation are given in Chapter 7. The performed work enables us to identify the the velocity of particle entrained in the AWJ under different conditions. This and some other conclusions obtained as the results of this study are provided in Chapter 8.

CHAPTER 2

DESCRIPTION OF AWJ SYSTEM

The first commercial application of a waterjet system was at Alton Box Board, Alton, Illinois, in 1971. The materials cut with the pure waterjet were limited to the non-metal materials with relatively low shear strength, such as food products, rubber, plastics, paperboard forms, etc. The limitation to cut metal materials prohibited its use as a universal tool. The advent of abrasive waterjet(AWJ) cutting technology in the early 80's produced a new tool in machining every known material [6-10].

Jet cutting, including WJ and AWJ cutting, offers many advantages. Some of these depend on the specific applications under consideration, but among these advantages are the following:

* It is estimated that production cost savings of at least 50% have been realized compared to the conventional machining technologies[11].
* The processes of cutting produce minimal or no dust, which makes operation less hazardous.
* It cuts without heat, which eliminates thermal distortion and fire hazards is therefore prevented.
* The WJ or AWJ is a true point, omni-directional cutter, hence cutting of complicated shapes is easily accomplished.

* Reaction forces from jet cutting are relatively low, hence structural support hardware requirements are dedicated to the mass of actuating components and their dynamics, not to the tool cutting force.

In addition to the advantages mentioned above, each application identifies additional ones, such as less noise, faster cutting speed, smooth cutting surface, etc., based on specific considerations.

To pressurize the water, a special system of components has been developed. The equipment employed in this study, the Streamline waterjet cutter manufactured by the Ingersoll-Rand Co., is divided into four major parts: the hydraulic unit, the nozzle body, the abrasive feeding system, and the robotic work cell.

The principal machine in the hydraulic unit is the intensifier, a special type of pump. A basic system pressurizes a large piston at hydraulic pressure about 1,500 to 3,000 psi. The control system cycles the piston in a double acting motion. The piston is mechanically connected to a smaller diameter piston and the resultant pressure in the smaller piston cylinder is intensified by the ratio of the areas of the large and small pistons. Using this principle it is possible to create a water flow having pressure between 50,000 and 60,000 psi. A series of check valves allow the water to enter the high pressure cylinder

on the suction stroke, and leave on the discharge stroke. A booster pump is used to assure continuous flow into the suction side of the high pressure cylinders. Filters and softeners are used to condition the water. High pressure tubing and swivels are used to connect the intensifier to the cutter, i.e. the nozzle.

In a pure waterjet cutting system, the nozzle is normally a small sapphire orifice with a diameter between 0.1778mm to 0.3556mm. In abrasive waterjet cutting system, the same nozzle as in pure waterjet cutting is used in conjunction with a secondary nozzle, known as carbide tube, with 0.8636mm, 1.09mm, and 1.6mm of internal diameters. The carbide tubes are made from tungsten carbide to resist wear.

A vibratory feeder is used to control the feedrate of the abrasives. In the course of the experiment, the size of the abrasive varied from 220 to 50 mesh with garnet sand being the material. The typical Tyler sieve analysis is shown in Fig. 3 [12].

The movement of the cutter is controlled by a 5-axis robotic workcell with Allen-Bradely 8200 controller. The programming capability of the controller enables the development of straight and arc trajectory for the cutter. The positioning accuracy is +/- 0.005" and the repeatability is also +/- 0.005" [13].

CHAPTER 3

LITERATURE SURVEY

3.1. Study of Waterjet

An abrasive waterjet(AWJ) is formed when a high-velocity waterjet mixed with abrasive particles is expelled through a carbide tube. The study of the behavior of the waterjet prior to mixing with particles is therefore essentially useful for the study of the entrained particles.

There are relatively few published papers dealing with high velocity waterjets which are applicable to our study. Dunne and Cassen investigated the velocity discontinuity and instabilty of a liquid jet having velocity higher than the speed of sound in air [14]. Schlieren photography was used in his study to observe the development of jet and to determine its velocity. An investigation of the distribution of momentum in a continuous liquid jet of supersonic velocity was given by Semerchan [15]. The average velocity of the jet was determined from the measurement of the discharge rate of water and compared with the value computed from Bernoulli's equation. Kinoshita studied the compressibility of waterjet by the measurement of the Mach number of the flow, which was determined from Schlieren photography [16]. A complete review of jet study is given in Reference [17].

3.2. Study of Particle Motion in a Fluid stream

The motion of particles entrained in a stream of fluid has been investigated in connection with a variety of industrial applications. Several equations were proposed for particles entrained in a lamminar flow. The forms of these equations depends on the forces considered in a particular study. Finnie [18] employed an equation goverening the motion of particle subjected to the drag force. This equation has the form:

$$\frac{4}{3} * \pi * r^3 * \rho_p * \frac{dV}{dt} = \frac{Cd}{2} * \rho_a * \pi * r^2 * (U-V)^2$$

where

r : particle radius

V : particle velocity

ρ_p : particle density

U : air velocity

ρ_a : air density

Cd : drag coefficient

A deduction of the equation of the motion of particles subjected to different forces is given in [19]. The various applications of this equation are discussed in [20-30].

The motion of particle in a turbulent flow is discussed in [31] and in some other studies. Tchen [32] and Hjelmfelt [33] derived an equation of the motion of particles and

discussed the particle response to the oscillatory motion of the carrying fluid. As a result of their work, the following equation was proposed:

$$\frac{\pi d^3}{6} * \rho_p * \frac{dU_p}{dt} = 3 * \pi * \mu * \rho_f * d * (U_f - U_p)$$

$$+ \frac{\pi d^3}{6} * \rho_f * \frac{dU_f}{dt} + \frac{1}{2} * \frac{\pi d^3}{6} * \rho_f * \left(\frac{dU_f}{dt} - \frac{dU_p}{dt} \right)$$

$$+ \frac{3}{2} * d^2 * \sqrt{\pi \rho_f \mu} * \int_{t_o}^{t} dt' * \frac{(dU_f/dt') - (dU_p/dt')}{t - t'} + F_e$$

Here

t_o is the starting time

the index f refers to the fluid

the index p refers to the particle

U is the velocity

d is the particle diameter

ρ is the density

F_e is an external force

A numerical solution of this equation at various initial and boundary conditions is given in [34-39].

3.3 Study of Particle Motion in an AWJ

Despite intensive study of motion of particles entrained in a fluid stream for different engineering applications, the information about the motion of particles in the AWJ formed by the nozzle head as used in this study are limited. Particularly, there is no direct determination

of particle velocity.

A simplified equation for the prediction of the particle velocity is given in [40]. Its derivation is based on the conservation of momentum. The equation is as given below.

$$V_w * m_w = (m_a + m_w) * V'$$

where

V_w is the water velocity prior to mixing with particle

V' is the mixture velocity at the exit of nozzle

m_w is the mass flow rate of water

m_a is the mass flow rate of abrasive

Assuming the velocity of particle contained in the mixture equal to V', we obtained

$$\frac{V_a}{V_w} = \frac{1}{1 + (m_a/m_w)}$$

However, this model does not consider the specific conditions of AWJ, for example, the pressure drop occurring within the carbide tube and the drag friction during the mixing process. The present study is concerned with the construction of the equation which is specifically applicable to AWJ.

An experimental technique for estimation of the

particle velocities was developed by Swanson[7]. In his experiment, conventional garnet sand mixed with steel particles of comparable size are entrained by the waterjet and the resulting mixture is directed through a pair of current-carrying coils spaced 1.2" apart. The particle velocity is determined by the measurement of the time between the signals induced by the steel particles entrained in the AWJ. This technique, however, allows us to measure only the mean velocity of a particle travelling through a considerably long distance compared to the jet diameter, which is only 0.05". Also, in this method, since the coil encloses the jet completely, the obtained velocity may represent the velocity of a particle on the periphery of the jet. Moreover, the obtained velocity is the velocity of added steel particle, rather than the actual abrasive particles used for cutting.

Isobe presented a theoretical model to calculate the velocity of a single particle by solving the equations of particle motion in the waterjet[8]. The following assumption were made in his derivation.

1. Shape of particle is spherical.
2. Gravity and air resistances are small enough to be neglected.
3. The angle between the velocity vector and the longitudinal axis of the waterjet is relatively small. Therefore, the velocity component in longitudinal direction was used to represent the velocity of waterjet.

The final form of the equations proposed by Isobe are as follows:

$$\frac{d^2X}{dt^2} * m + C_D * \left(\frac{dX}{dt}\right)^2 * \frac{\rho * \pi * R^2}{2} = 0$$

$$\frac{d^2X}{dt^2} * m + C_L * \left(\frac{dX}{dt}\right)^2 * \frac{\rho * \pi * R^2}{2} = 0$$

where

X : longitudinal coordinate

Y : transversal coordinate

R : radius of particle

ρ : density of particle

m : mass of particle

C_D : drag coefficient

C_L : lift coefficient

The above equation does not consider the energy dissipation in the turbulent flow which is an important factor in the determination of AWJ behavior. Also, the effects of interaction between particles has been neglected in this derivation.

In addition to the above model, Isobe also obtained the average velocity of abrasive particles by counting the numbers of the impact craters on an aluminum plate, which he used as a test piece. However, the obtained velocity may

represent the velocity of the particle on the periphery of the jet and the accuracy of the results is strongly correlated to the counting method.

3.4 Measurements of Velocity of Particle in the AWJ

The conventional probe instruments used to measure the velocity of the flow can not applied in this study due to the presence of the particles. For this reason, only the non-instrusive instruments such as photography and laser velocimeter can be considered. The use of photography to determine the particle velocity in an AWJ is difficult due to the size and velocity of the object. Also, the water droplets of the jet make the picture indistinct. Laser velocimeter, on the other hand, is non-instrusive and also involes a very small measuring volume. In general, there are two different types of laser velocimeter based on the difference of their operational principles, i.e., Laser Doppler Anemometer(LDA) and Laser Transit Anemometer(LTA) [41]. LTA is chosen for the purpose of this study due to the excessive cost of LDA. The following survey, therefore, is limited to the measurement of LTA.

The operational principle of LTA was first reported by Schodl [42] and the test using LTA was carried out in a supersonic wind tunnel with Mach number up to of 2.2. In his study, the time measurements, taken at the same measuring

point, were represented in the form of probability distribution. The maximum value of the probabilty was taken to calculate the mean value of velocity of the flow at the measuring point. He also found that the angle between the directions of flow and beam plane was strongly correlated to the determination of the maximum probability. The greater the angle between the direction of the flow and beam plane, lesser the maximum value of probability. Beyond an angle of 1.5 degree, the measured data became randomly distributed and failed to determine the value of velocity. The results of Schodl measurement were compared with hot-wire measurement and agreed very well.

After the work of Schodl, Eckardt [43] used the same method to measure the velocity in the internal flow of a radial discharge impeller, running at tip speed up to 400 m/sec.

Mayo [44] used LTA to measure the central axial velocity of the jet with 1" diameter by incoporating the data management system(DMS) into the LTA. The DMS automatically rotates the two focused beams about a common center through a sequence of angles so that the flow direction can be determined by comparing the maximum value of probability taken at different angles.

Loh and Tan [45] employed LTA to measure the velocity of air jet with the pressure up to 5 atm. In their work, the

possible cases relating to the travel of the particles were discussed. The results of their measurement were in agreement with the results obtained from the Schlieren photography measurement.

Smart [46] measured the velocity and flow angle in the rotating blades of turbomachinery by the use of LTA. The obtained results were compared with the data received by the use of Bernoulli's equation with the substitution of the measured pressure. The comparison between measured and computed results shows the validity of the measurement in his study.

From the above review, it is clear that the LTA technique can be used for the determination of particle velocity in a flow. However, considerable efforts need to be made in every different applications due to the occurrance of incorrect data which will be discussed in the next chapter. Moreover, the comparison of the results measured by LTA and other available methods is necessary to validate the feasibility of LTA measurement.

In addition, the available sources concerned with LTA theory and applications do not provide any practical guides for the use of this technique. The provided information is limited to the physical principles and the results of applications. All elements of the used measurement procedure

were developed in the course of this work and are discussed in detail later in this study.

CHAPTER 4

EXPERIMENTAL APPARATUS AND PROCEDURE

4.1 Experiemntal Apparatus

Laser Transit Anemometer(LTA) is an optical instrument for nonintrusive measurements, which produces no interference with the flow. It has a unique lens system that splits a single incoming laser beam into two equal intensity beams and focuses the beams into a small region. Thus, a particle passing through the focal point of either of these split beams generates a scattering light of high intensity. The design of LTA is such that it ensures the generation of the signals is due to only those particles passing through the focal points. With a knowledge of the the distance between the two foci and the time taken for a particle to travel through these two focal points, it is possible for us to calculate the velocity of the particle. The operational principle of LTA will be discussed later in detail in the section "Discussion of LTA Measurement".

The measuring system used in this study has been developed by Dantec Electronic Co. and a 15 mW He-Ne laser is used as the light source. As shown in Figure 4, the system consists of an optical head and a data processing system [47].

4.1.1 OPTICAL HEAD

The setup of the optical head is illustrated in Figure 5 [48]. The beam splitter BS1 receives the source light and creates two beams. The beam plane formed by these beams can be rotated by two polarizers P1 and P2 to ensure its coincidence with the direction of the flight of particle. The two beams are focused by the lens system to form the measuring volume and the image of two focal points is received by the same lens system and transmitted via the mirrors M1 and M2 to the beam splitter BS2. The scattered light, generated by a particle passing through the measuring volume is detected and converted to the voltage signals by the photomultiplier PM. Thus, the signals are transmitted to the data processing system for the determination of the particle velocity by measuring the time period between the signals, which is illustrated in Figures 6 and 7. More detailed description of these Figures is given in the following section.

4.1.2 DATA PROCESSING SYSTEM

The Data Processing System of the LTA measurement has three major functional components. They are 1). Counter Processor 2). Oscilloscope 3). Computer.

The Counter Processor receives the voltage signals from

the photomultiplier in the optical head and conveys these signals, both in analog form to the Oscilloscope and also in digital form to the Computer.

The function of the computer is to determine the time period between two successive signals which are fed from Counter Processor and hence calculate the velocity. To do so, the signals have to be converted into the digital square wave form. This is done by means of a pair of preset trigger levels which are in the Counter Processor. As illustrated in Fig. 7, one of the trigger is set at the lower voltage level of -150mV and the second one is set at -50mV. When the voltage level of a signal goes below the lower trigger level, the output goes to "1". And when the signal again crosses the -50 mV level, the output goes to "0". The wave form of such an output is also given in the same figure. Thus, it can be seen that for a signal to be accepted, its amptitude should be below -150mV. The voltage level of the received signal can be amplified by means of the attenuator inside the Counter and is displayed on the Oscilloscope. By monitoring these displayed signals, one can set the voltage level of signal for the digitization by the Counter Processor. The form of such displayed signals is shown in Figures 9-14. The horizontal division represents 1 micro second and the vertical division represents 75 mV.

The time period t between two successive logical "1"s is then determined by the computer and the velocity is

computed as per the equation

$$V = d/t$$

where

d : distance between the two focal points

These velocity values are continuously displayed on the LTA counter for every time interval. These values are then recorded for the calculation of mean value of the velocity and is discussed in full detail in the section 4.2 "Discussion of the LTA measurement. The picture of this counter and the used Oscilloscope is shown in Fig. 8.

The application of the above principle of LTA technique to measure the particle velocity is described in detail in the later section.

4.2 Discussion of LTA Measurement

4.2.1 Prevention of Incorrect Data

The LTA operates by detecting scattered light from small particles as they pass through two focal points formed by two highly focused laser beams. As shown in Figures 7, when a particle passes through the first focal point, it generates a start pulse and the stop pulse is generated by the same particle while crossing the second focal point.

The velocity is determined by measuring the time of flight of particles moving successively from one beam to another and the known separation of the two beams. However, in a turbulent flow, not every particle entering the measuring volume will meet both laser beams and emit the start-stop pulses. Additionally, two successive pulses may be generated by two different particles. As illustrated in Fig. 15, there are three possible cases regarding the travel of particles and the generation of voltage signals, they are as follows [45].

1. A particle travels directly from the first focus A to the second focus B within certain time period T.
2. After a particle passes through focus A(or B), no other particle crosses focus B(or A) during time T.
3. After a particle passes through focus A(or B), another particle crosses focus B(or A) during time T.

The time interval resulting from the pulses in case 1 is the correct representation of the particle velocity.

The pulse generated in the case 2 is disregarded by the computer since there is no successive pulse within the set time T. A time T is chosen and set, so that two successive pulses occurring within this time window T is considered by the computer for velocity calculation. The determination of T is based on the knowledge of an approximate value of particle velocity. This value in our study was determined by the Schlieren photography method. The velocity was found in

the range of 400 to 660 m/sec for which the average time interval is 1 microsecond. After considering all factors, the time window was set at 2.05 microsecond, which was the nearest available setting on the system.

The velocity calculated from the time interval generated in case 3 is not the particles velocity. The occurrence of such a pair of pulses is mainly due to the following factors:

1). The mean distance between particles is smaller than the distance between two focal points.

2). The two focal points are not aligned along the direction of the flight of the particles.

The correct and false time intervals occurring in case 1 and 3, respectively, can not be identified by the Data Processing System. However, the correct data has eminent probability if the occurrence of incorrect time interval is much less than the occurrence of correct one. As it was shown by [44], the distribution of observed time intervals can be, in most general case, approximated by the curve shown in Fig. 16. This curve in general consists of two regions. The observed data with higher occurrence probabilty were distributed in region A and were considered as the correct data. Region B indicated the observed data with lower occurrence probability and represented the noises occurred during the experiment. Therefore, the arithmetic mean

velocity calculated from all the observed time intervals can represent, with acceptable accuracy, the particle velocity. The difference between the peaks at the region A and B determines the quality of the measurement which is controlled by the probability of the occurrence of the false values. In general, it is possible to reduce the occurrence of false time interval by a correct experimental setup. They are:

1). The distance between the two focal points is kept shorter than the mean distance between the particles.
2). The two focal points are aligned as perfectly as possible with the direction of the flight of particles.

The determination of the suitable distance between the two foci is a major issue in the design of optical head of LTA system. As reported in several publications on the application of LTA [42-46], the distance should be in the range 0.3mm to 0.5mm in order to provide satisfactory measurements. For the LTA used in our study, such value was chosen as 0.45mm and was found to be suitable for our measurement.

The effect of the alignment between the direction of the beam plane and the direction of the flight of the particle on the probability of the occurrence of the incorrect time interval was discussed in [42]. Great difficulty was encountered during the measurement to align the direction of particle flight and two foci due to the size

of the jet, laser beam and the speed of jet. As shown in Fig. 17, a magnifying lens(25X) was used to enlarge the image of the jet at low pressure(600 kPa) and the image of the laser beams. Then the laser beam plane which consisted of the two beams was moved and rotated to coincide with the jet axis. The image of these two beams is shown in Fig. 18. Thereafter, the measurements were performed at the desired pressure which is 325 MPa in this study. The axis of jet was positioned at the focal points. The focal length of LTA optical head is given by manufacturer and is equal to 600mm.

4.2.2 Measurement in Pure Waterjet

The velocity measurement by the use of LTA is based on the measurement of the time of flight of particle. However, as reported in [42], the velocity of pure waterjet can be measured by LTA based on the flight of submicron particles which are normally contained in a real fluid. The velocities of such particles are strongly correlated with the water velocity [49]. The size difference between the added particles and particles contained in the water determines the difference in the intensity of the light, scattered by both kinds of particles. This enables us to differentiate between the signals obtained from added particles and those obtained from contained particles. In measuring the velocities of added particles, the signals generated by submicron particles become noise signals by the selection of an appropriate amplifier gain. Thus, the time intervals measured between

such noise signals were ignored by data counter system.

4.3 Measurement Procedure

The purpose of this study is to find the correlation between particles velocities and conditions of AWJ formation. An AWJ is formed when a high-velocity waterjet(sapphire waterjet) mixed with abrasive particles is expelled through a carbide tube. The study of the behavior of the waterjet prior to mixing with particles is therefore essentially useful for the purpose of this study. The velocity of the sapphire waterjet formed by the highly pressurized water passing through the sapphire nozzle was first measured. Then, the velocity of carbide waterjet formed by sapphire waterjet passing through the carbide tube was also measured. The velocities of particles entrained in the corresponding AWJ were thereafter measured.

From the above discussion, the obtained value representing the mean velocity of the particles which pass through the measuring point is determined statistically from a large sample of measurement data. The sample number for pure waterjet(either sapphire or carbide waterjet) was chosen in the range of 150-200 in order to obtain such statistical mean value. For the measurement of entrained particles, the number was reduced to 100-150 considering the wear within the carbide tube due to the abrasive particles passing through.

The experimental matrix used in the determination of particle velocity is shown in Table 1. A factorial approach to the experimental design was adopted for this study. The experiments were conducted in two suites. The first suite was an investigation covering all the combination of the diameters of sapphire and carbide nozzles. The second suite was to study the effects of other parameters on the particle velocity under certain sapphire and carbide nozzles. The determination of the values of abrasive mass flow rate used in all diameter combination is based on the consideration of the wear within the carbide tube. This approach facilitates the construction of an empirical model to describe the relative importance of the various parameters investigated and ensure that the data taken was sufficient for a sound statistical analysis.

The determination of the experimental conditions was based upon several important factors. These factors were based not only upon practical considerations to conduct the experiments, but were also chosed based upon the available range of the sapphire and carbide diameters and the available particle size as well as the commonly used in industry today.

All available sizes of d_c and d_n were tested at a contant mass flow rate value of 68 g/min and a mesh value of #220. In all twelve combinations of d_c and d_n were used in the experiment. The abrasive particle of size #220 mesh and

the low mass flow rate of 68 g/min were chosen to keep the wear of the carbide nozzle to a minimum.

Both d_n and d_c were kept at a highest value at higher mass flow rate during the experiemnt so as to prevent the clogging of the carbide tube. The diameter 0.254mm and diameter 0.1778mm were tested with different particle sizes as it is the most widely used and most practical sapphire nozzle for almost all types of cutting applications. To determine the transition of the water to water-particle flow, minimal detectable flow rate(13 g/min) was used at 7 different nozzle combinations. The selected matrix enabled us to evaluate all possible nozzle combinations, the possible range of the mass flow rate and the a prctical range of the particle size.

CHAPTER 5

VALIDATION OF THE MEASUREMENT TECHNIQUE

The validation of the measurement using LTA as proposed in this study becomes necessary since the application of LTA in determining the velocities of high speed waterjets and water-particle jets have not been found in available literature.

The validity of the results of the above technique for our purpose is demonstrated by a comparison of the results of LTA measurements with the data obtained by the well established techniques, such as force measurements and Schlieren photography, which will be shown in the following section. Additionally, the measured velocities of the waterjet were compared with the theoretical prediction obtained from Bernoulli's equation.

5.1 Bernoulli Equation

The velocities of waterjet can be calculated theoretically from Bernoulli's equation as follows:

$$V_W = (2*P*g_c/\rho)^{1/2}$$

where

P : pressure drop across the sapphire nozzle

ρ : water density

The computed and measured results are given in Figure 19. The higher values obtained from Bernoulli's equation in comparison with the measured data are due to the fact that the pressure drop within the nozzle is not considered in our computation. The ratio of measured and computed velocities at different water pressure is shown in Fig. [20]. It is observed that the value of measured velocity is about 85% of the value of velocity computed from Bernoulli's equation at same pressure.

5.2 Force Measurement

The forces of the WJ stream were measured with Piezoelectric Force Transducer [50], and the obtained values were used to calculate the waterjet velocities using the equation:

$$V_w = (F/\rho * A)^{1/2}$$

where

V_w : mean waterjet velocity

F : measured force of waterjet

ρ : water density

A : axial surface area of waterjet

The accuracy of the determination of the velocity by this method is strongly affected by area determination. The measurement of axial surface area of waterjet is difficult because of the magnitude of the jet diameter and its impact

pressure. The value of A used in this study was determined by the measurement of the area of the hole pierced during 60 seconds by the waterjet on the stainless steel plate with 0.55mm thickness.

The mean velocities obtained by force measurement and the velocities measured by LTA were given in Figure 10. The decay of mean velocity along axial direction of waterjet, as shown in the experimental results, is due to the effect of drag friction of the surrounding space. The mean velocity of waterjet at the exit of the nozzle is known to be equal to the central velocity [51]. The capability of LTA to measure the centerline velocity in a jet is confirmed by the comparison of both data obtained at very close stand-off distance, which is shown in the Fig. 21.

To enhance this confirmation, an experiment was performed based on the fact that the centerline velocity of the jet has the maximum value along the transversal direction [49]. The velocity measurement by the use of LTA were carried out by moving the jet along transversal direction and the measuring point remaining at same position. The obtained probability distribution of the velocity at different distances from the center of jet were shown in Figs. 22-28. The corresponding mean velocity was given in Fig. 29. It is observed that the velocity of the centerline of the jet, which was measured by the method mentioned in the Chapter 4,

has the maximum value. Therefore, the use of LTA to measure the centerline velocity in a jet is concluded.

It is also found that the obtained probability beyond 1.143mm from the centerline of jet became randomly distributed and failed to determine the value of velocity. The reason for that is the direction of jet flow in that region is not aligned with the direction of the beam plane due to the divergence characteristics [52]. Thus, the probability of the occurrence of the false value is higher than the correct one. The importance of the alignment between the direction of beam plane and the direction of the object in the LTA measurement was discussed in detail in Chapter 4.

5.3 Schlieren Photography

Figure 30 shows the Schlieren photograph of an abrasive waterjet, which is used for comparing the results of LTA. Some Mach lines were observed at the boundary of jet. The Mach number of the flow can be determined from the photograph by measuring the shock angle. The velocities of the liquid phase or the entrained particles were obtained by using the equation:

$V = M*C$

where

M = Mach number = $(1/SIN\theta)$

C = speed of sound in air = 340 m/sec

in which

Θ = shock angle

One important fact to be noted is the velocities of the entrained particles. By Schlieren photography technique it was not possible to distinguish between the velocities of the liquid phase and entrained particles. The values obtained from the Schlieren photograph are found to be in the range of 430m/sec to 660 m/sec, whereas values as measured by LTA technique are in the range of 400m/sec to 500 m/sec. The higher value observed in the case of Schlieren measurement are most probably the liquid phase velocities. The suitability of LTA as a means of the measurement of particle velocity certified by the comparison of the results obtained from both techniques.

Upon the comparison of the results presented, the LTA instrument can allow us to measure:

1). the velocity of pure waterjet.

2). the velocity of particle entrained in an AWJ.

3). the centerline velocity of pure waterjet or the velocity of particle entrained in the centerline of an AWJ.

The results obtained by the use of LTA for the purpose of this study are presented in Chapter 7.

CHAPTER 6

REGRESSION ANALYSIS

Regression analysis enables us to ascertain and utilize a relation between a variable of interest, called a dependent or response variable, and one or more independent or predictor variables. The analysis is often used to predict the response variable from the knowledge of the independent variable.

In most empirical studies where interest centers on a dependent variable Y, the value of Y is not uniquely determined when the level of the independent variable is specified. A tendency of the dependent variable Y varies systematically with the independent variable X by a line or curve of statistical relationship. A scattering of observations around the line or curve of statistical relationship, is partly due to the factors in addition to the independent variable X affect the dependent variable Y, and partly due to the inherent variability of Y [53].

A regression model then assumes that each observation on the dependent variable Y_i consists of:

1. A regression component reflecting the line or curve of statistical relationship.
2. A random component reflecting the scatter or deviation

about the line or curve of statistical relationship.

For example, the basic regression model, where the statistical relation is linear, takes the form:

$Y_i = B' + B"*X_i + e_i$

where

Y_i is the response in the ith observation.

X_i is the value of independent variable in the ith observation.

B' and B" are regression components and are called regression parameters.

e_i : is the random component and is called error term.

Ordinarily, the regression parameters B' and B" are unknown and must be estimated from sample data. The error terms are the data that are used to identify the dispersion of all Y values around the estimated equations. The determination of the values of B' and B" with minimum deviation is given in [54,55].

The linear regression equation describes a constant amount of increase in the dependent variable associated with a unit increase in the independent variable. The data obtained in experiment, however, does not always follow the linear hypothesis tendency. But, many possible nonlinear mathematical relationships between the two variables X and Y can be transformed to linear relationships between two new

variables by applying a relatively simple mathematical operation to the original nonlinear form [56].

Consider the exponential relation, for example,

$Y = B' * e^{B''X}$

the nonlinear relationship is transformed to a linear relation, by taking the natural logarithm of both sides of the equation, as follows:

$Ln\ Y = Ln\ B' + B'' * X$ or

$W = b' + B'' * X$

This mathematical operation yields a linear relationship instead of an exponential relationship. The regression parameters in the new linear regression equation can be estimated from transforming the sample data by taking the natural logarithm of each Y_i, and then performing the simple linear regression analysis on the transformed data set.

There are many software packages available to find the regression parameters of estimated regression equations. These packages calculate the value of correlation coefficient to show the degree of association between response values and estimation. TempleGraph, developed by Mihalisin Associates [57] and used in this study, is a software package, which allows one to analyze data via regression operation and represent the obtained results graphically. A comparative study of four regression models such as linear,

exponential, power, and natural logarithm is used to construct the empirical equation for the prediction of the particle velocities in different conditions of AWJ formation. The selection of a desired regression model was based on the comparison of the values of correlation coefficients associated with each regression model. The selection of the dimensionless groups involved in the empirical equation, either independent or dependent variables, were determined based on the results of regression analysis. A number of trials were performed to choose the one with highest correlation coefficient, conforming the physically acceptable process pattern.

CHAPTER 7

EXPERIMENTAL RESULTS AND DISCUSSIONS

7.1 Velocities of Sapphire Waterjets($V_{s.w.}$)

The waterjet formed by the highly pressurized water and passing through the sapphire nozzle is called sapphire waterjet for distinction in this study. The measurements, by the use of LTA, to determine the center velocities of sapphire waterjet were first performed. The diameters of sapphire nozzles used in the presented study were 0.1778mm, 0.254mm, 0.3048mm and 0.3556mm respectively, and the discharge pressure was maintained at 325Mpa. Figs. 31-35 show the probability distribution of velocity obtained at the stand-off distances(i.e., the distance from the nozzle exit) in the range from 6.35mm to 63.5mm with a 0.254mm nozzle diameter. The results shown in these figures indicate the relative frequency of the velocities. The Figures showing the frequency(i.e., the number of occurrence) distribution of velocity obtained with other nozzle diameters are given in Appendix.

The values occurring with lower probability, which were distributed in the shielding region as shown in the given figures, have been discarded as being caused due to the "noise" associated with the measurement. The mean velocity of each measurement is estimated by taking the arithmetic

mean of only those values of the sample data(i.e. the observed velocities) which had a high probability of occurrence. The "cut-off" value is varied in each obtained probability distribution and is shown in given Figures. The variation of the accepted values of velocities is due to the errors of measurements, other than the turbulent longtitudinal pulsation of velocity. By comparing the probability or frequency distribution of velocity obtained at different stand-off distances with same nozzle, the scattering of jet velocities increases as the distance from the nozzle exit point increases. This change is due to the deterioration of the jet coherence in the course of its development. The values of mean velocities of sapphire waterjets estimated from the measurements with different nozzles are tabulated in Table 2 and shown in Fig. 36.

As observed from the results, the values of velocities of waterjets are slightly increased as the nozzle diameter decreased. Considering the energy loss along the piping line, however, it may be concluded that the velocities of waterjets formed by different nozzle diameters at constant discharge pressure of water are virtually the same and about 700 m/sec. It is also observed that the center line velocity of sapphire waterjet tend to decrease along the axial direction. Such a velocity decay indicates that the waterjet energy has dispersed in the transverse direction.

7.2 Velocities of Carbide Waterjets($V_{c.w.}$)

The abrasive particles are entrained into the nozzle head to mix with sapphire waterjet and the AWJ that is formed by such mixture gets expelled through the secondary nozzle(named carbide tube or slurry nozzle). The waterjet formed by the sapphire waterjet and expelled through the carbide tube without entraining any abrasive particles is called carbide waterjet to distinguish from the sapphire waterjet. The diameters of carbide tubes used in the experiments were 0.863mm, 1.09mm and 1.6mm. The length of the tube was 50.8mm.

The acceleration of entrained particles is a result of momentum transfer from sapphire waterjet and the acceleration process occurring within the carbide tube. Therefore, the velocities of the particles are strongly correlated with the superiority of the alignment between the sapphire nozzle and carbide tube. Thus, the velocities of carbide waterjets has to be determined in order to identify such superiority. The existing method for the determinination of the superiority of the alignment is based on the observation of the strength of the carbide waterjet discharged at low pressure(about 1,000 psi). The procedure for the alignment of sapphire and carbide nozzles, used in our setup, is as described below.

The sapphire nozzle is placed at the center of a housing which is threaded to the high pressure water pipe. This housing is detachable from the pipe in order to facitate the replacement of worn sapphire nozzle. Three screwed holes at 120 degree pitch are at its bottom end. The holes have screws in them to hold the carbide nozzle in position and adjust its axis in relation to the axis of the sapphire nozzle.

Initially, the waterjet is manually maintained at 1,000 psi so that the coherence of the jet coming out of the carbide nozzle can be seen visually, and the position of carbide nozzle can be adjusted manually. It is thus possible to determine the superiority of the alignment based upon the visual observation of the jet. If there is no disturbance in the jet, i.e., no waterdrop around the periphery of the jet, then the alignment procedure is said to be completed. Although this is not an accurate method, it is the commonlly accepted procedure applied in the industry so far.

Figure 37 illustrates the probability distribution of velocity of carbide waterjet. The Figures showing the frequency distribution of velocity of the carbide waterjets are given in Appendix. The estimated mean values of velocities obtained in the measurements are given in Table 3. The multiple values shown in the same diameter combination, as observed from given Table, were the values of the velocities of carbides waterjets formed by assembling the

same sapphire and carbide nozzles differently, i.e., the sapphire and carbide nozzles were disassembled after the first measurement and the same nozzles were assembled again for second measurement and so on. As observed from the given results, the variation of the values obtained at the same diameters of sapphire and carbide nozzles indicates the uncertainty of the velocities of carbide waterjets. The above mentioned phenomena is also confirmed by the Figure 38 which gives a graph of value of $(V_{c.w.}/V_{s.w.})$ against $(d_n/d_c)^2$. A clear inference from the graph would be that the velocity values of the carbide waterjet obtained at same value of $(d_n/d_c)^2$ are inconsistent. This is due to the variation in the alignment of the carbide and sapphire nozzles in successive set-ups. A perfect alignment should ensure the velocities of carbide and sapphire waterjets to be the same provided the same sapphire and carbide nozzles are used.

7.3 Velocity of Entrained Abrasive Particle(V_a)

Typical probability distribution of velocities of particles is shown in Fig. 39. The Figures showing the frequency distribution of velocity of particles entrained in different AWJs are given in Appendix. The mean values of velocities estimated from the measured results are given in Table 4 - 8. The multiple values shown in the Table were

taken repeatedly for the same AWJ to check the effect of wear of the carbide tube on the particle velocity. The average of those multiple values was used to represent the particle velocity at that condition. No clear tendency is found by comparing the value of V_a at different conditions such as diameter of sapphire or carbide nozzle. However, some tendencies are noticed by comparing the values of ($V_{c.w}$ - V_a), where the carbide waterjet and the AWJ were formed by the same sapphire and carbide nozzles. The reason for the use of the velocity difference between the carbide waterjet and the corresponding entrained particles is to nullify the effect of the alignment and the energy loss due to the interaction between the waterjet within the carbide tube. Therefore, the variation of ($V_{c.w}$ - V_a) virtually represents the variation relative to V_a.

7.3.1 Effects of Diameter of Carbide Tube(d_c)

A graph of ($V_{c.w}$ - V_a) against the diameter of carbide tube (d_c) was constructed and shown in Figure 40. From the constructed figure it is found that the value of ($V_{c.w}$ - V_a) increases with the increase of d_c. The increasing value of ($V_{c.w}$ - V_a) in the figure can be actually interpreted as the decrease in the value of V_a. The decreasing trend in the value of V_a with the increasing value of d_c suggests the acceleration of the particles are highly dependent on the rebound force obtained from the wall of the carbide tube.

7.3.2 Effects of Diameter of Sapphire Nozzle(d_n)

Figure 41 shows a graph of ($V_{c.w.}$-V_a) against the diameter of sapphire nozzle (d_n). It indicates that the value ($V_{c.w}$-V_a) tends to decrease, i.e. V_a increases, with the increasing of the d_n. It is realized from the fact that the water flow rate of sapphire waterjet is increased by the increasing of the diameter of sapphire nozzle. As a result of the increasing of water flow rate, more momentum is delivered to accelerate the entrained particles and their velocities, therefore, are increased.

7.3.3 Effects of Particle Size

The size distribution of the particles in different mesh numbers is shown in Figure 3 [12]. Fig. 42 shows the probability of velocity of particles entrained in an AWJ, and is based on separate measurements for injecting different mesh numbers of particles. As observed from the given figure, the patterns of the probability distribution of the velocities are similar and the values are in the same range. This indicates that the variation of the velocities of entrained particles is practically independent of the size of added particles. The reason of this similarity of velocity distribution is the disintegration of the added particles during the acceleration process, which was confirmed by the

results given in Ref.[58].

7.3.4 Effects of Abrasive Mass Flow Rate(m_a)

The values of mean velocities of particles entrained in an AWJ for different mass flow rates are shown in Fig. 43. The velocity values of particles tend to decrease with the increasing of mass flow rate(m_a) at constant diameters of sapphire and carbide nozzles. Conversely, as the mass flow rate decreases, the value ($V_{c.w.}$-V_a) also decreases and as the mass flow rate approaches to zero, $V_{c.w.}$-V_a is equal to zero. Thereby, it suggests that at a very mass flow rate, the velocity of the carbide waterjet is equal to the velocity of the entrained particle. This is also obvious from the fact of theory of momentum transfer that as the mass flow tends to reduce, the velocity tends to increase.

7.5 Resulting Equation

On the basis of the above results it has been finally possible to construct an empirical equation that can be used to predict the particles velocities by certain known conditions of AWJ formation. By known conditions we mean the knowledge of diameters of sapphire and carbide nozzles, abrasive mass flow rate and particle size distribution. A number of trials were performed to select the correct independent and dependent dimensionless variables for such an equation. The foremost creteria for the selection of these

variables was the correlation coefficient obtained by conducting the regression analysis of the variables.

The regression analysis of the values of the parameters such as $V_{s.w.}$, $V_{c.w.}$, V_a, d_n, d_c and m_a was carried out. The results with higher correlation coefficients are shown in Figures 44-46. It was observed that the relation between $(V_{c.w.}-V_a)/V_{s.w.}$ and $(Q_a/Q_w)^{(dn/dc)^2}$ had the highest value of coefficient in the case of power regression model. The resulting equation is given as follows:

$$Y = a * X^b$$

where

$Y = (V_{c.w.}-V_a)/V_{s.w.}$

$X = (Q_a/Q_w)^{(dn/dc)^2}$

$a = 0.6274$

$b = 2.5571$

Q_a : volume flow rate of abrasive

Q_w : volume flow rate of water

The above equation $Y=aX^b$ is derived using the volume flow rare instead of mass flow rate. The main reason behind this is the availability of the information for potential applications of this equation for different types of fluid media.

7.5 Discussion

7.5.1 Application of Resulting Equation

The obtained resulting equation enables us to predict the value of the velocity of particle entrained in an AWJ for given values of the diameters of sapphire and carbide nozzles and the abrasive mass flow rate. The procedure for the computation of particle velocity using this equation is illustrated as follows:

1). The value of $(V_{c.w} - V_a)/V_{s.w}$ is obtained from given values of d_n, d_c and m_a($Q_a = m_a/\rho$).

2). The value of $V_{s.w}$ is determined by the product of a coefficient and the velocity computed from Bernoulli's equation. As discussed in Chapter 5, this coefficient is used to take into account the pressure drop that occurred within the sapphire nozzle. The value of this coefficient is chosen as 0.85 which is determined from the ratio of measured and computed velocity as shown in Fig. 20. As it was discussed in our study, the velocity of the sapphire waterjet at 325 MPa is constant and equal 822 m/sec as computed using Bernoulli equation. Therefore, after taking to account the above value of the coefficient, 0.85, the value of $V_{s.w}$ used for our computation is equal to 699 m/sec.

3). As mentioned in the preceding section, the ratio of

$V_{c.w.}/V_{s.w}$ depends on the superiority of the alignment between the sapphire and carbide nozzles. As of today, there is no available data which can provide us such information to determine this ratio. Ideally, this ratio is expected to be equal to 1 and this value is used in our computation.

The computed velocities and the corresponding measured particle velocities are shown in Figure 47. The difference between these two values does not exceed +/- 100 m/sec.

7.5.2 Limitations of the Resulting Equation

The characteristics of an AWJ formed in the certain range of diameter ratio of sapphire and carbide nozzles is expected to be different with an AWJ formed in the some other range of such diameter ratio. For example, an AWJ formed with very small ratio of d_n/d_c has the same characteristics as a free jer(jet submerged in the air) whereas the AWJ formed with the ratio of d_n/d_c equal to 1 is essentially considered as the flow in a straight pipe. Therefore, the use of the obtained equation is limited to the diameter ratio in the range employed in this study, which changes from 0.11 to 0.41. For the diameter ratio outside this range, further study is required.

As mentioned in the preceding Chapters, the parameters involved in this study are the diameters of sapphire and carbide nozzles, the size of added particles and its mass

flow rate. The other parameters such as the length of carbide tube and water pressure are kept constant during the measurement. Therefore, the obtained equation is only applicable to calculate the velocities of particles in an AWJ under considered conditions. However, it may be expected that the kinematic variable $(V_{c.w}-V_a)/V_{s.w}$ can be also used in the construction of the equation for a wide range of experimental process.

Despite the above mentioned limitations, the results provided in this study is the only available equation which can be used to predict the velocities of particles entrained in an AWJ The parameters considered in this study are the actual parameters used in AWJ cutting technology so that the obtained results can be used by the industry.

CHAPTER 8

CONCLUSIONS

8.1 LTA Measurement

Since the knowledge of physics of the acceleration mechanism of the particles entrained in an AWJ is still limited, no reliable theoretical data available as of today enable us to predict the particles velocities. Moreover, the experimental techniques which have been employed for such studies can not provide such informations due to the complex phenomena of the subject in question. It is expected that the applications of AWJ technology can be extended if those informations can be acquired properly.

An optical instrument(LTA) was used to measure the velocities of the particles entrained in the AWJ. Those values were compared with the ones obtained by the other means. The application of the measurements using LTA for the AWJ in question is validated and the conclusions of this study related to the measurements by LTA can be drawn as follows:

1. LTA can be used for the measurement of the velocities of the waterjet and abrasive waterjet. The technique for this measurement was developed and validated.
2. LTA can discriminate the velocities of the water and

entrained particles in an AWJ.

3. LTA enables us to determine the center line velocity of jet.

8.2 Analysis of the Results of the Measurement

An AWJ is the combination of sapphire waterjet, carbide waterjet and entrained particles. The velocities of the sapphire and carbide waterjets are measured prior to the measurement of velocities of entrained particles. The results of the measurement of the waterjets indicate:

1. Velocities of sapphire waterjets formed at constant water pressure of 325MPa by different nozzle diameters are almost equal to 700 m/sec. The observed difference between the velocities of the jets generated by different sapphire nozzles are due to the difference in the pressure drop along the pipeline.

2. In our experiments, the velocities of entrained particles range from 243m/sec to 634m/sec.

3. The velocities of carbide waterjets are strongly correlated to the alignment between the sapphire and the carbide nozzles. The existing alignment technique does not allow us to generate the carbide waterjets having a constant value of velocities at same sapphire and carbide nozzles and constant water pressure. The estimated variation of the velocity of carbide waterjet due to the effect of the

alignment is in the range of 20%.

4. The kinematics of the carbide waterjet is determined by the dimensionless group $(V_{c.w.}-V_a)/V_{s.w.}$.

5. In a general form, the correlation between the kinematic characteristics of the jet and conditions of its formation are given by the following equation:

$$\frac{V_{c.w.}-V_a}{V_{s.w.}} = 0.627 * \left(\frac{Q_a}{Q_w} (d_n/d_c)^2 \right)^{2.557}$$

6. The following effects have been observed from the statistical analysis of our data:

a. The velocities of the entrained particles are increased with the increase of the diameter of the sapphire nozzle.

b. The velocities of entrained particles increase as the diameter of carbide tube decreases.

c. The mean values of the velocities of entrained particles decrease as the abrasive mass flow rate increases.

d. There is a weak correlation between the velocities of the entrained particles and the size of the added particles.

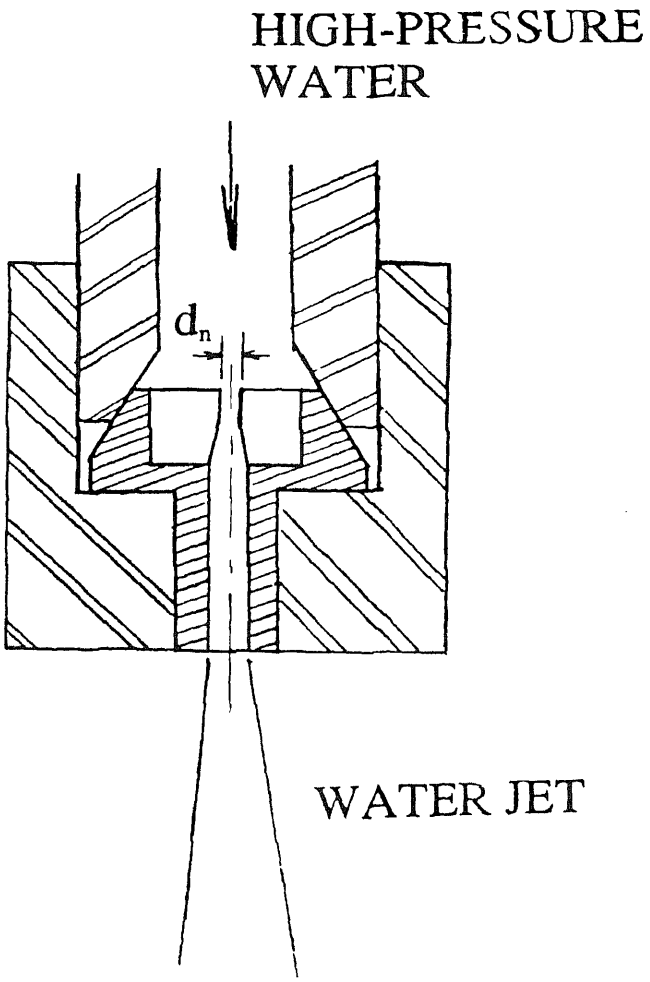

Fig. 1: Schematic of Sapphire Waterjet

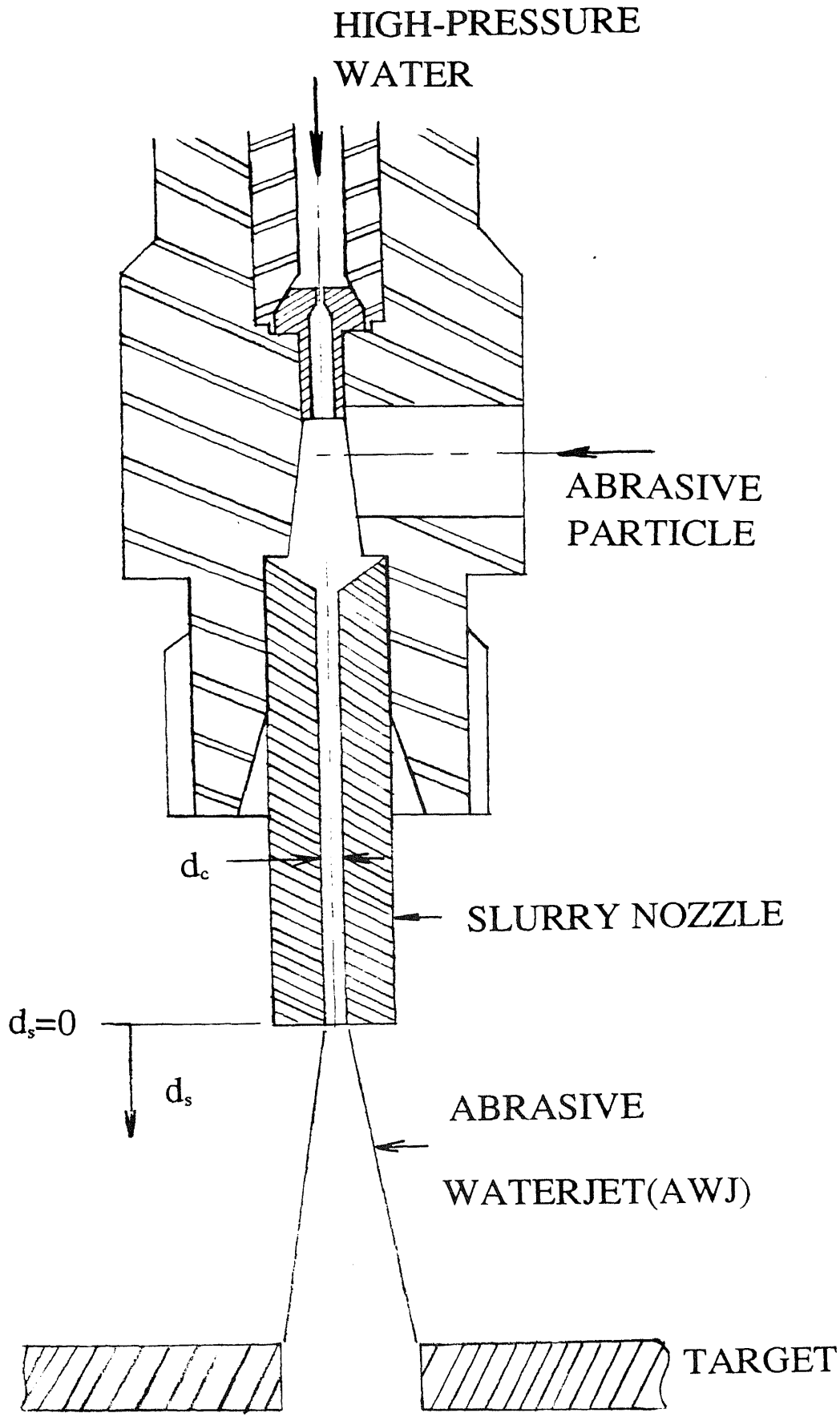

Fig. 2: Schematic of the Assembly for the AWJ Formation

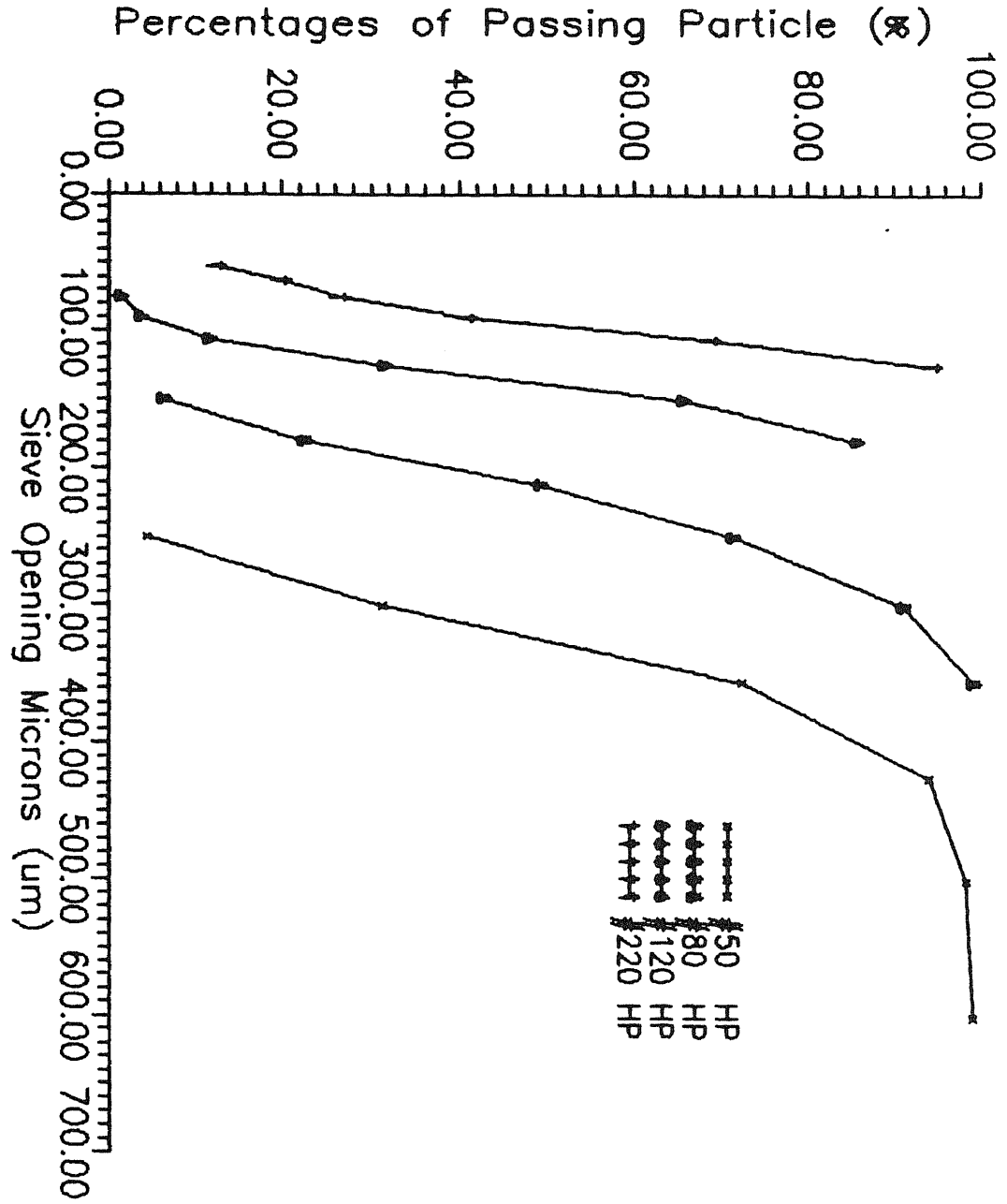

Fig. 3: Size Distribution of Added Particles

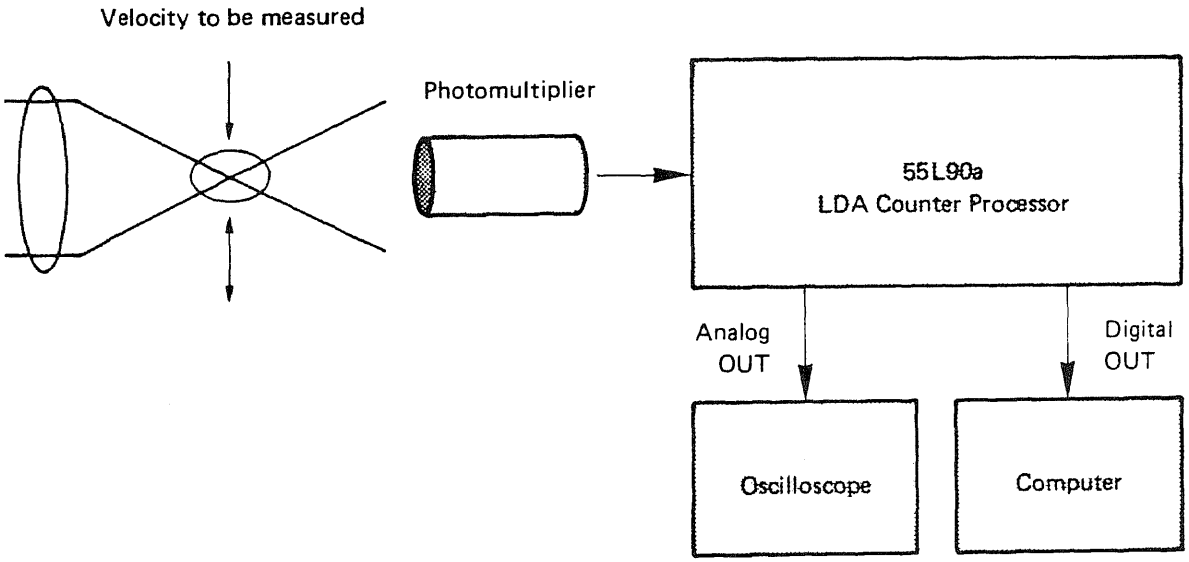

Fig. 4: Block Diagram of the Data Management System

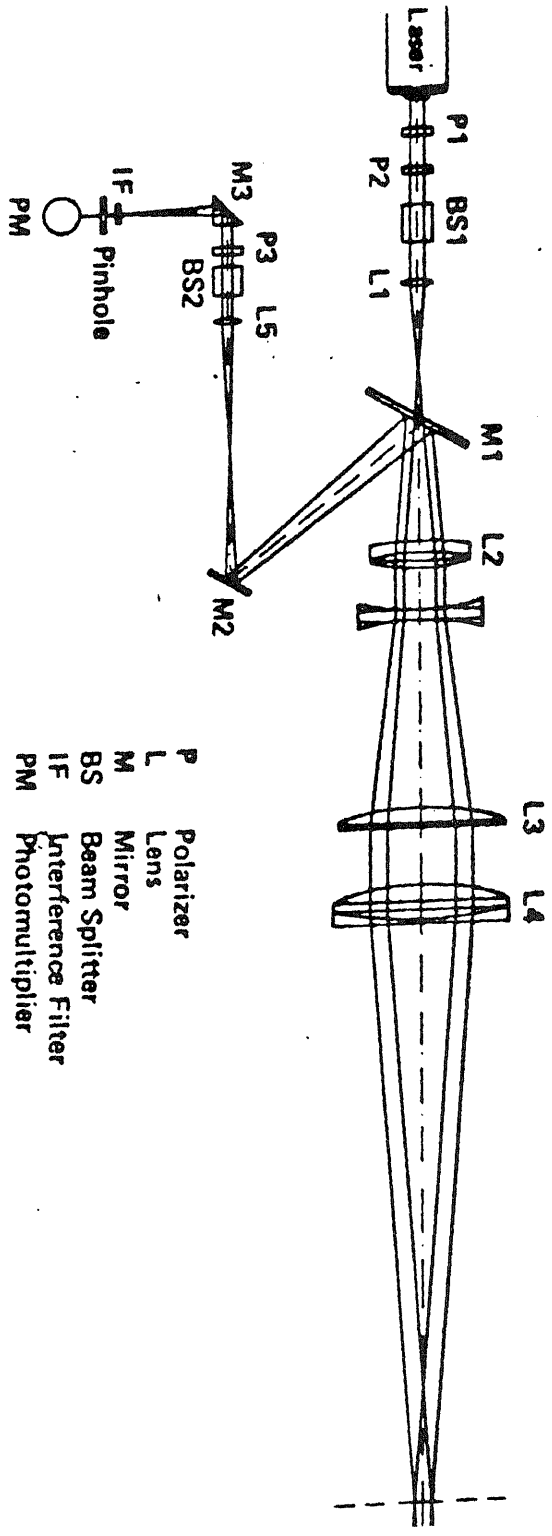

Fig. 5: Sketch of the Optical Head of LTA

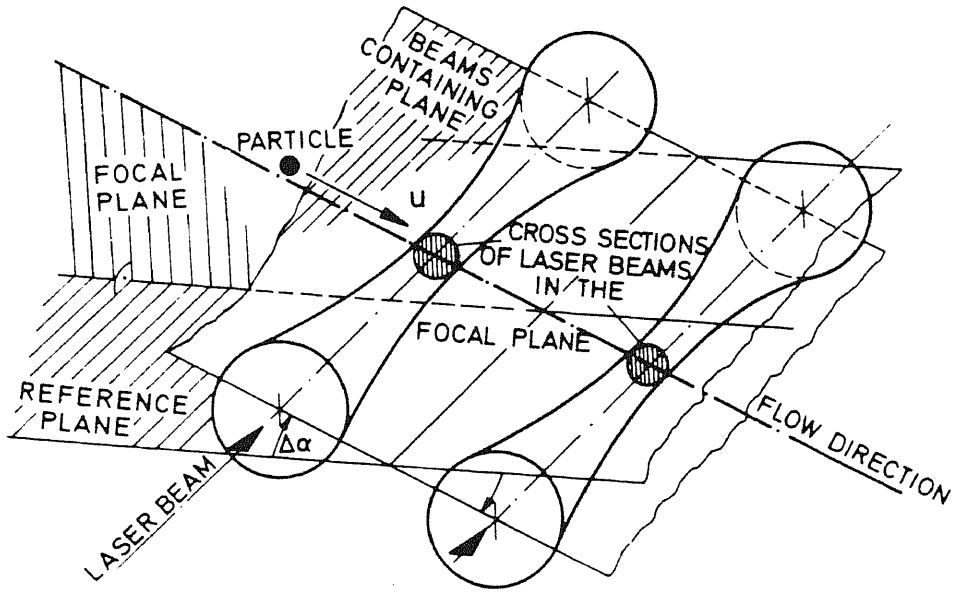

Fig. 6: Sketch of the LTA Measuring Volume

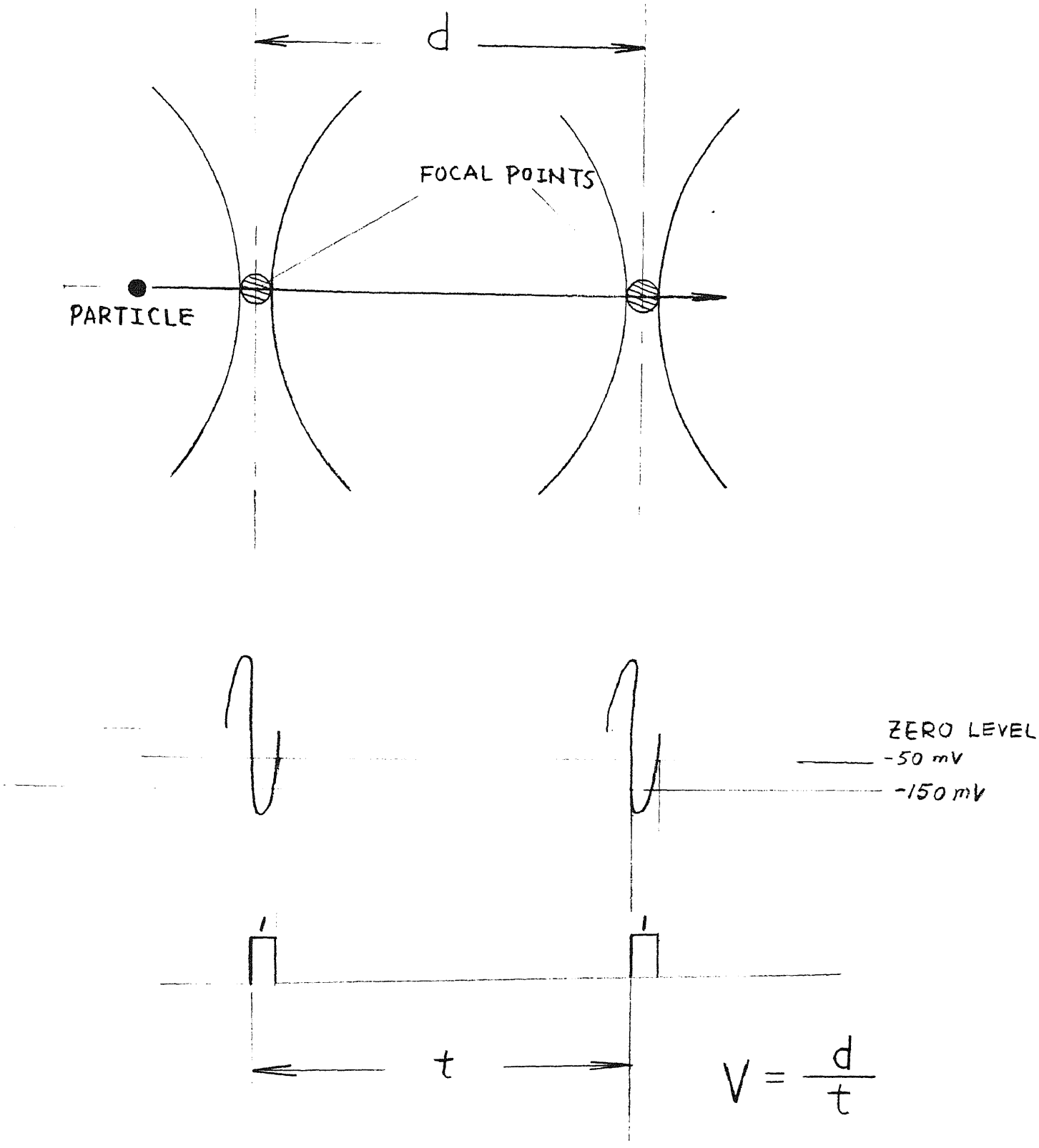

Fig. 7: Wave Form of Output Signals for Digitization

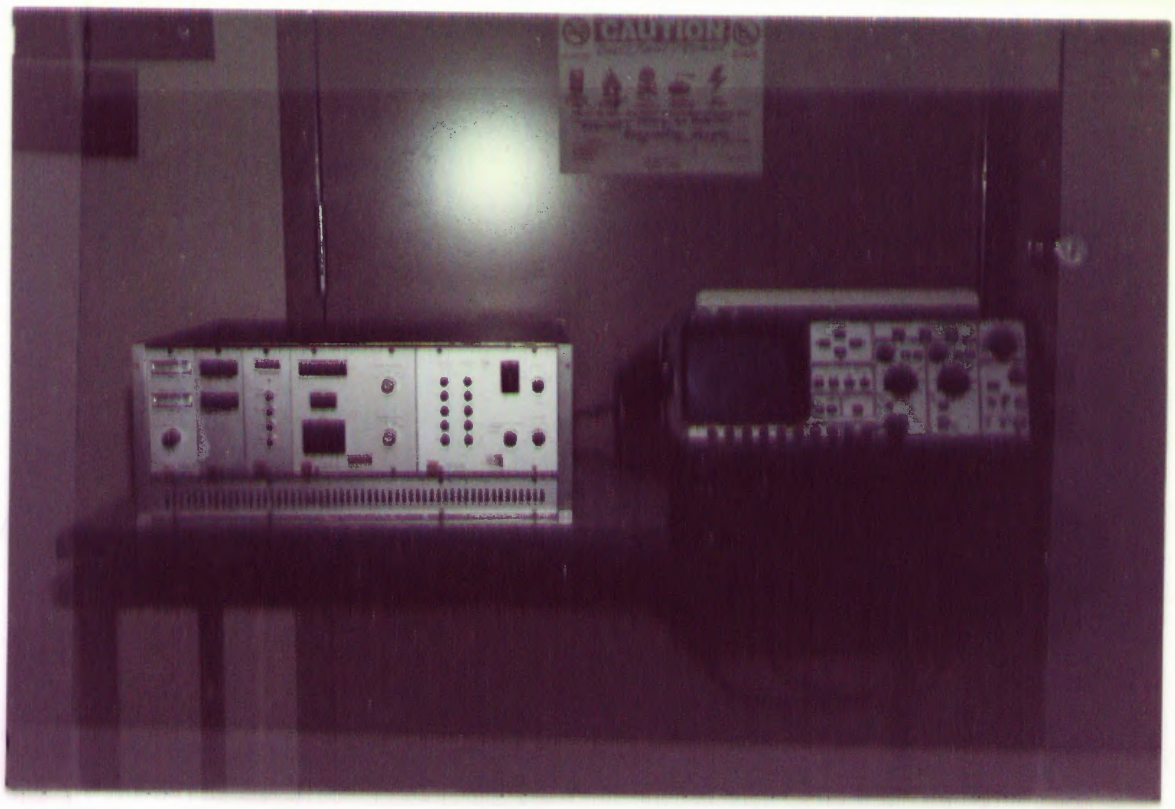

Fig. 8: Picture of Counter and Oscilloscope

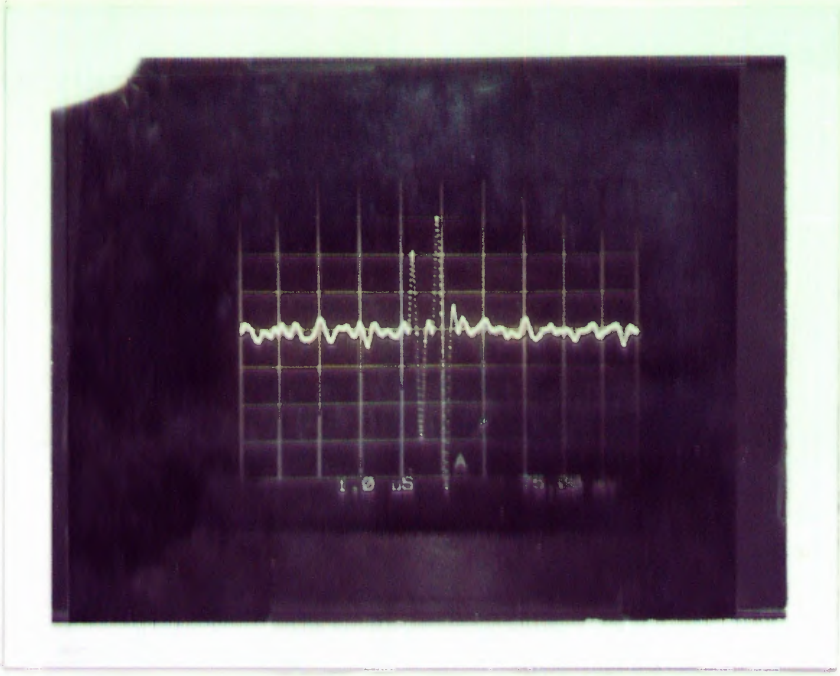

Fig. 9 : Oscillogram of Signals from LTA Measurement on Sapphire Waterjet: dn=0.3556mm

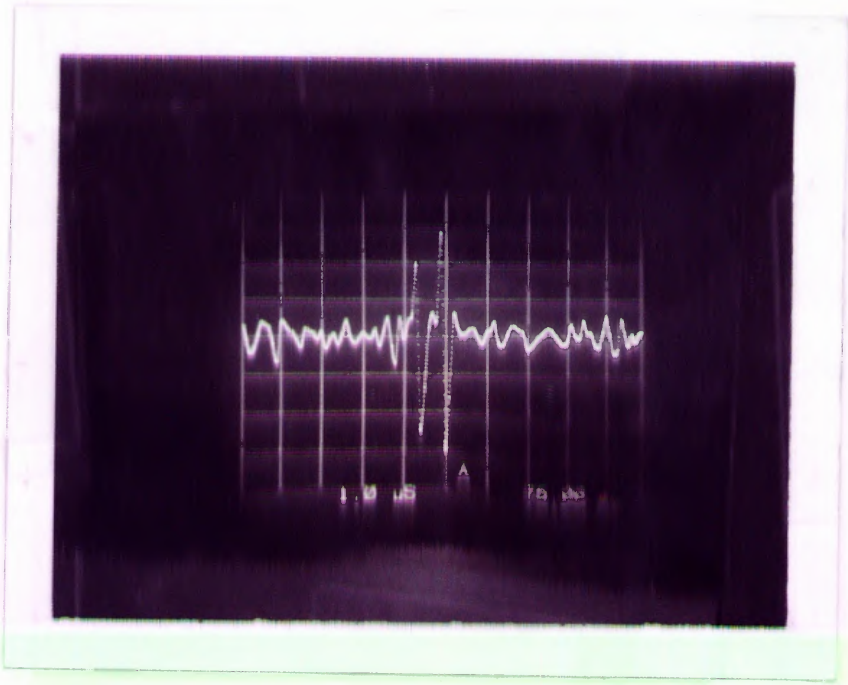

Fig.10: Oscillogram of LTA Signal;Sapphire Waterjet: d_n=0.254mm

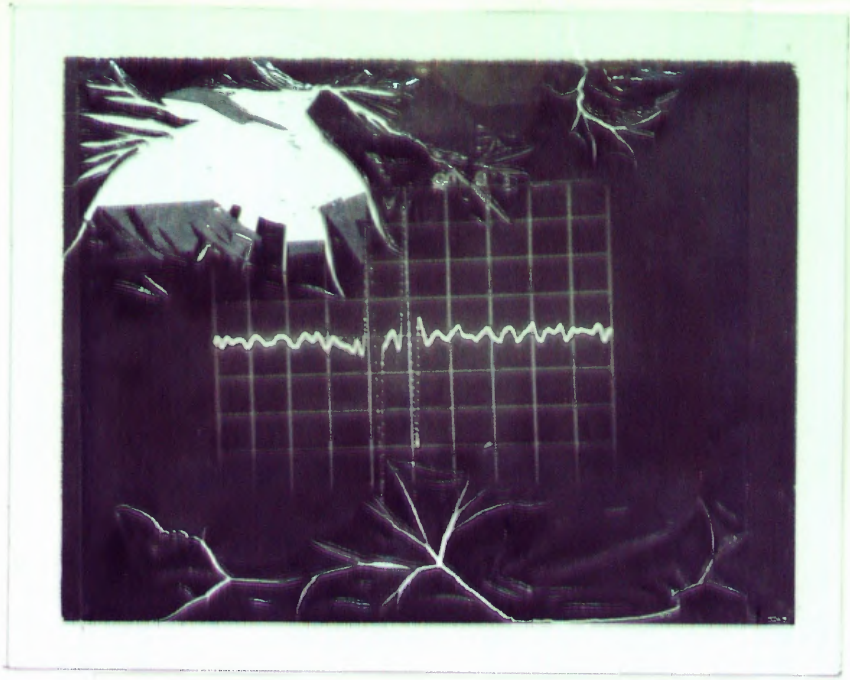

Fig. 11: Oscillogram of Signals from LTA Measurement on Carbide Waterejt: dn=0.1778mm; dc=1.09mm

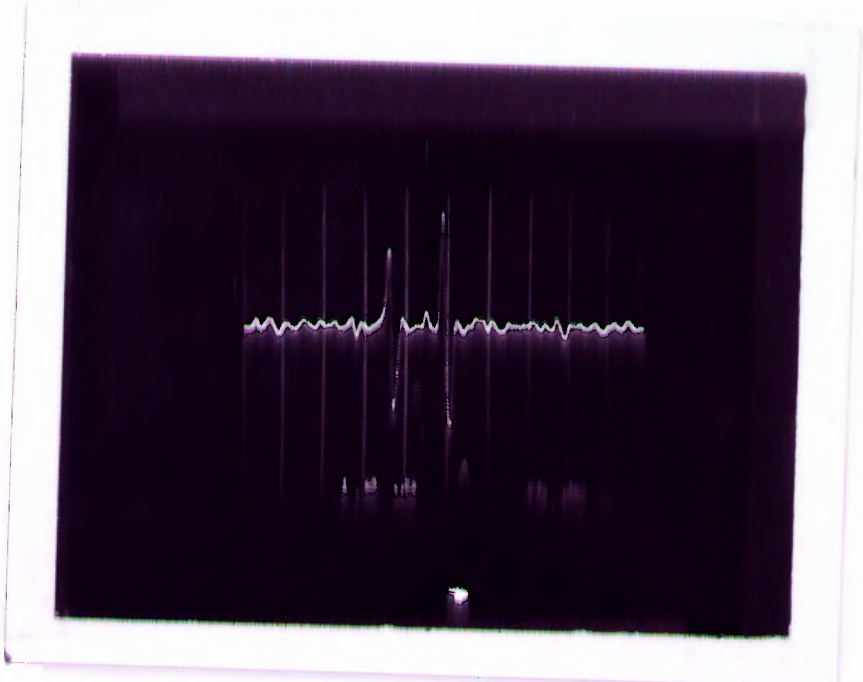

Fig.12: Oscillogram of LTA Signal; Carbide Waterjet: d_n=0.254mm; d_c=0.8636mm

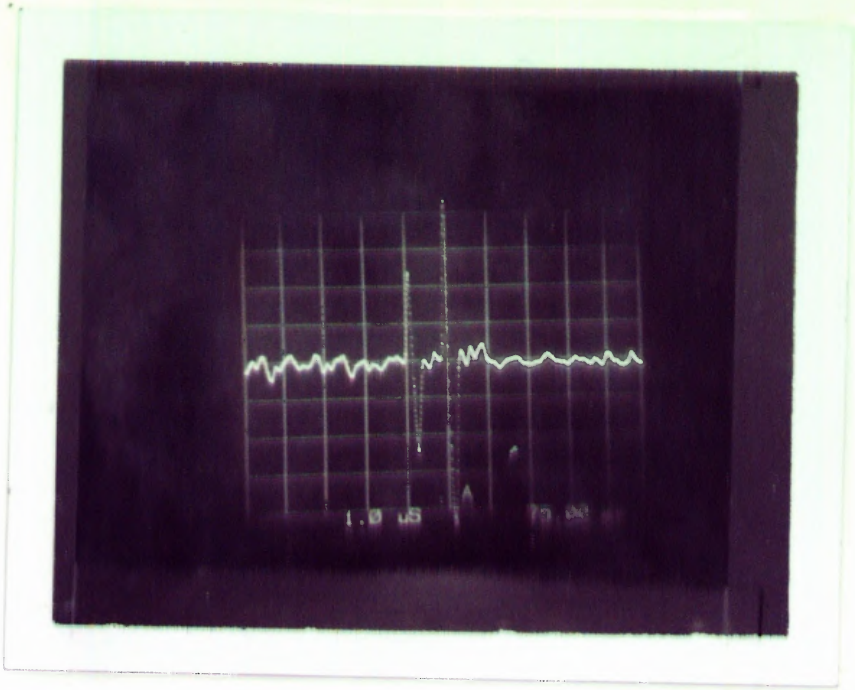

Fig.13: Oscillogram of Signals from LTA Measurement on Abrasive Waterjet: dn=0.3556mm; dc=0.8636mm; ma=68g/min;da=#220

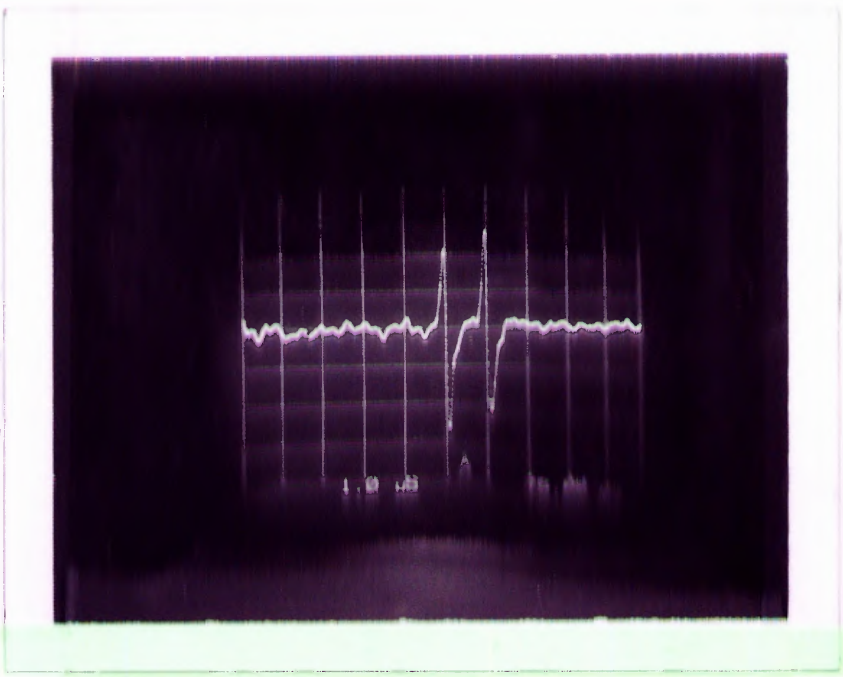

Fig.14: Oscillogram of LTA Signal; Abrasive Waterjet: d_n=0.254mm; d_c=0.8636mm; m_a=68g/min; d_a=#220

1). Pulse Generation Due to Single Particle

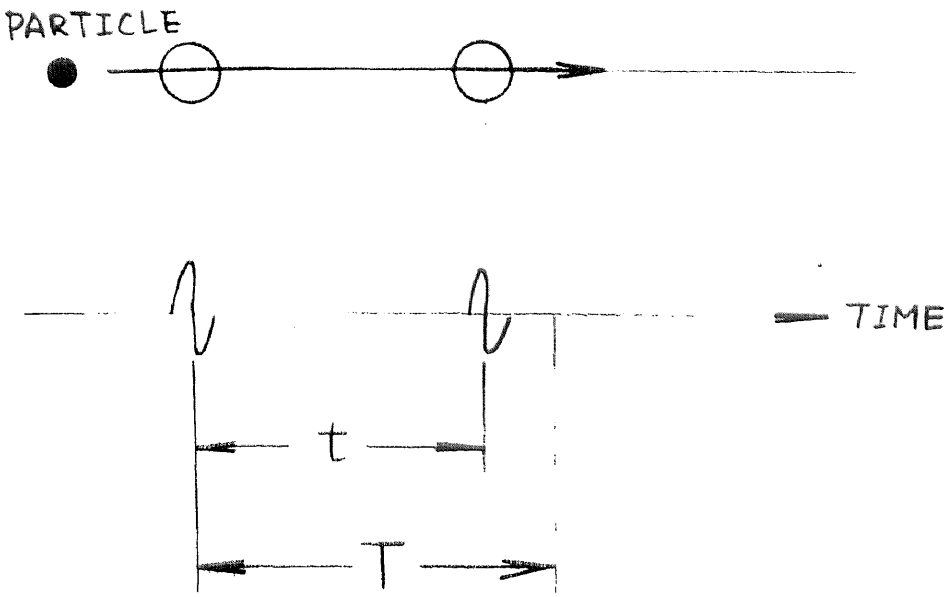

2). Pulse Generation with Incorrect Time Interval

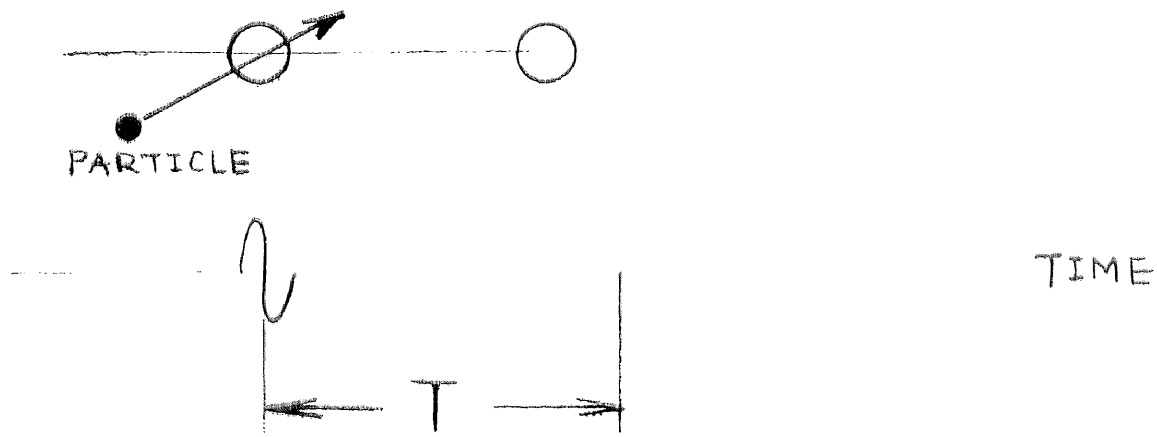

3). Pulse Generation Due to 2 Different Particles

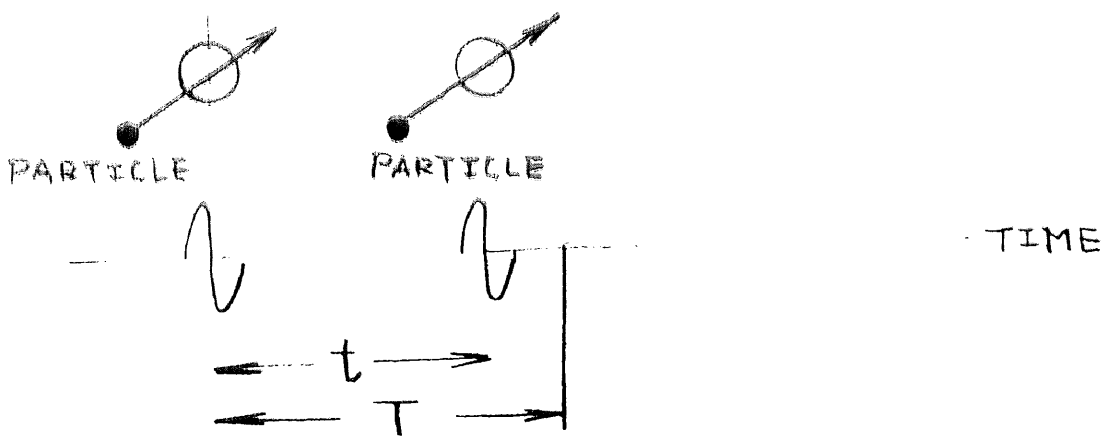

Fig.15: Possibility of Pulse Generation

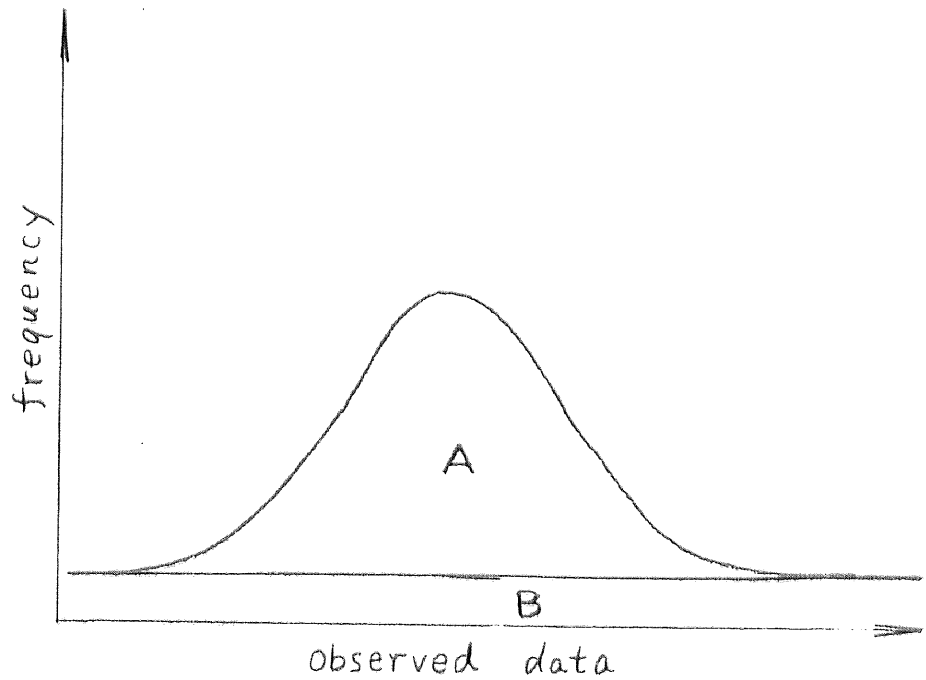

Fig.16: Frequency Distribution of Observed Data

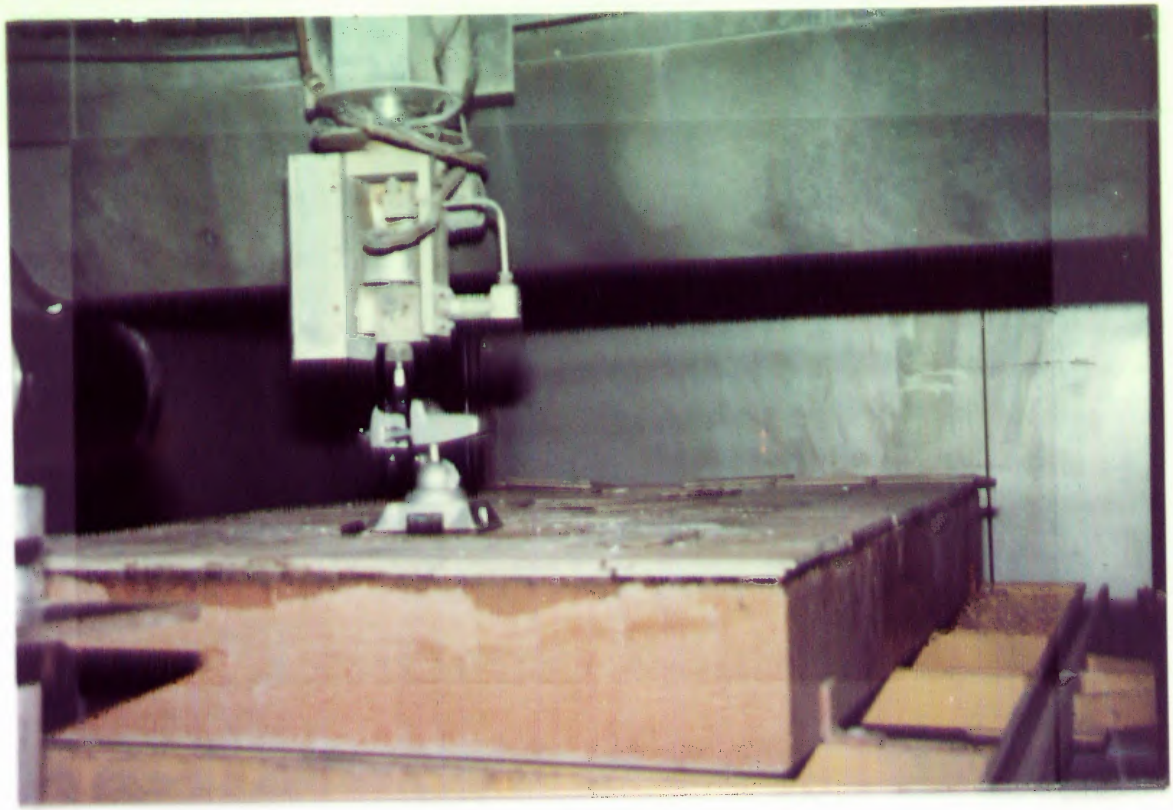

Fig.17: Picture of the Experimental Setup for the Alignment of the Measurement

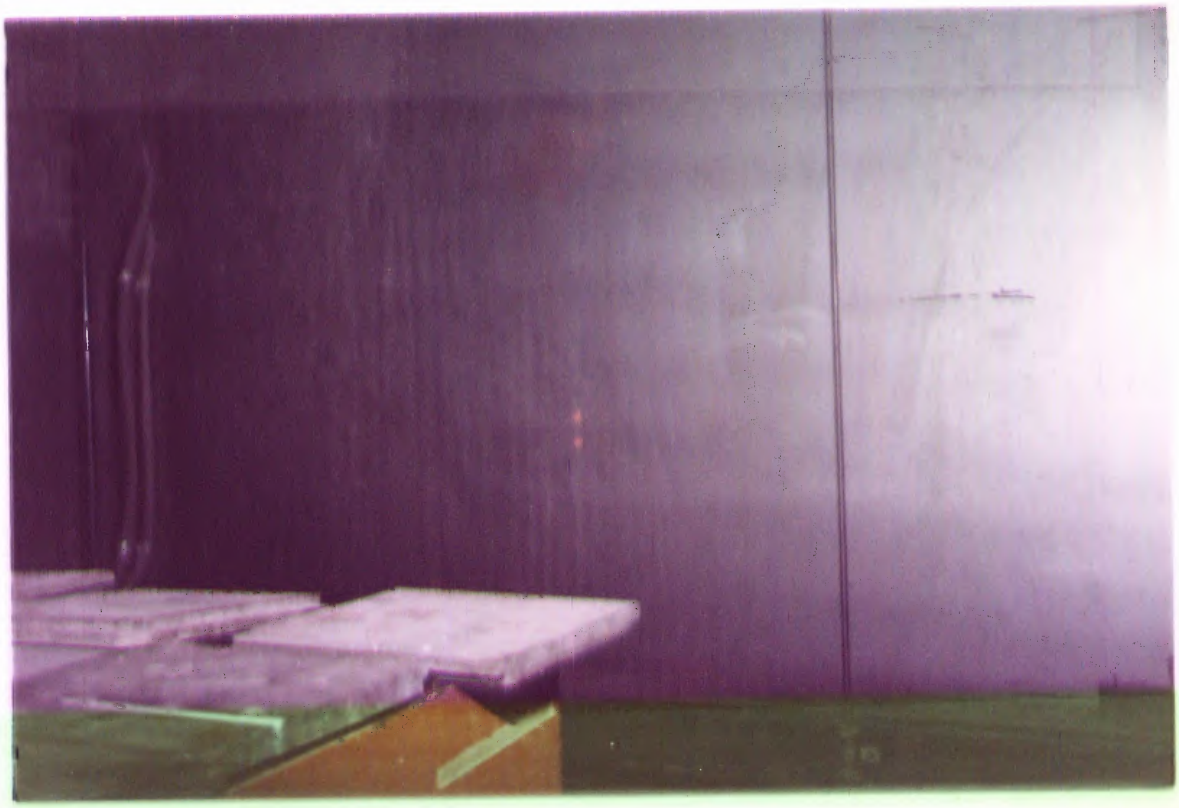

Fig.18: Picture of the Image of Laser Bems

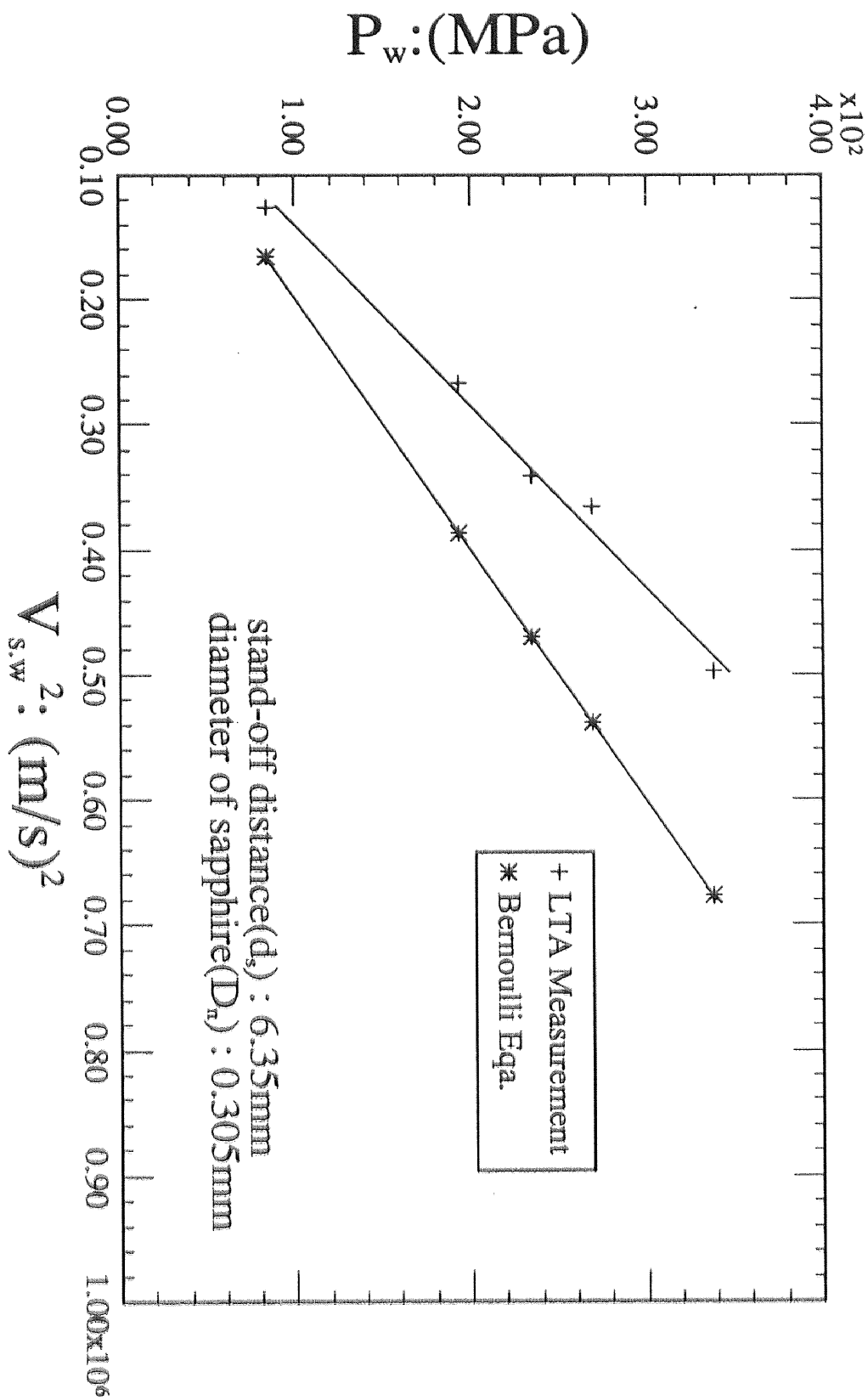

Fig.19: Comparison between LTA Measurement and Bernoulli Equation Computation(P_w v.s. $V_{s.w}^2$)

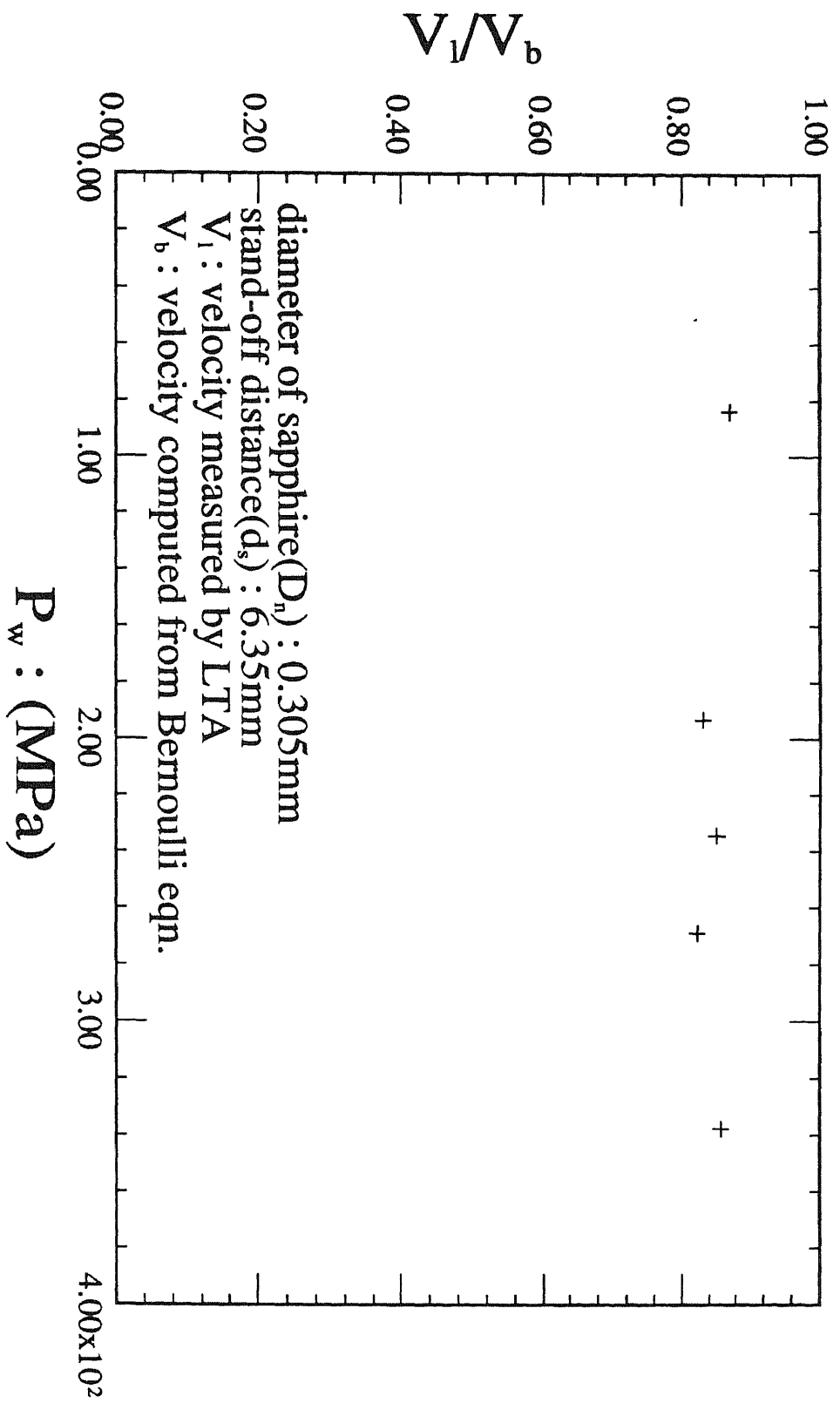

Fig.20: Comparison between LTA Measurement and Bernoulli Equation Computation(V_l/V_b v.s. P_w)

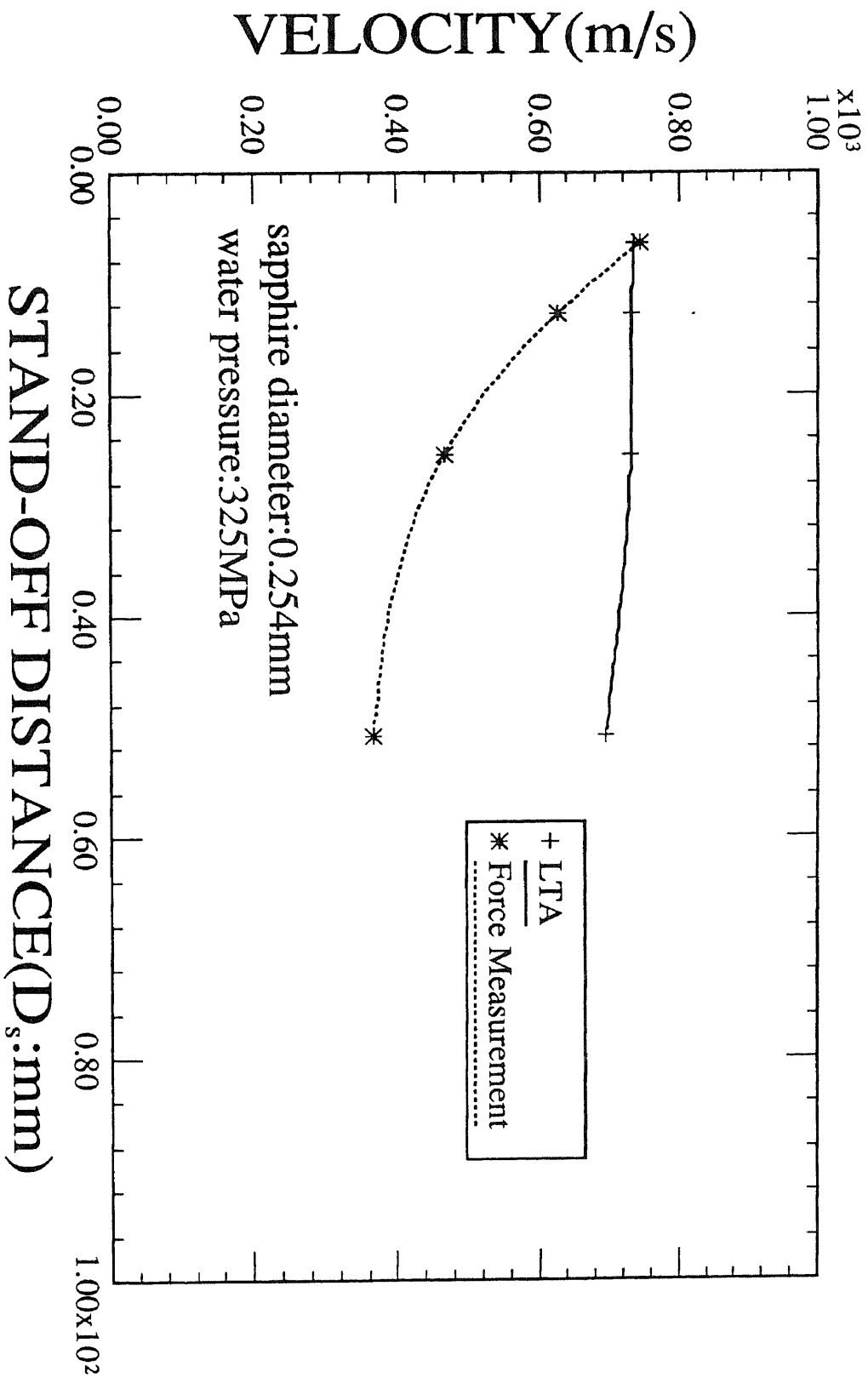

Fig.21: Comparison between Velocities Determined by LTA and Force Transducer Measurements

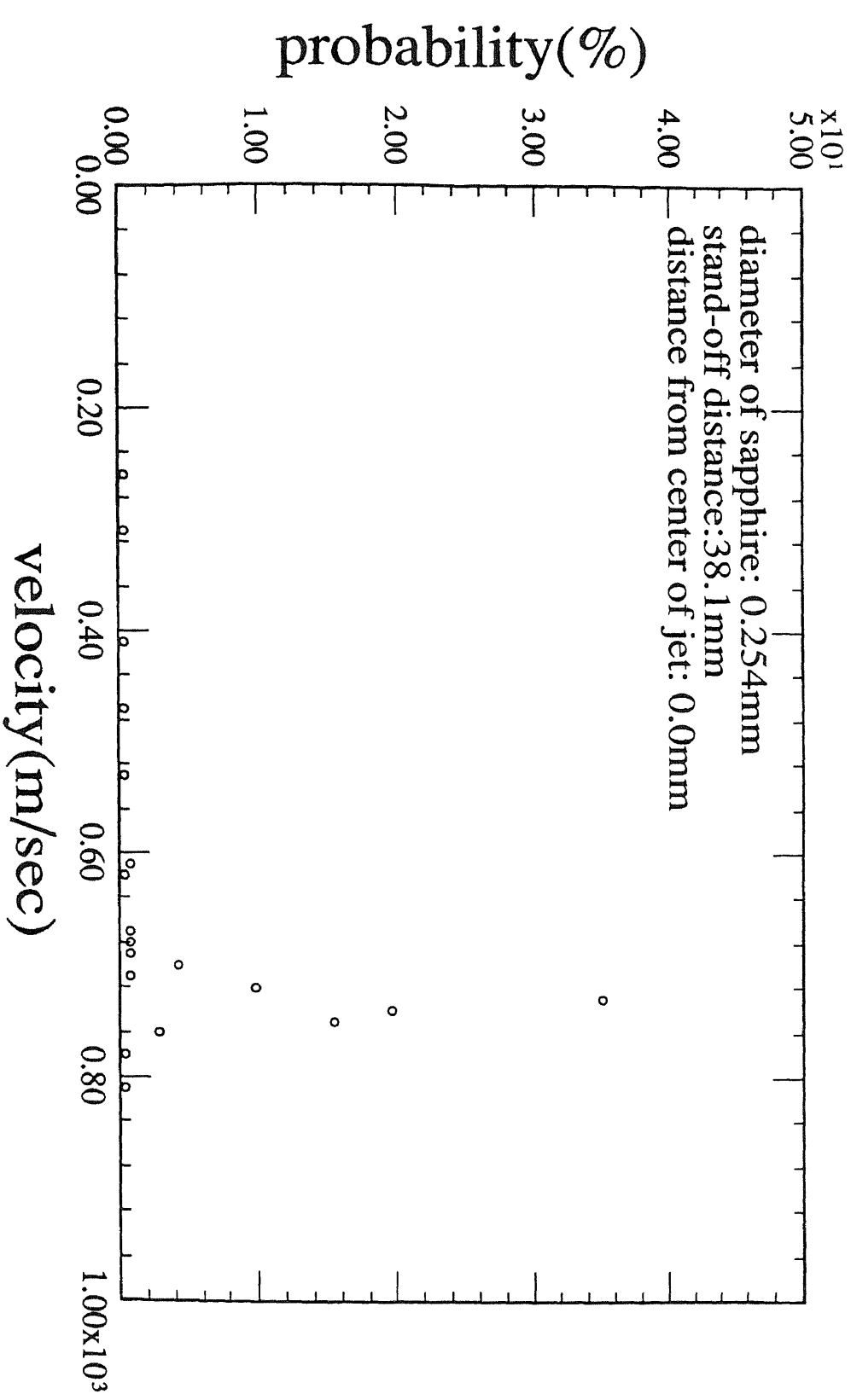

Fig.22: Probability Distribution of Velocities of Sapphire Waterjet at 0.00 Radial Distance

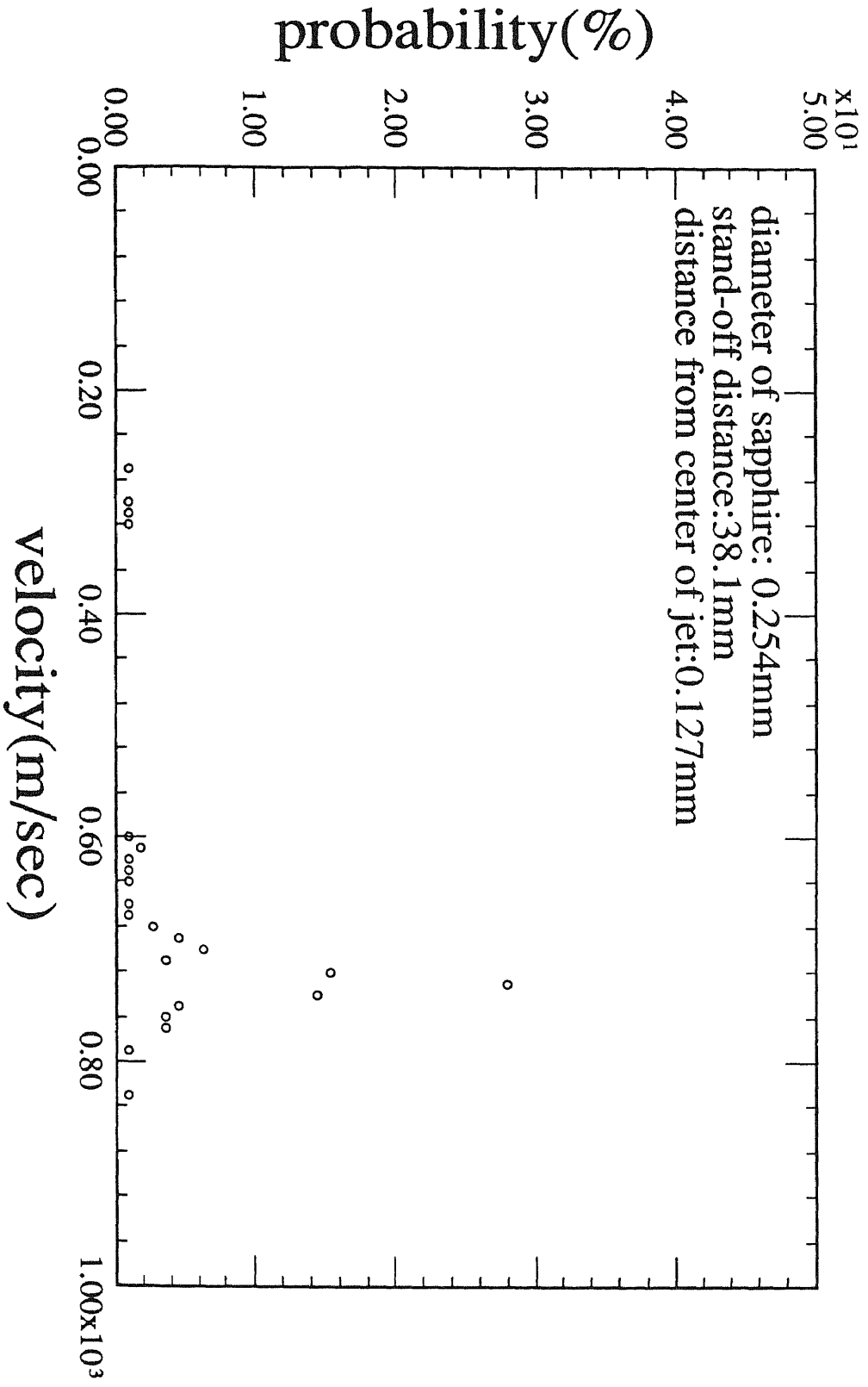

Fig.23: Probability Distribution of Velocities of Sapphire Waterjet at 0.127mm Radial Distance

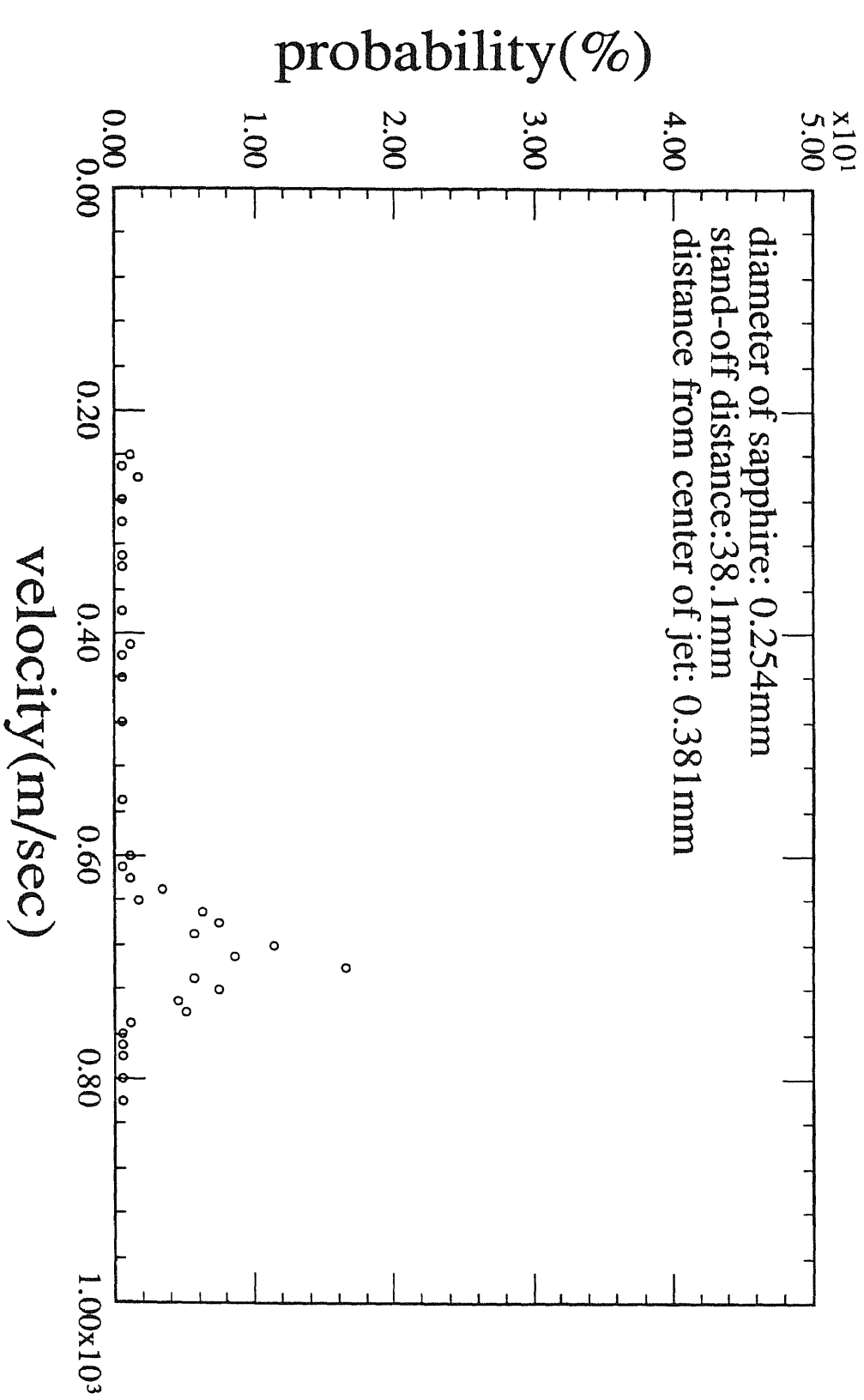

Fig.24: Probability Distribution of Velocities of Sapphire Waterjet at 0.381mm Radial Distance

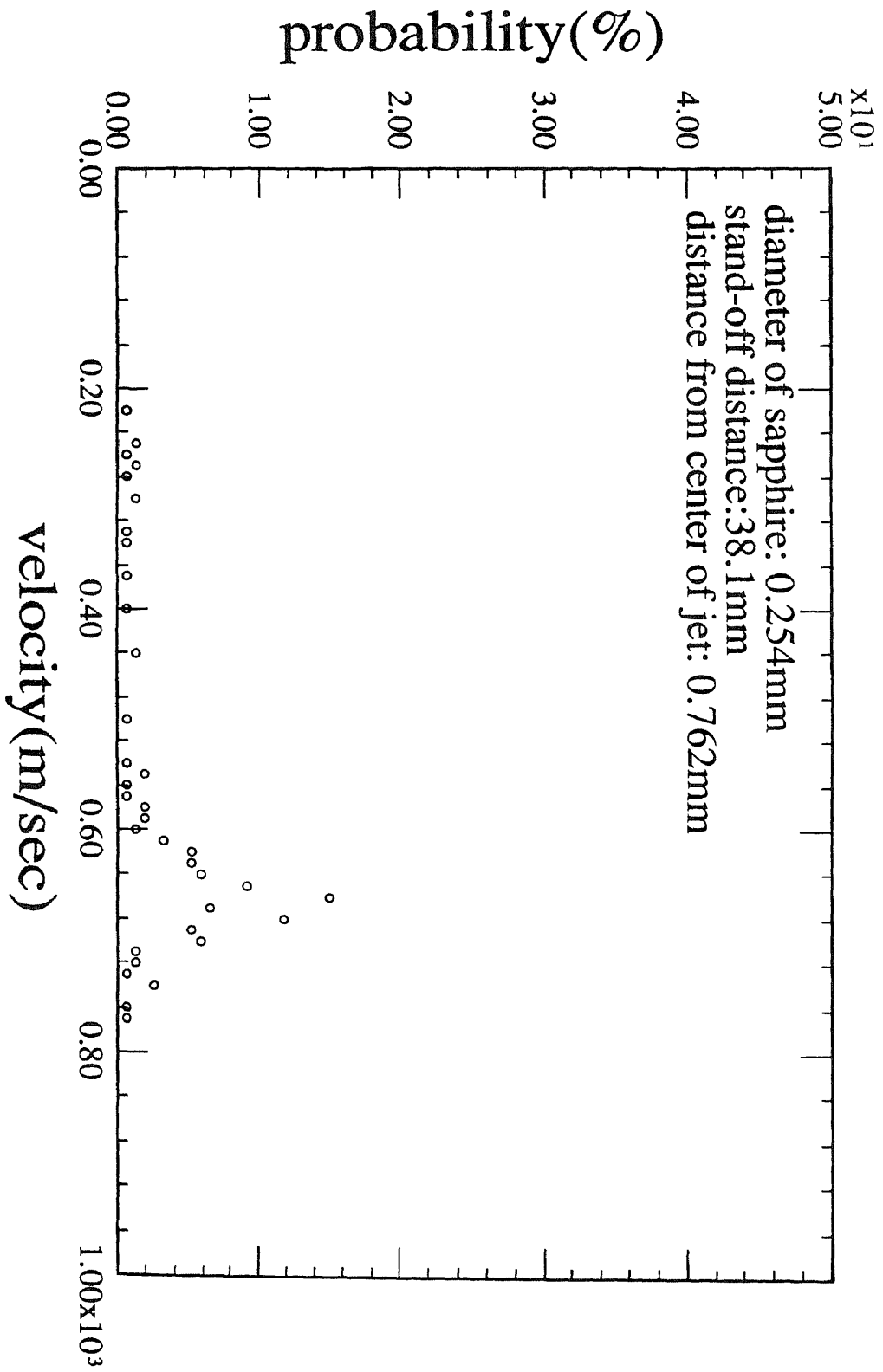

Fig.25: Probability Distribution of Velocities of Sapphire Waterjet at 0.762mm Radial Distance

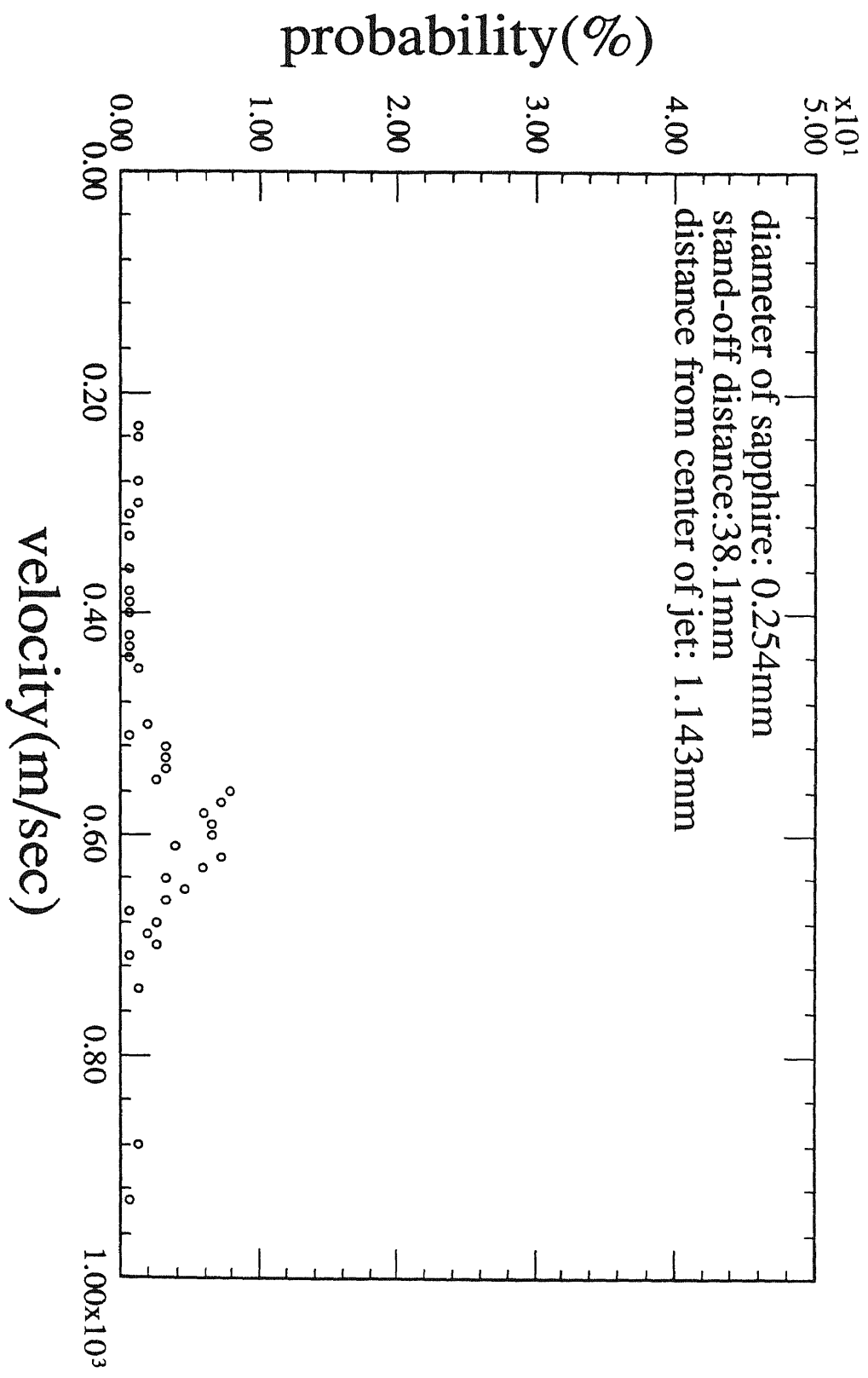

Fig.26: Probability Distribution of Velocities of Sapphire Waterjet at 1.143mm Radial Distance

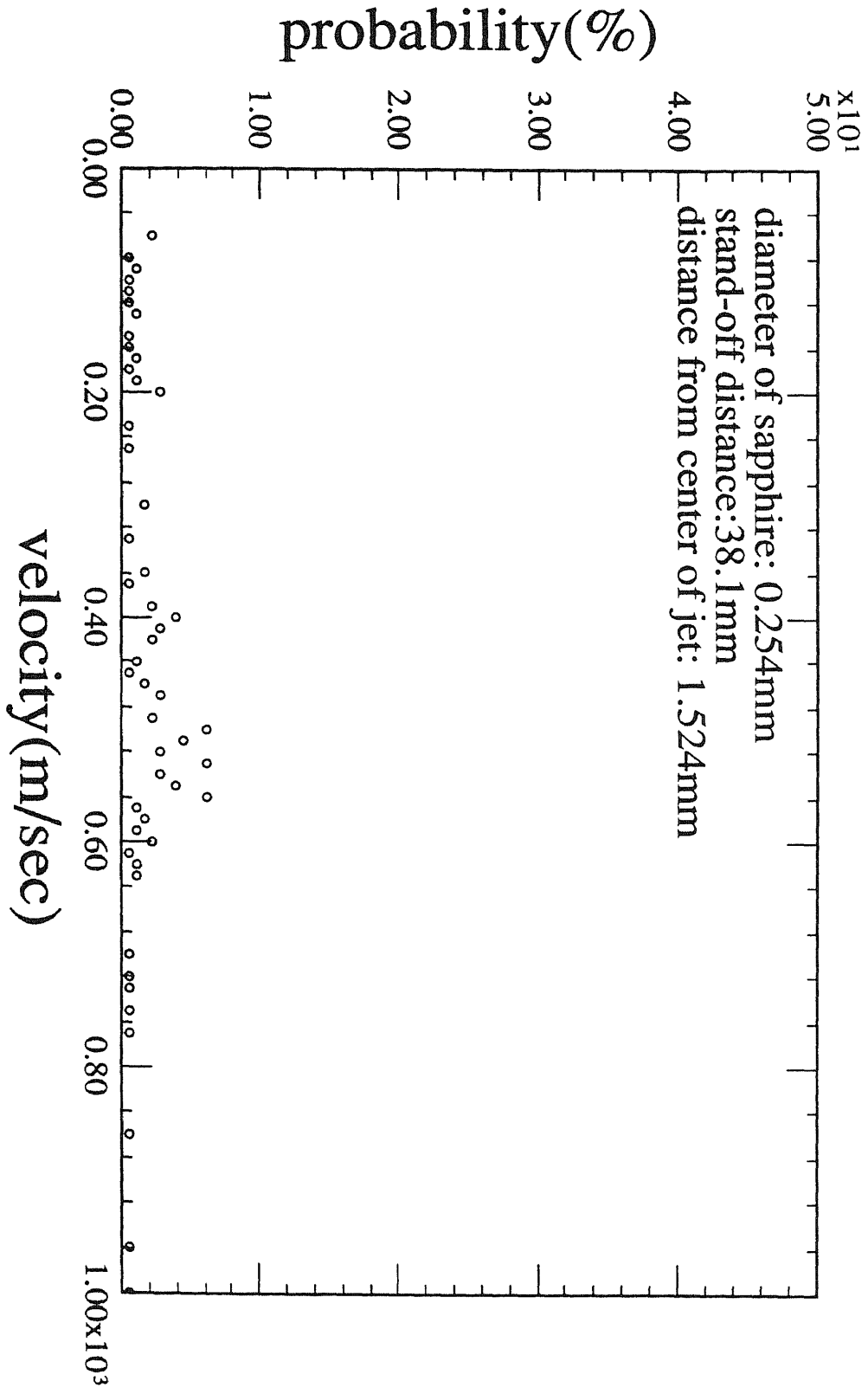

Fig.27: Probability Distribution of Velocities of Sapphire Waterjet at 1.524mm Radial Distance

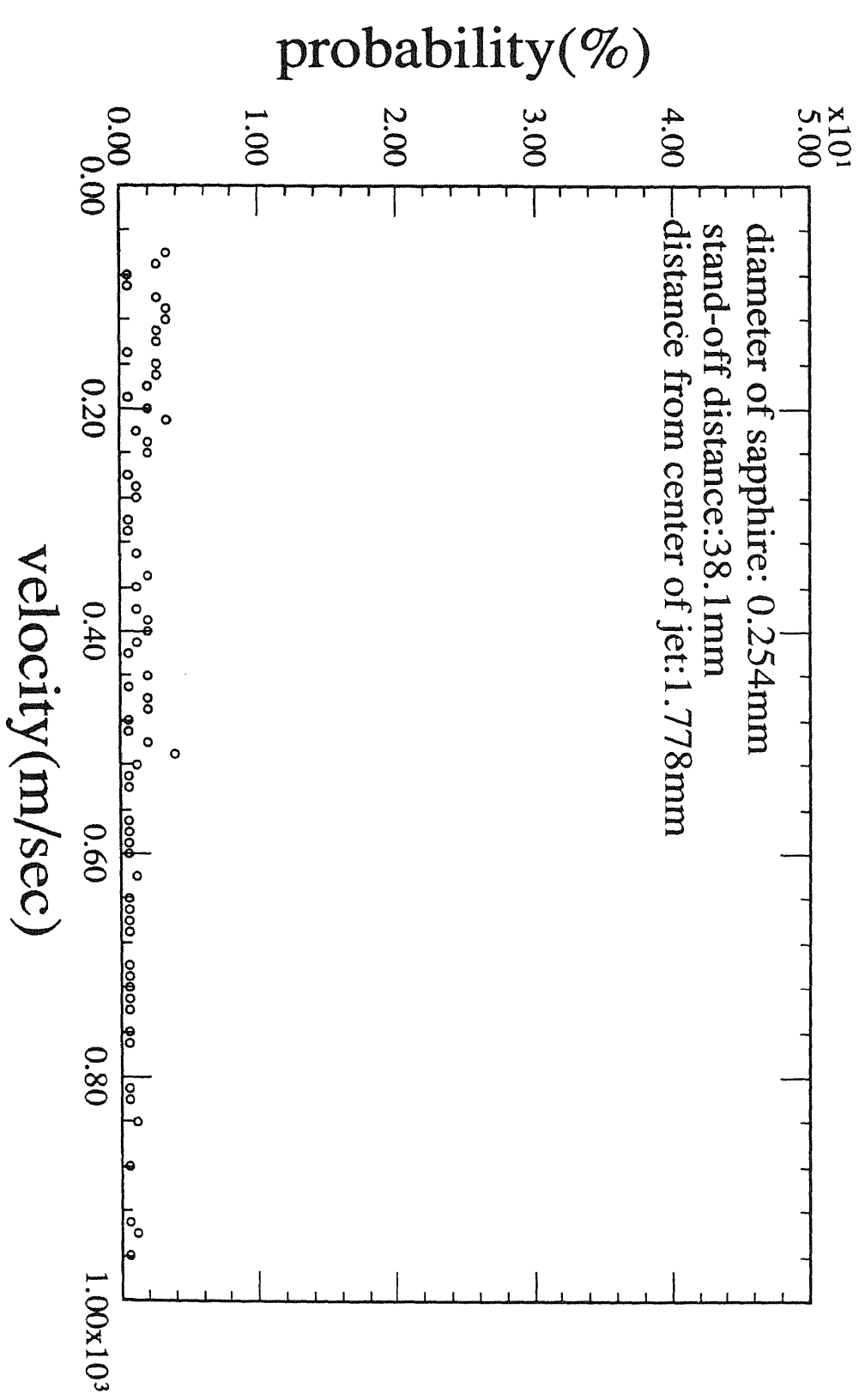

Fig.28: Probability Distribution of Velocities of Sapphire Waterjet at 1.778mm Radial Distance

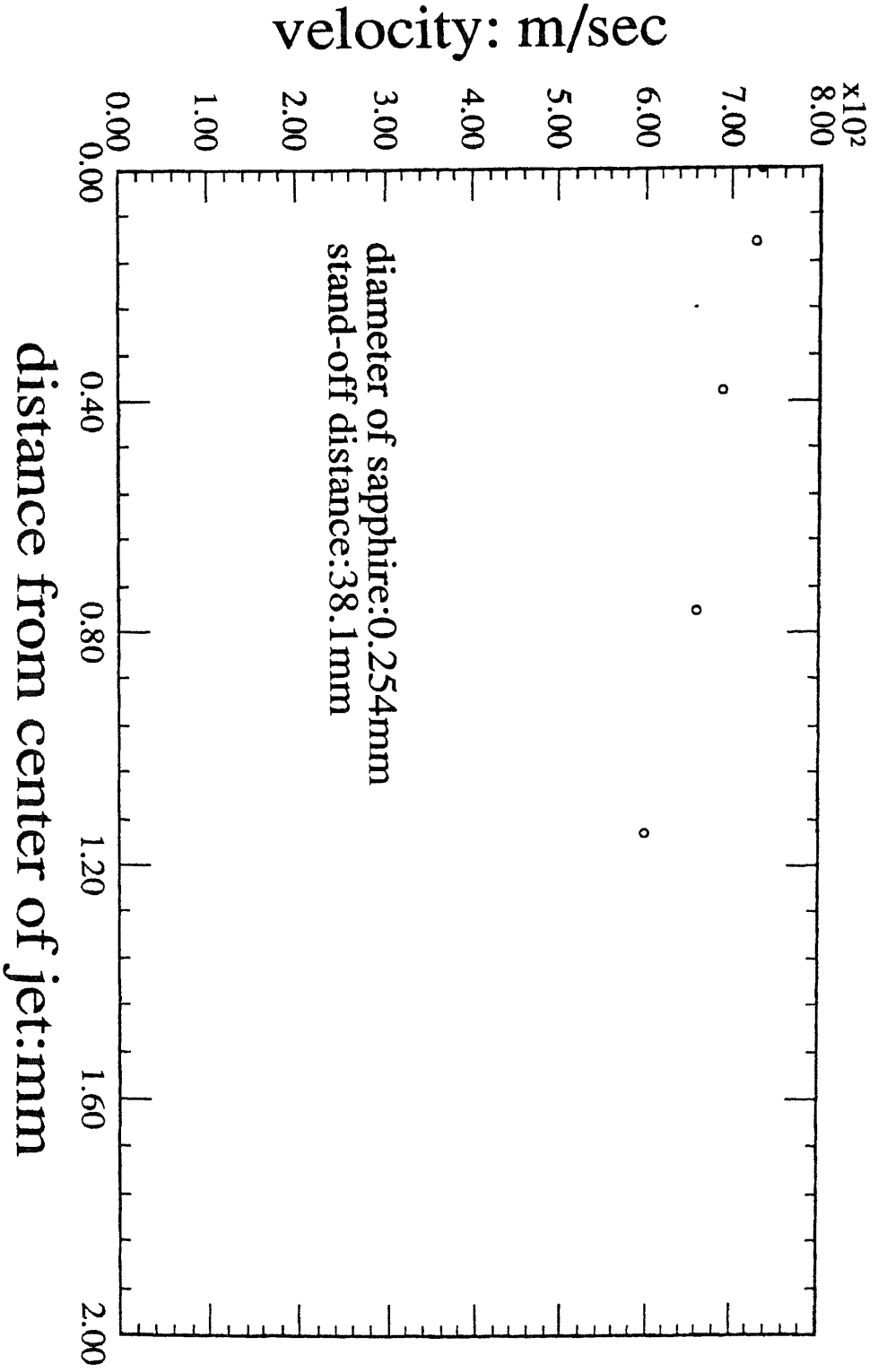

Fig.29: Estimated Velocities of Sapphire Waterjet at Different Radial Distances; d_n=0.254mm

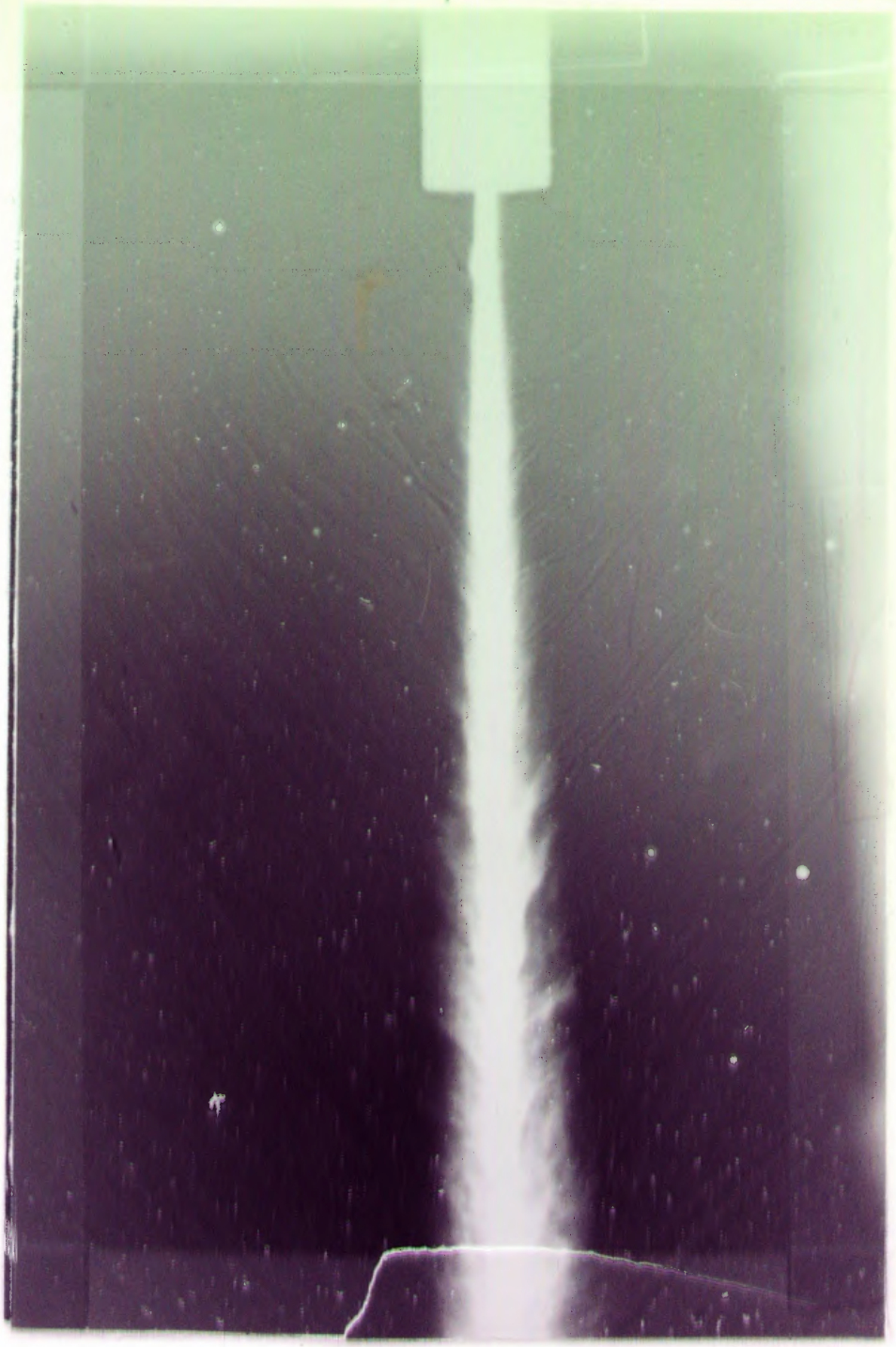

Fig.30: Schlieren Photograph of AWJ;
d_n=0.254mm, d_c=0.8636mm, m_a=68g/min

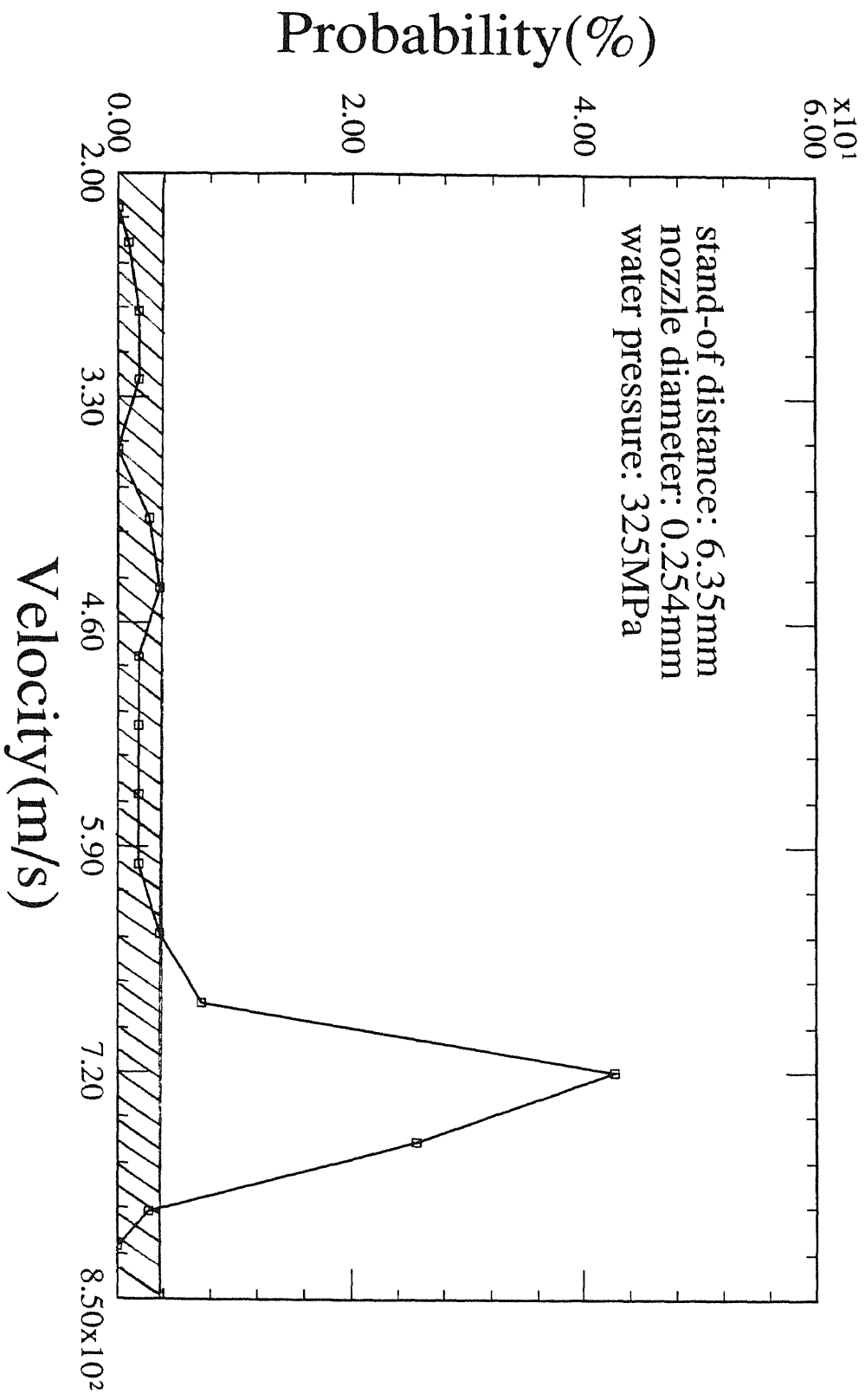

Fig.31: Probability Distribution of Velocities of Sapphire Waterjet at 6.35mm Stand-off Distance

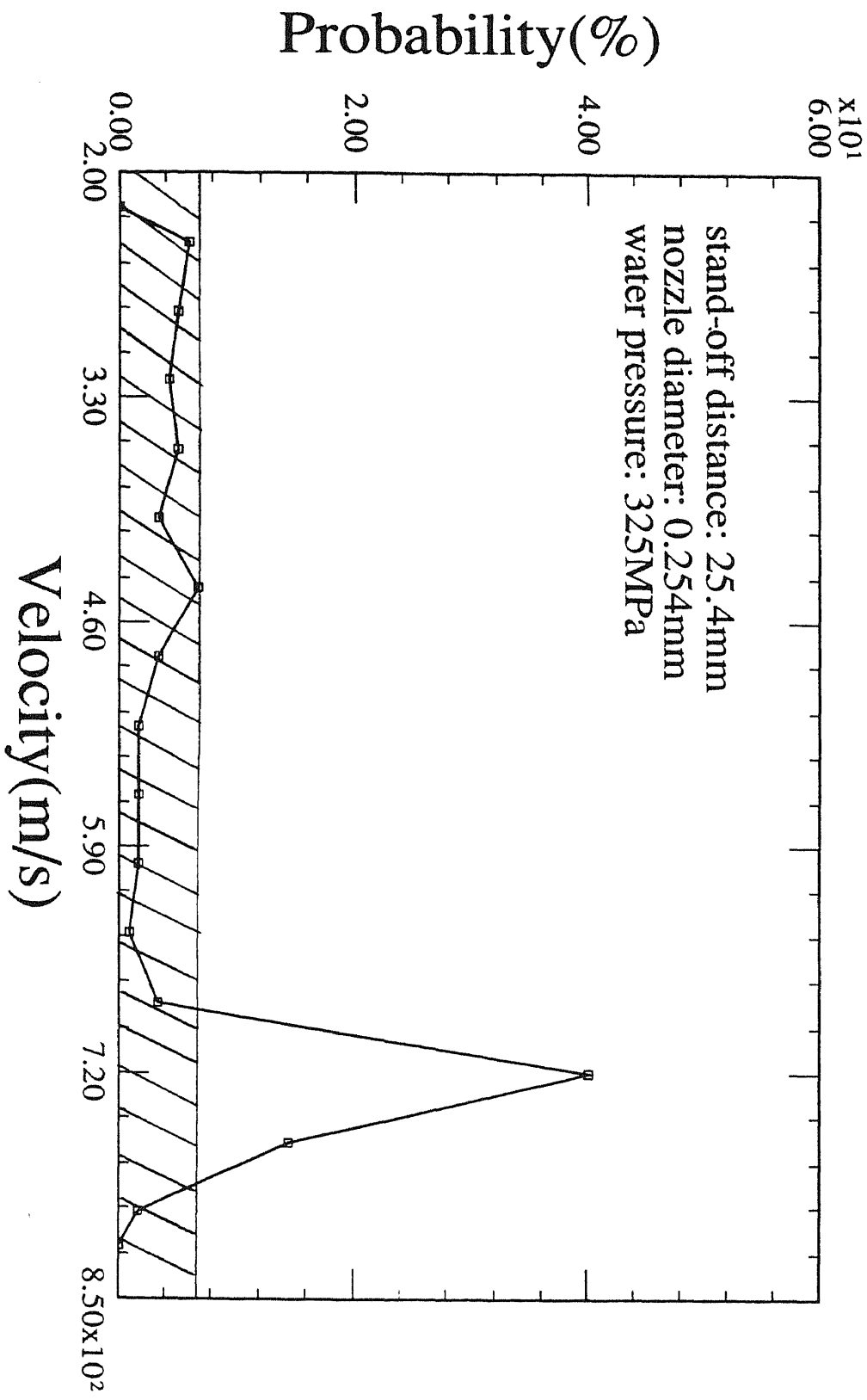

Fig.32: Probability Distribution of Velocities of Sapphire Waterjet at 25.4mm Stand-off Distance

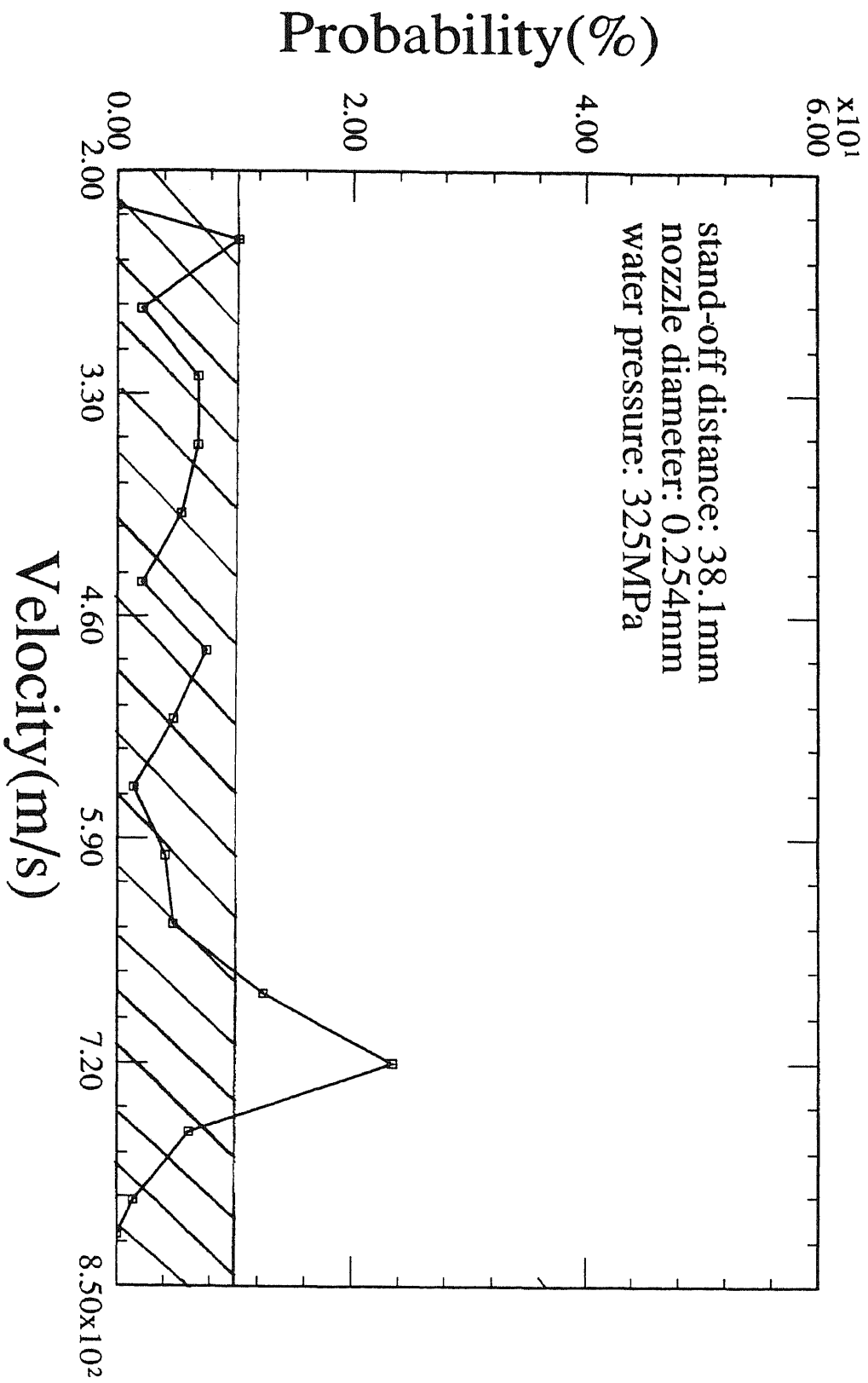

Fig.33: Probability Distribution of Velocities of Saphhire Waterjet at 38.1mm Stand-off Distance

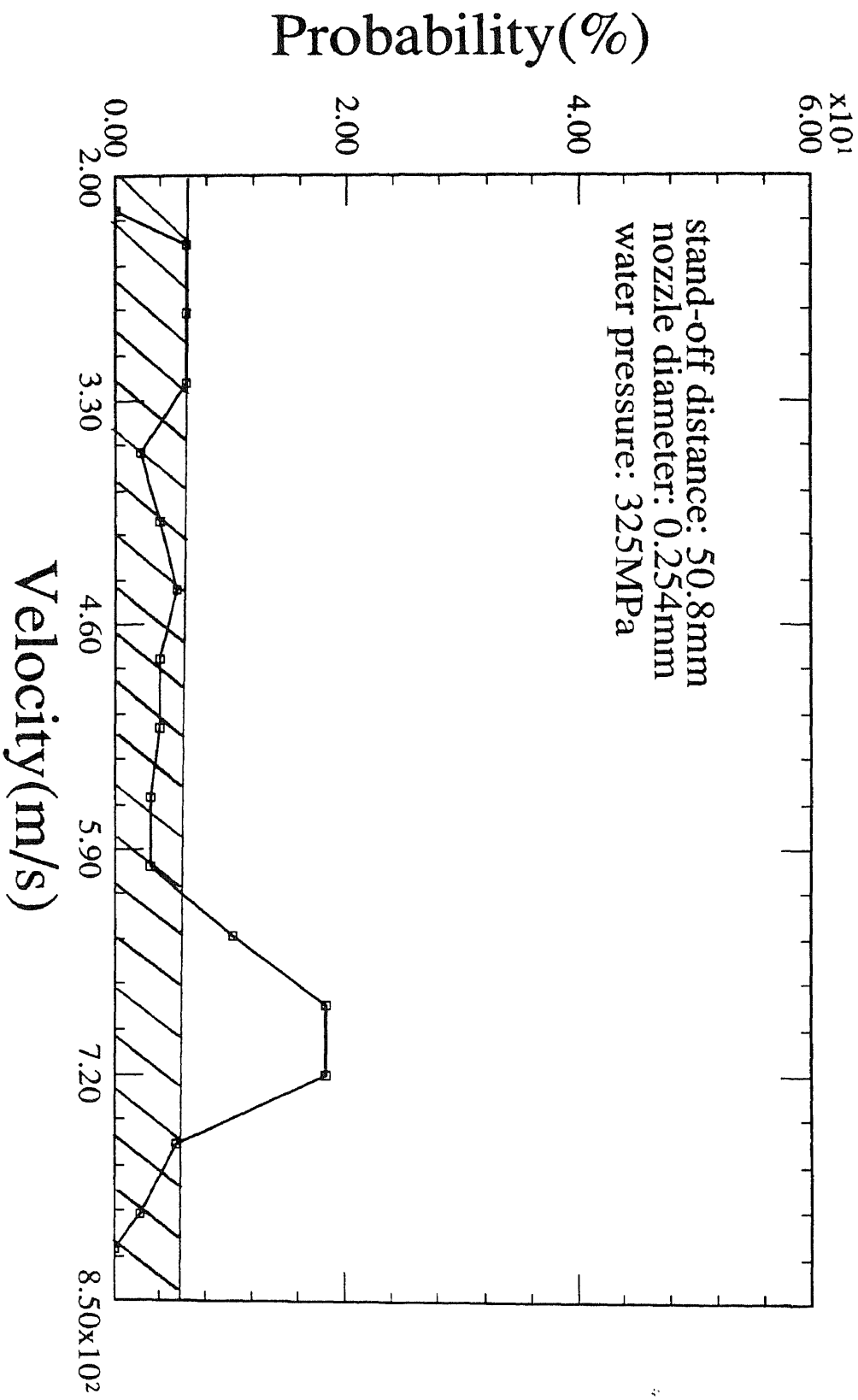

Fig.34: Probability Distribution of Velocities of Sapphire Waterjet at 50.8mm Stand-off Distance

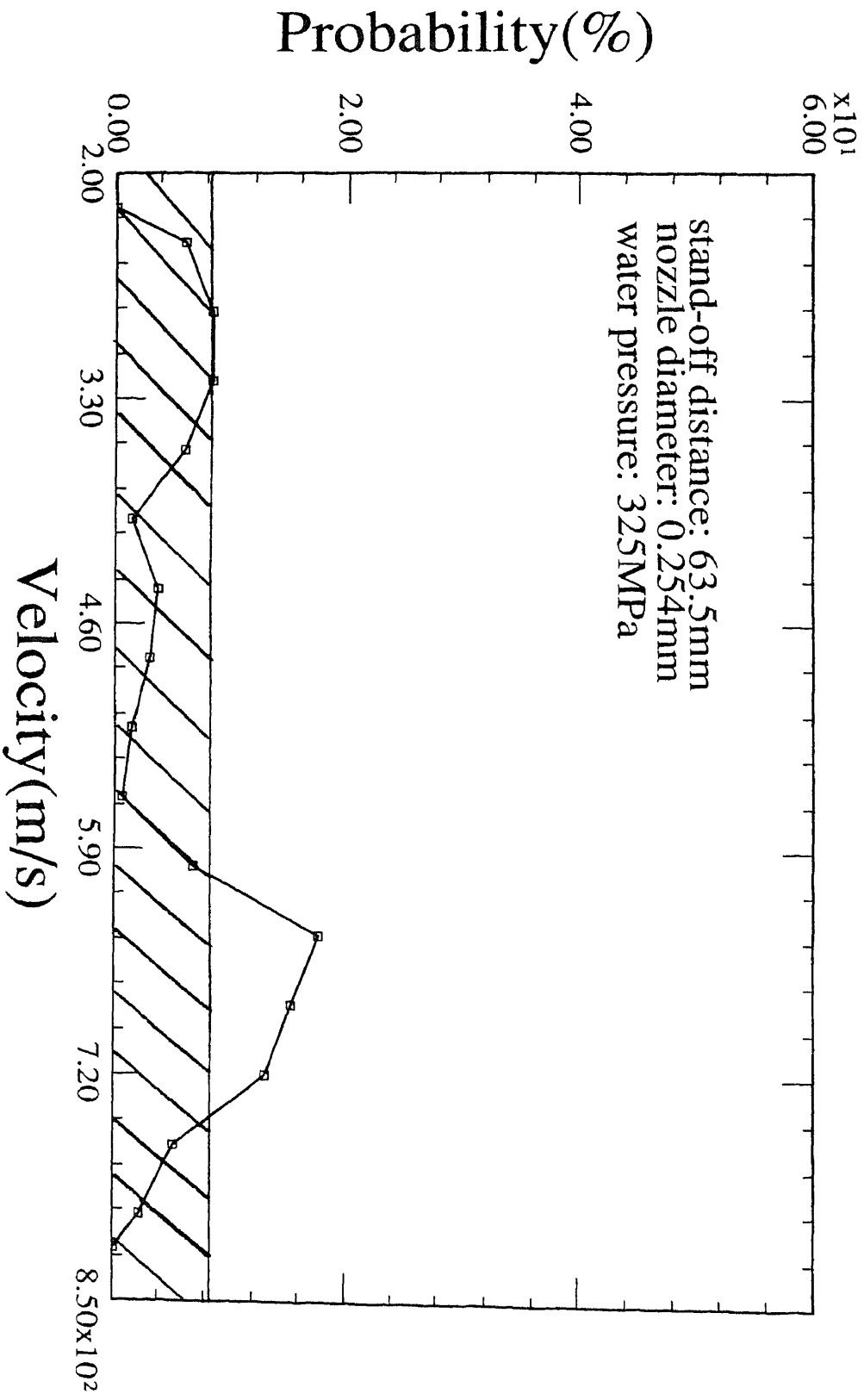

Fig.35: Probability Distribution of Velocities of Sapphire Waterjet at 63.5mm Stand-off Distance

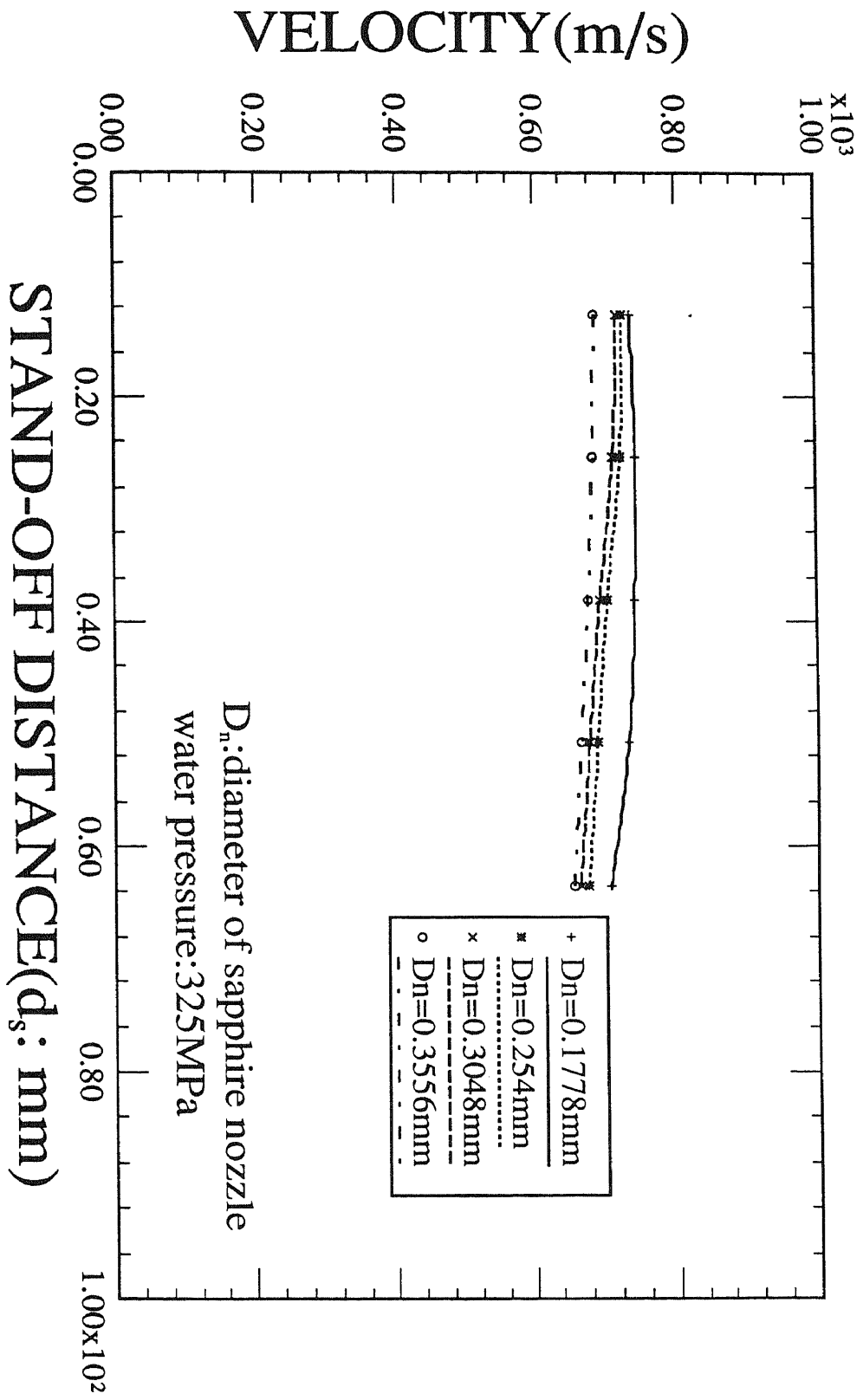

Fig.36: Estimated Velocities of Sapphire Waterjets at Different Stand-off Distances

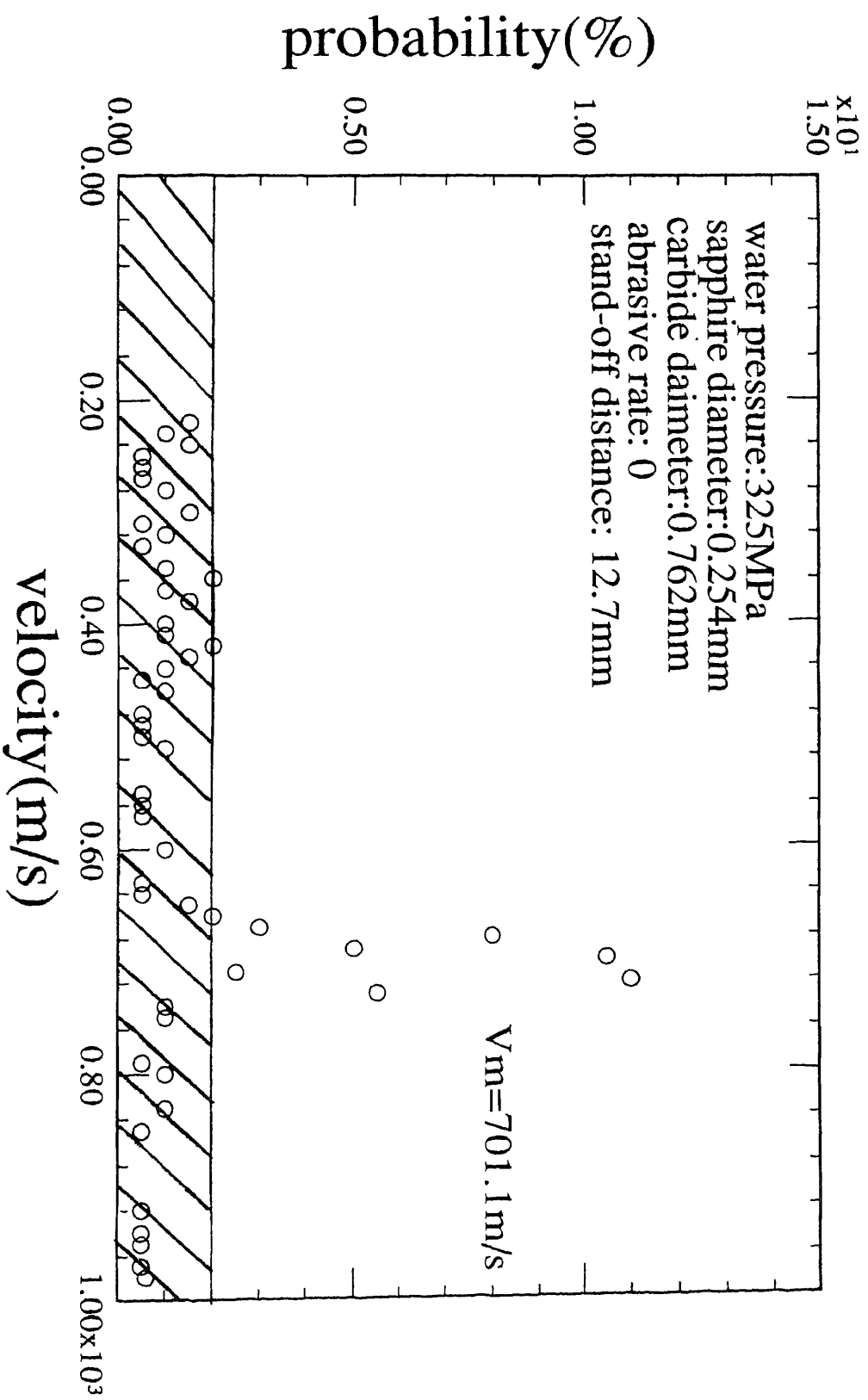

Fig.37: Probability Distribution of Velocities of Carbide Waterjet; d_n=0.254mm; d_C=0.762;d_S=12.7mm

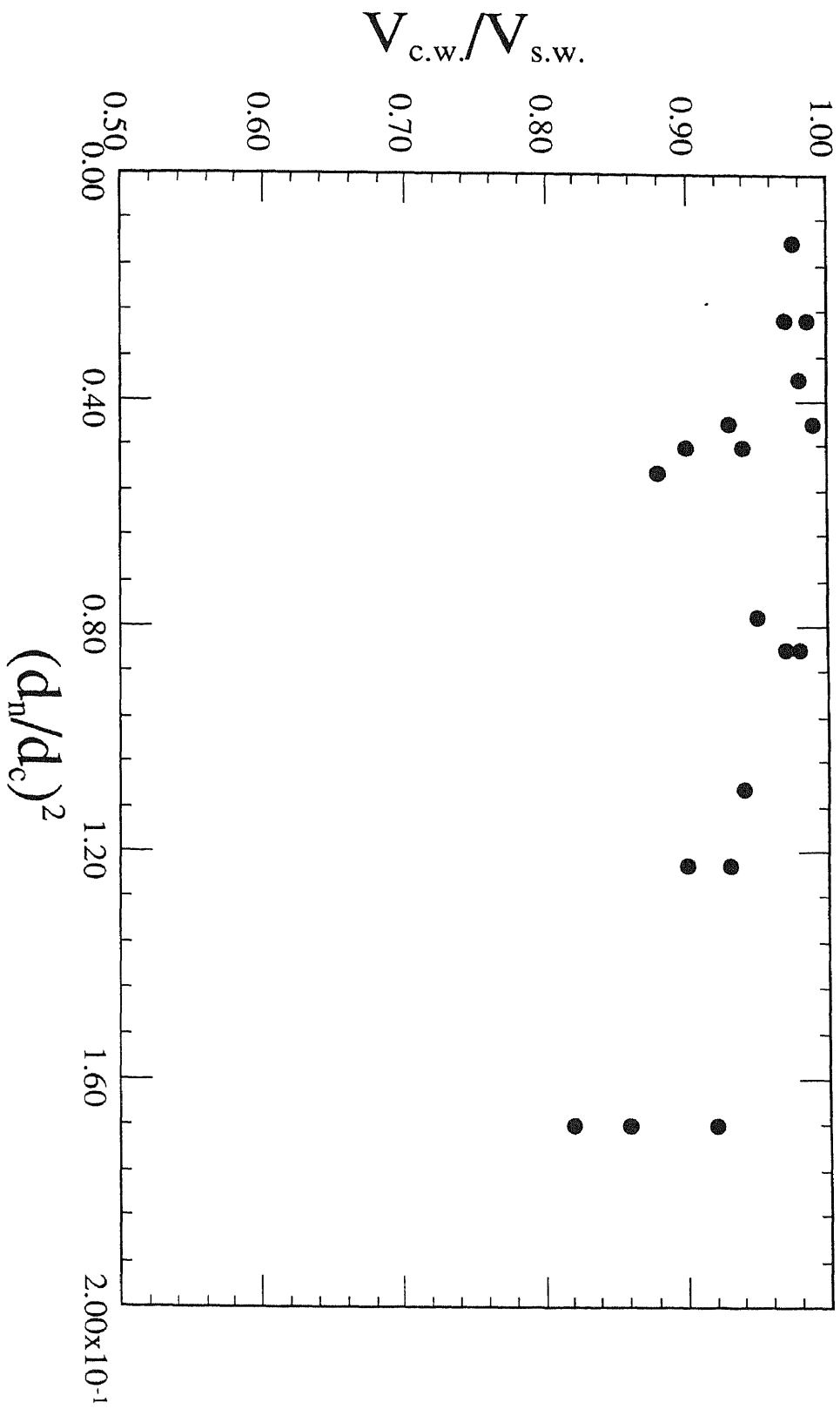

Fig.38: Velocity Ratio of Carbide and Sapphire Waterjets Versus the Diameter Ratio of Carbide and Sapphire Nozzles

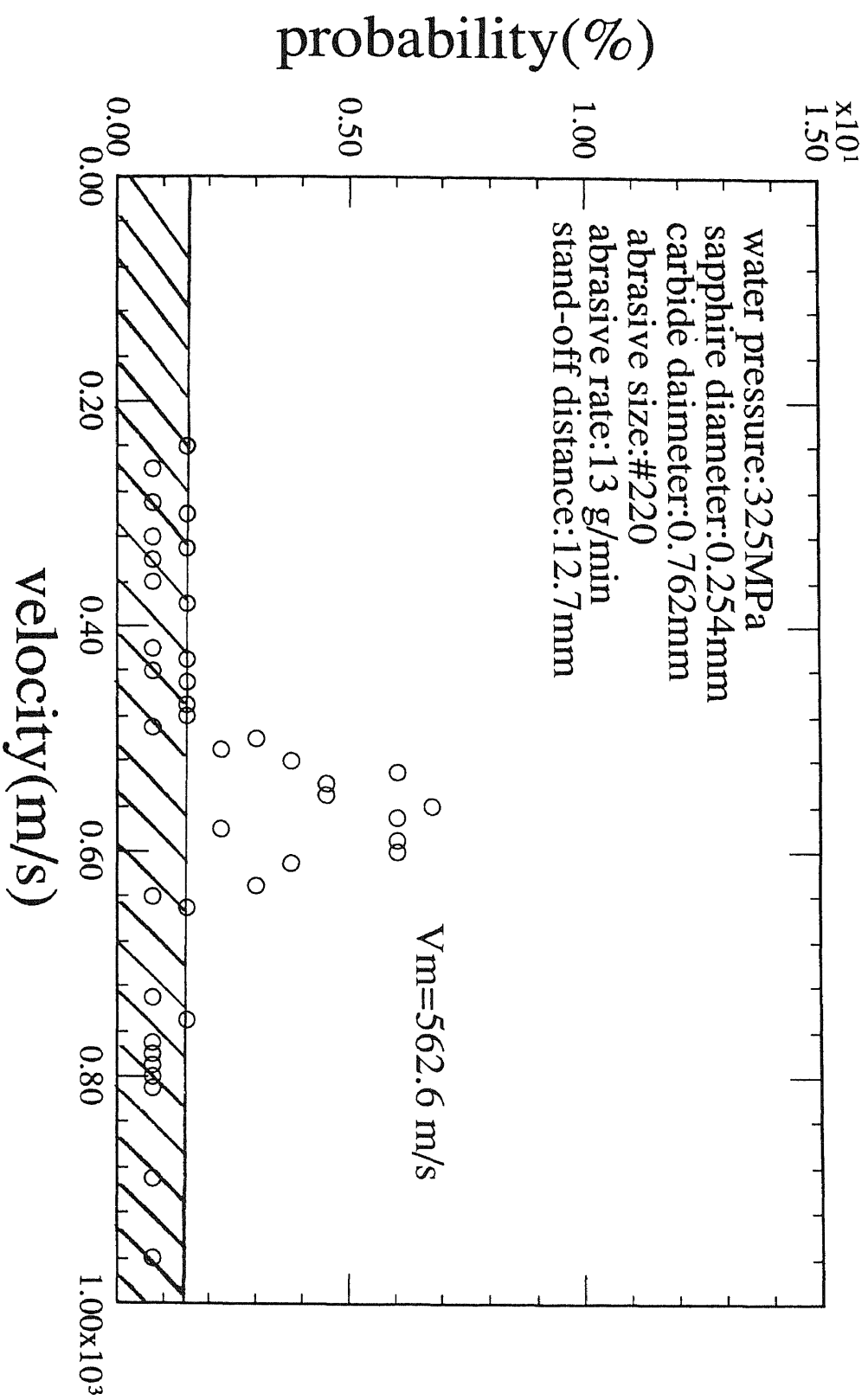

Fig.39: Probability Distribution of Velocities of Entrained Particles within an AWJ; m_a=13g/min; d_n=0.254mm; d_c=0.762;d_a=#220; d_s=12.7mm

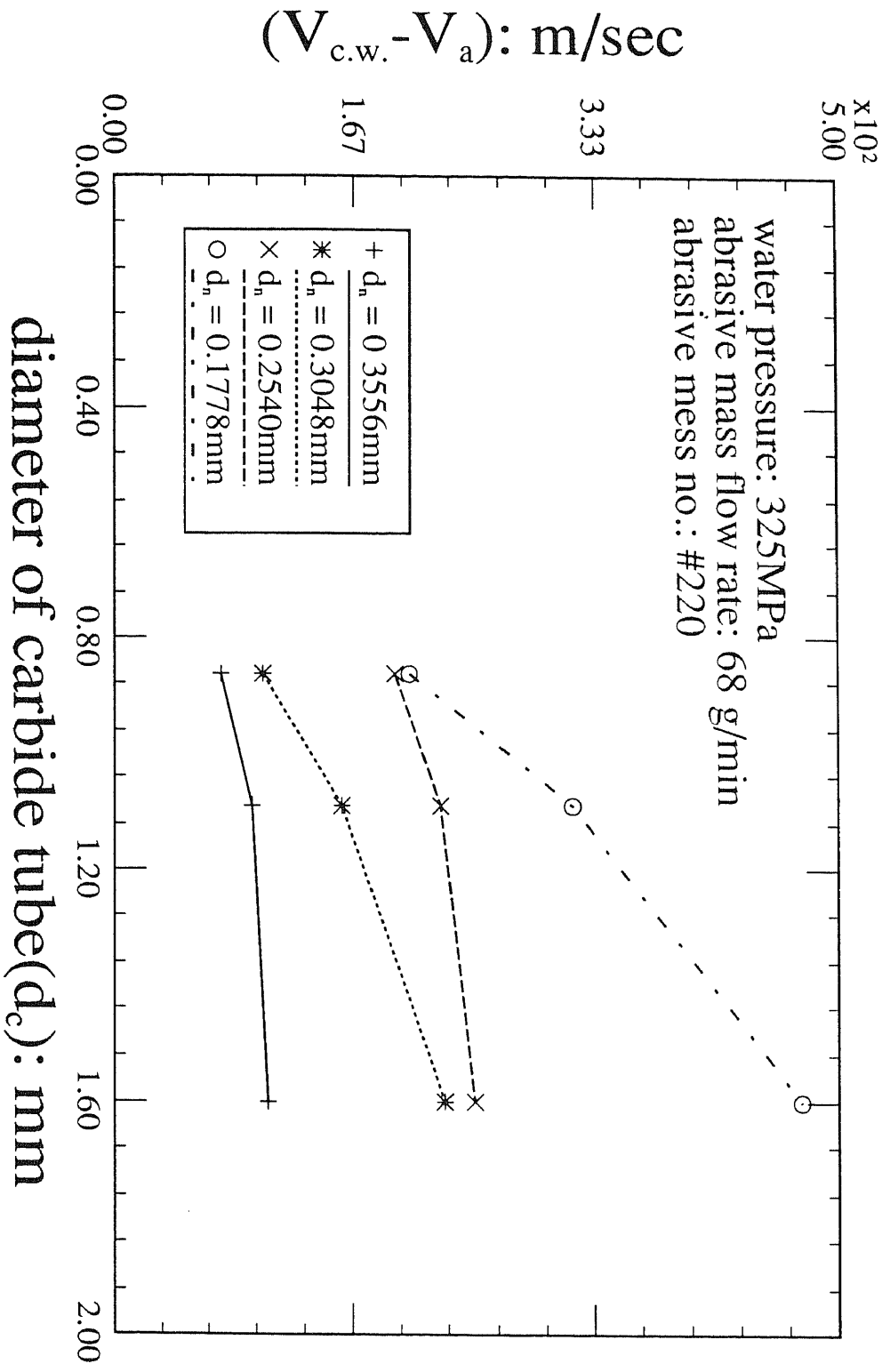

Fig.40: Effect of Carbide Tube Diameter on $(V_{c.w}-V_a)$

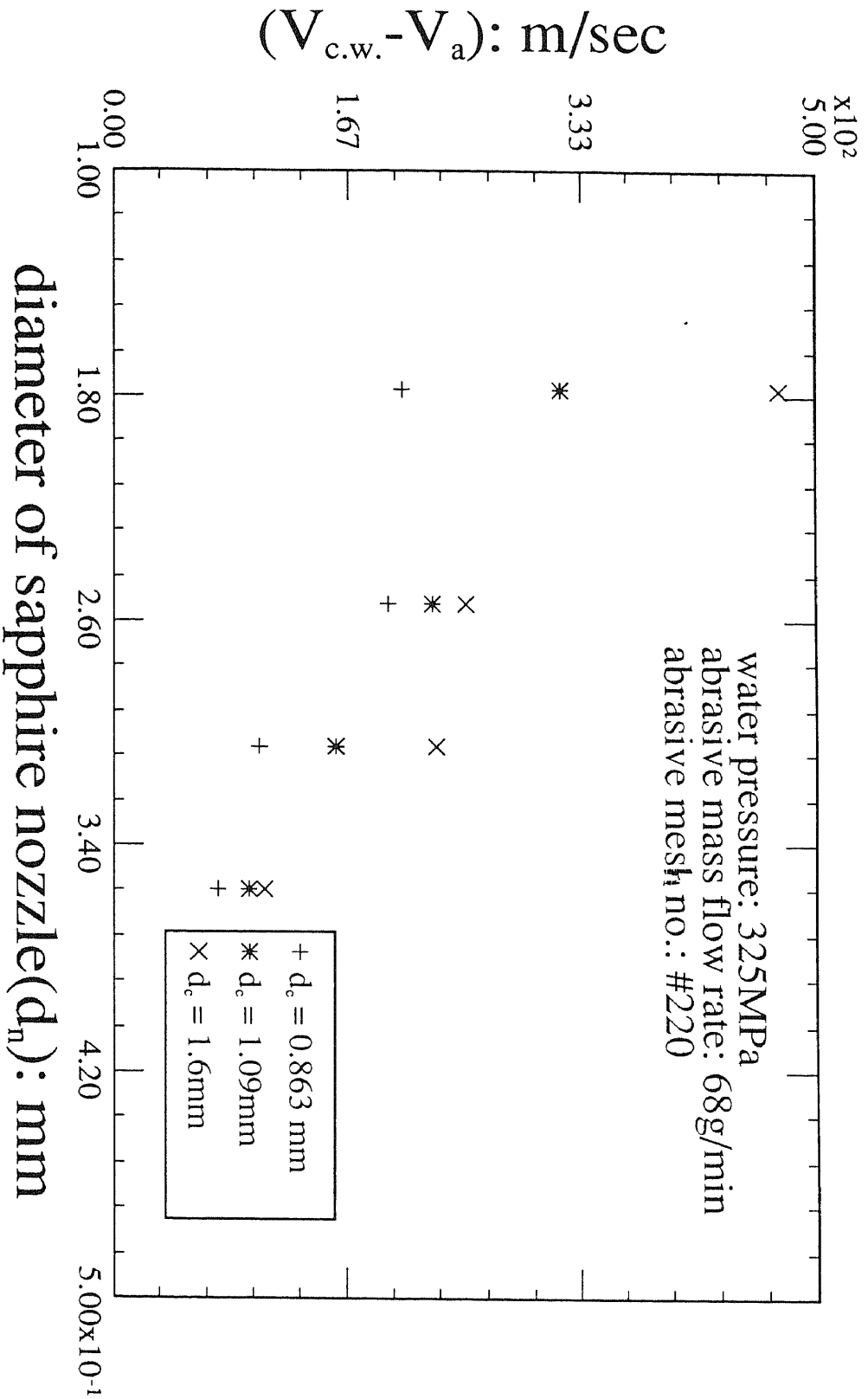

Fig.41: Effect of Sapphire Nozzle Diameter on $(V_{c.w}-V_a)$

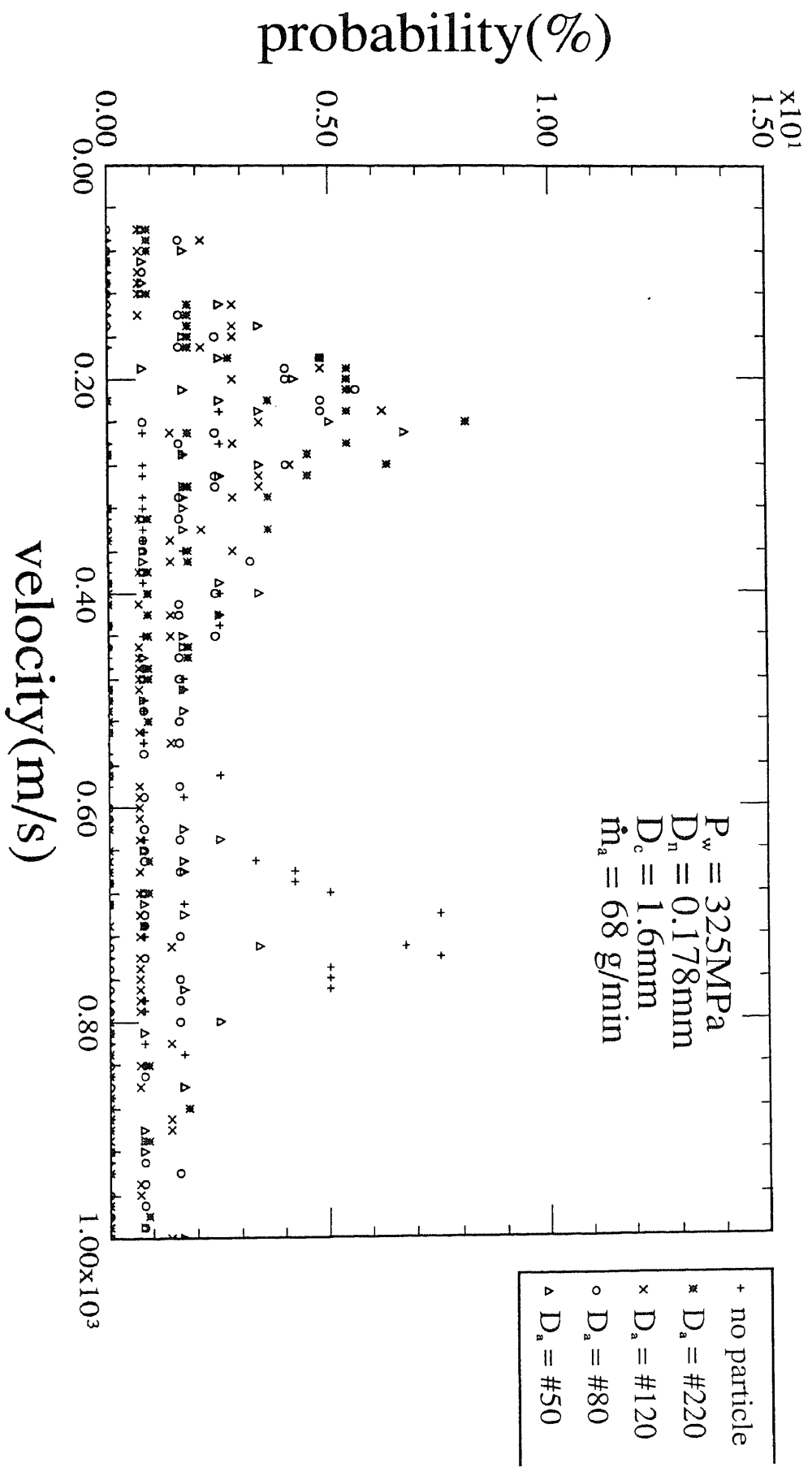

Fig.42: Probability Distribution of Velocities of Different Size Particles Entrained in an AWJ

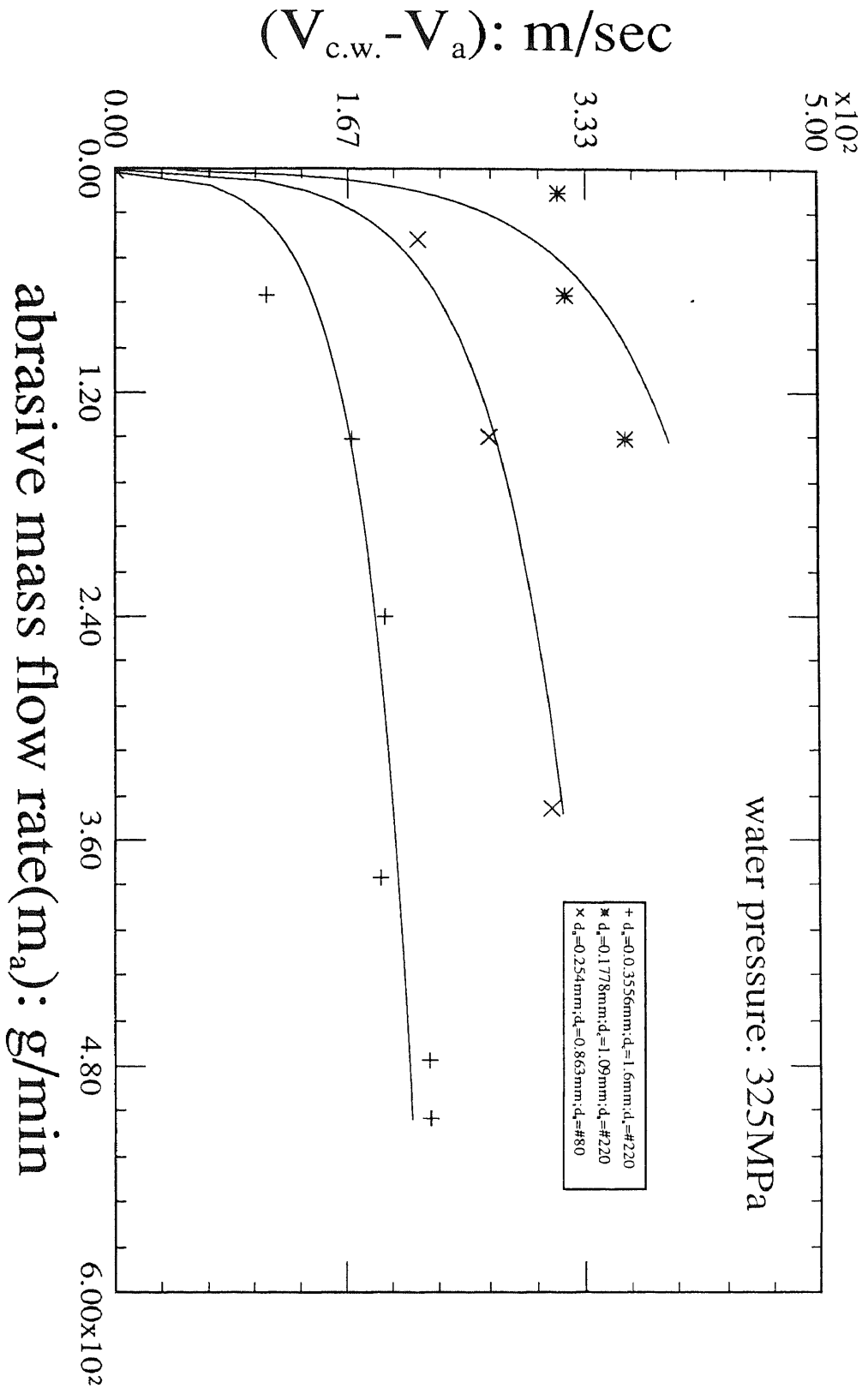

Fig.43: Effect of Abrasive Mass Flow Rates on $(V_{C.W.}-V_a)$

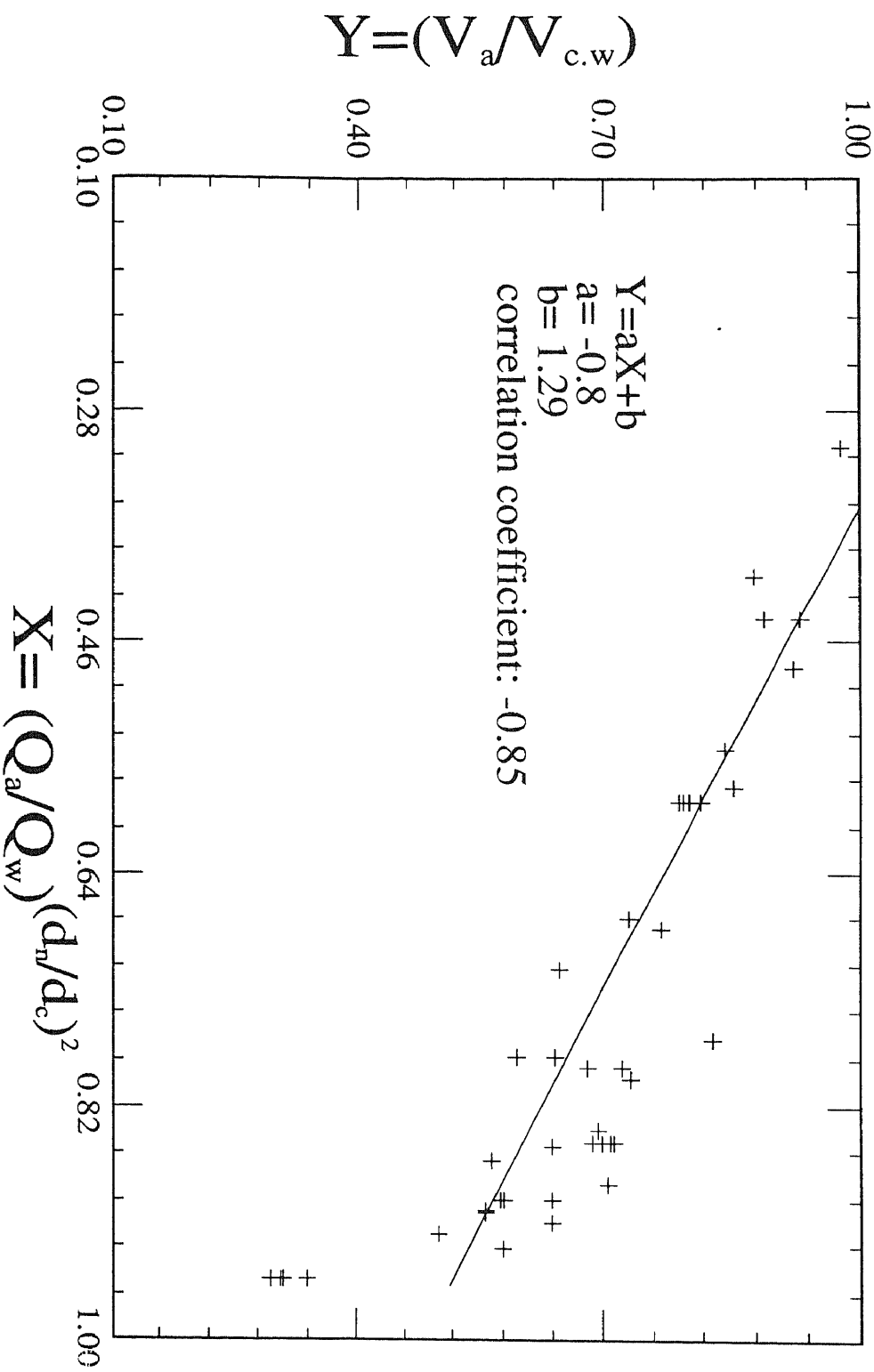

Fig.44: Correlation between $(V_a/V_{c.w.})$ and $(Q_a/Q_w)(dn/dc)^2$

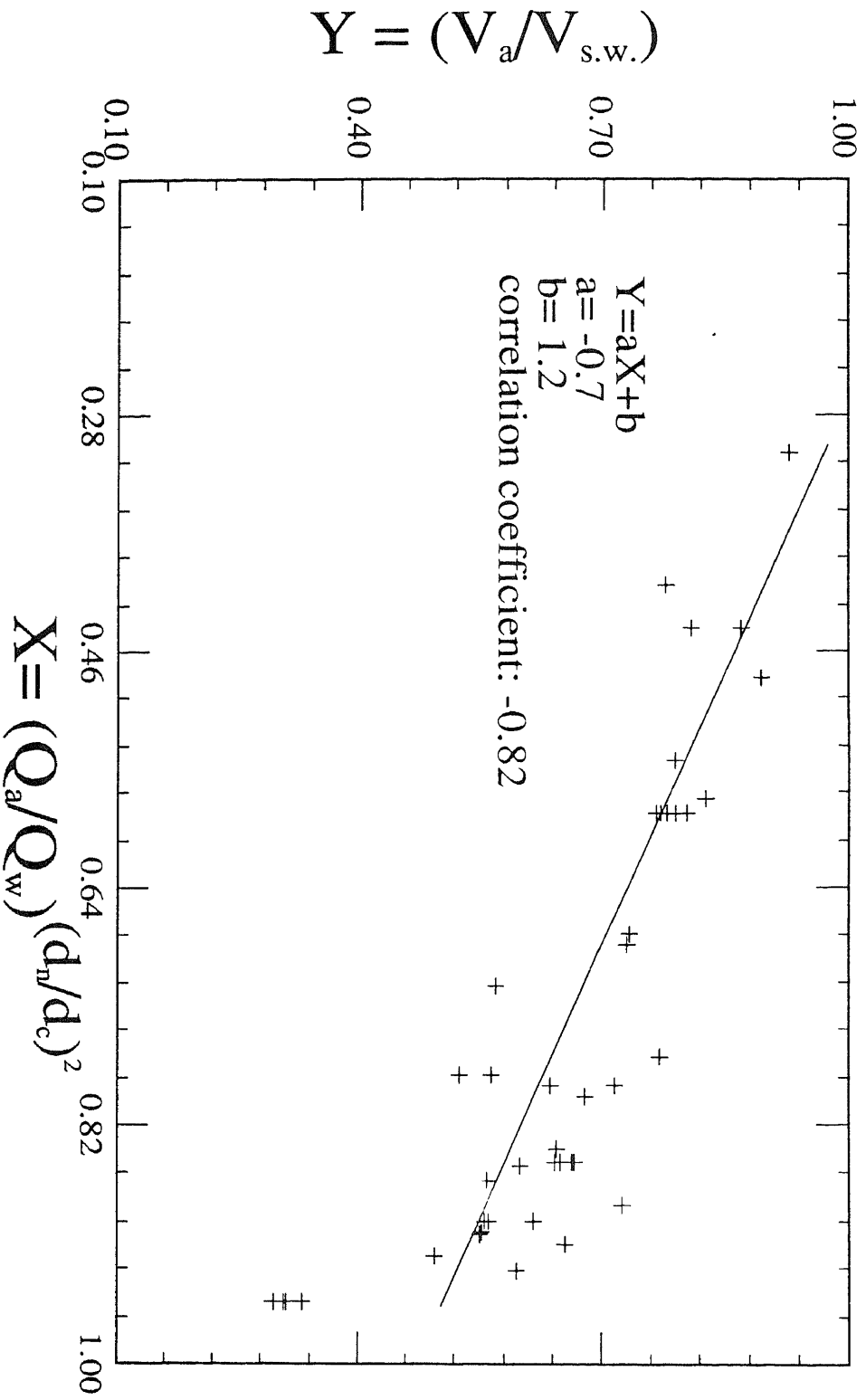

Fig.45: Correlation between $(V_a/V_{s.w.})$ and $(Q_a/Q_w)^{(dn/dc)^2}$

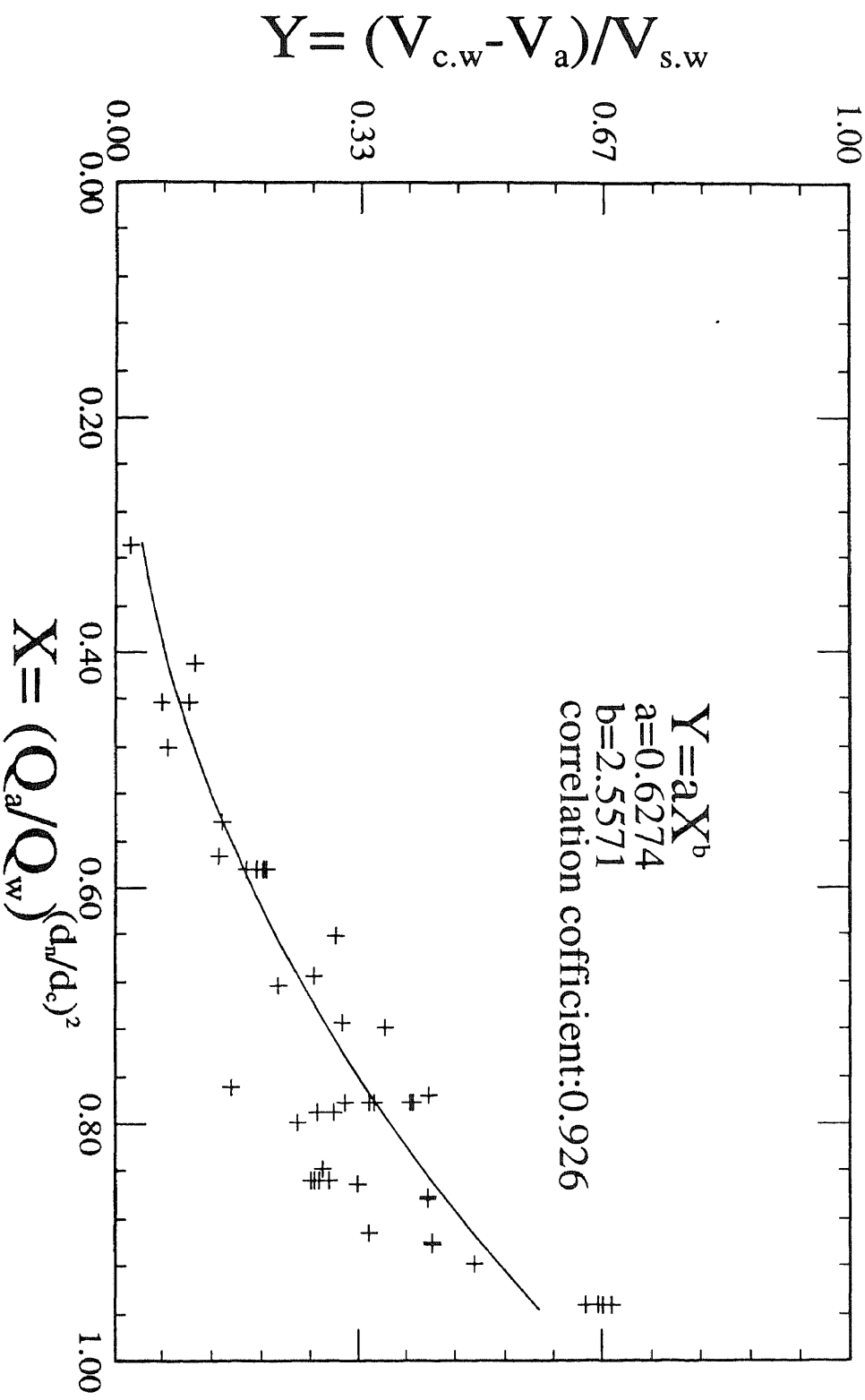

Fig.46: Correlation between $(V_{c.w.}-V_a)/V_{s.w.}$ and $(Q_a/Q_w)^{(dn/dc)}$

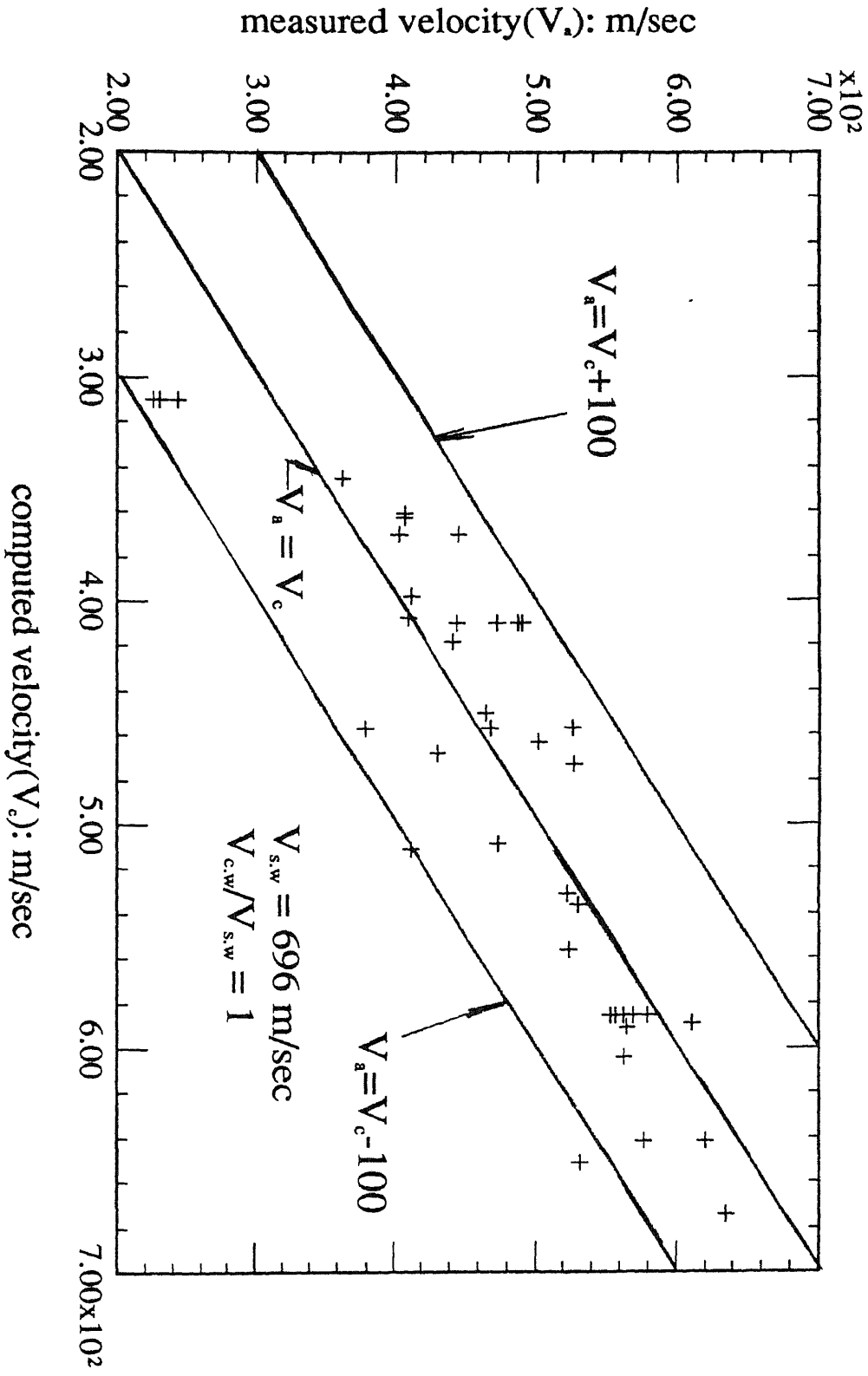

Fig.47: Comparison between Computed and Measured Particle Velocity

Dc \ Dn	0.3556 (mm)	0.3048 (mm)	0.254 (mm)	0.1778 (mm)
	Ma(g/min)			
0.863 (mm)	13, 68	13, 68	13, 68 ,38* 144*, 343*	13, 68
1.09 (mm)	13, 68	68	13, 68, 68*	13, 68, 145
1.6 (mm)	68, 145 380, 477 240, 508	68	68, 68*, 68+	68, 68* 68+, 68x

Footnotes:

No Symbol: #220
* : #80
\+ : #120
x : #50

Table 1: Experimental Matrix

dn \ ds	12.7	25.4	38.1	50.8	63.5
0.1778	735.2	741.4	738.8	728.3	713.2
0.254	717.4	716.4	694.1	677.2	671.7
0.3048	717.9	711.6	693.1	677.8	664.8
0.3556	704.4	697.6	686.8	664.6	664.1

Footnotes: Unit: m/sec
1. dn(mm): diameter of sapphire nozzle
2. ds(mm): stand-off distance

Table 2 : Mean Velocities of Sapphire Waterjets

dc \ dn	0.3556	0.3048	0.254	0.1778
0.863	605.8 576.2 648.7	649.3 666.4	701.1 697.7	727.8 687.3
1.09	661.5	680.7	634.2	725
1.6	662.9	634.6	696.1	717.9

Unit: m/sec

Footnotes:
1.dn(mm): diameter of sapphire nozzle
2.dc(mm): diameter of carbide tube

Table 3 : Estimated Velocities of Carbide Waterjets

dc \ dn	0.3556	0.3048	0.254	0.1778
0.863	531.2	562.7	530.0	490.4 487.7 472.9
1.09	565.0	522.5	407.7	405.8
1.6	526.9	405.0	445.4	243.1

Unit: m/sec

Footnotes:
1. dn(mm): diameter of sapphire nozzle
2. dc(mm): diameter of carbide tube
3. abrasive mass flow rate: 68 g/min
4. abrasive mesh no.(d_A): #220

Table 4: Estimated Velocities of Entrained Particles; m_A= 68 g/min; d_A=#220

dc \ dn	0.3556	0.3048	0.254	0.1778
0.863	634.7	620.3	562.6 569.6 556.7 579.7 553.0	526.0 468.5
1.09	611.3	577.0	410.7	410.8

Unit: m/sec

Footnotes:
1. dn(mm): diameter of sapphire nozzle
2. dc(mm): diameter of carbide tube
3. abrasive mass flow rate 13 g/min
4. abrasive mesh no.: #220

Table 5: Estimated Velocities of Entrained Particles; m_A=13 g/min; d_A=#220

m_A	Va
13	410.0
68	405.0
145	363.0

Footnotes:
1.m_A(g/min): abrasive mass flow rate
2.Va(m/sec): mean particle velocity

Table 6: Estimated Velocities of Particles at Different Mass Flow Rates;
da = #220; dn = 0.1778mm; dc = 1.09mm

m_A	Va
38	523.6
144	474.1
343	430.4

Footnotes:
1.m_A(g/min): abrasive mass flow rate
2.Va(m/sec): mean particle velocity

Table 7 : Estimated Velocities of Particle at Different Mass Flow Rates;
da = #80; dn = 0.2540mm; dc = 0.863mm

m_A	Va
68	526.9
145.0	465.3
240.0	444.2
380.0	444.2
477.0	409.1
508.0	408.4

Footnotes:
1.m_A(g/min) : abrasive mass flow rate
2.Va(m/sec) : mean velocity of particle

Table 8 : Estimated Velocities of Particles at Different Mass Flow Rates;
da = #220; dn = 0.3556mm; dc = 1.6mm

REFERENCE

1. Hashish, M.,"A Modeling Study of Metal Cutting with Abrasive Waterjet", Transactions of the A.S.M.E. Journal of Engineering Materials and Technology, Vol.106, Jan., 1984, p.p. 88-100.

2. Swanson, R.K., Kilman, M., Cerwin, S. and Tarver, W., "Study of Particle Velocities in Water Driven Abrasive Jet Cutting", Proceedings of 4th U.S. Water Jet Conference, 1987.

3. Isobe, T., Yoshida, H. and Nishi, K., "Distribution of Abrasive Particles in Abrasive Water Jet and Acceleration Mechanism", Proceedings of 9th International Symposium on Jet Cutting Technology, 1988.

4. Geskin, E.S. and Chen, W.L. etc., "Investigation of Anatomy of an Abrasive Waterjet", Proceedings of 5th American Waterjet Conference, August 29-31, 1989.

5. Goldstein, R. J., Fluid Mechanics Measurements, Ohemisphere Publishing Corporation, 1976

6. Geskin, E.S., Chen, W.L., and Lee, W.Z., "Glass Shaping by the Use of Abrasive Waterjet", Glass Digest, Nov., 1988, p.p 60-64.

7. Donnan, P. H., " Abrasive Jet Cutting Development for Specialist Industrial Application", Proceedings of 7th International Symposium on Jet Cutting Technology, 1984, paper E2.

8. Hashish, M., "Application of Abrasive Waterjet to Metal Cutting", Proceedings of Conference on Nontraditional Machining, 1986, p.p. 1-11.

9. Yie, G.G., "Cutting Hard Material with Abrasive-Entrained Waterjet - A Progess Report", Proceedings of 7th International Symposium on Jet Cutting Technology, 1984, p.p. 481-492.

10. Hashish, M., "Cutting with Abrasive Waterjets", Mechanical Engineering, March, 1984, p.p. 60-69.

11. Haylock, R., "Waterjet Cutting", Preceedings of Automach Austrial'85, July 2-5, 1985.

12. Barton Corporation, Technical Data, 1987

13. Ingersoll-Rand Technical Report on the Performance of Robotic Work Station; 1986

14. Dunne, B. and Cassen, B., "Velocity Discontinuity Instability

of a Liquid Jet", J. Appl. Phys., vol.27, no.6, Jun. 1956, p.p.577-582.

15. Semerchan, A.A., Vereschagin, L.F., Filler, F.M. and Kuzin, N.N.,"Distribution of Momentum in a Continuous Liquid Jet of Supersonic Velocity", Sov. Phys. - Tech. Phys., vol.3, no.9, Sep. 1958, p.p. 1984-1903.

16. Kinoshita, T., "An Investigation of the Mechanism of a High Speed Liquid Jet and Its Practical Application", Proceedings of 2nd International Symposium on Jet Cutting, 1974.

17. Yanaida, K. and Ohashi, A., "Flow Characteristics of Water Jets in Air", Proceedings of 5th International Symposium on Jet Cutting, 1980.

18. Finnie, I., " Erosion by Solid Particle in a Fluid Stream", ASTM Technical Publication 307, 1961

19. Soo, S. L., Fluid Dynamics of Multiphase System, Waltham, Mass., Blaisdell Pub. Co., 1967.

20. Sheldon, G. L. and Finnie, I., " The Mechanism of Material Removal in the Erosive Cutting of Brittle Material", Journal of Engineering for Industry, Nov. 1966

21. Finnie, I., Wolak, J. and Kabil, Y. "Erosion of Metals by Solid Particles", Journal of Materials, 1967

22. Neilson, J.H. and Gilchrist, A. "Erosion by a Stream of Solid Particles", Wear II, 1968

23. Tilly, G.P., "Erosion Caused by Airborne Particles", Wear 14, 1969

24. Sheldon, G. L. and Kanhere, A., " An Investigation of Impingement Erosion using Single Particle", Wear 21, 1972 .

25. Tilly, G.P, "A Two Stages Mechanism of Ductile Erosion", Wear 23, 1972.

26. Young, J.P. and Ruff, A.W., "Particle Erosion Measurements on Metals", Journal of Engineering Materials and Technology, April, 1977.

27. Benchaita, M.T., Griffith, P. and Rabinowicz, E., "Erosion of Metallic Plate by Solid Particles Entrained in a Liquid Jet", Journal of Engineering for Industry, August, 1983.

28. Verma, A.P. and Lal, G.K., "An Experimental Study of Abrasive Machining", Int. J. Mach. Tools Des. Res., vol. 24, no1. 1984.

29. Verma, A. and Lal G.K., " Basic Mechanics of Abrasive Jet Machining", IE (I) Journal-PE, 1985.

30. Michaelides, E.E., "Motion of Particles in Gases: Average Velocity and Pressure Loss", Transactions of the ASME, Vol. 109, June, 1987.

31. Hinze, J.O., Turbulence, McGraw-Hill Book Company, Inc., 1959

32. Tchen, C.M., "Mean Values and Correlation Problems Connected with the Motion of Small Particles", Ph.D. Thesis, Delft, 1947.

33. Hjelmfelt, A.T., Jr. and Mockros, L.F., "Motion of Discrete Particles in a Turbulent Fluid", Appl. Sci. Res., 1965.

34. Danon, H., Wolfshtein, M. and Hetsroni, G., "Numerical Calculation of Two-Phase Turbulent Round Jet", Int. J. Multiphase Flow, vol.3, 1977, p.p. 223-234.

35. Melville, W. K. and Bray, K.N.C., "A Model of the Two-Phase Turbulent Jet", Int. J. Heat Mass Transfer, vol.22, 1979.

36. Maxey, M.R., and Riley, J.J., "Equation of Motion for a small Rigid Sphere in a Nonuniform Flow", Phys. Fluids, 26(4), April 1983.

37. Situ, M. and Schetz, J.A., "Numerical Calculations of the Breakup of Highly Loaded Slurry Jets.", Journal of Fluids Engineering, Sep. 1987.

38. Givler, R. C. and Mikatarian, R.R., "Numerical Simulation of Fluid-Particle Flows: Geothermal Drilling Applications", Journal of Fluids Engineering, Sep., 1987.

39. Ahmadi, G. and Ounis, H., "Dispersion of Small Rigid Spheres in a Turbulent Flow Field", Proceedings of International Conference on Mechanics of Two-Phase Flow, June, 1989.

40. Hashish, M., "On the Modelling of Abrasive-Waterjet Cutting", Proceedings of 7th International Symposium on Jet Cutting Technology, 1984, p.p. 249-265.

41. Thompson, H. D. and Stevenson, W.H., Laser Velocimetry and Particle Sizing, Ohemisphere Publishing Corporation, 1978.

42. Schodl, R., "A Laser Dual-beam Method for Flow Measurements in Turbomachines", ASME Parper No. 74-GT-157.

43. Eckard D., "Detailed Flow Investigation within a High-Speed Centrifugal Compressor Impeller". Journal of Fluids Engineering, Transactions of the ASME, September, 1976.

44. Mayo, W.T.,Jr., Smart, A.E. and Hunt, T.E., "Laser Transit Anemometer with Microcomputer and Special Digital Electronics: Measurements in Supersonic Flows", ICIASF'79 RECORD, 1979.

45. Loh Y. and Tan H., "A New Method for Processing the Signals from a Laser Dual-focus Velocimeter", The Institute of Physics, 1981.

46. Smart, A. E., Wisler, D.C. and Mayo, W.T., Jr., "Optical Advance in Laser Transit Anemometry", Journal of Engineering for Power, April, 1981.

47. Dantec Instruction Manual of Laser Transit Anemometer, 1987.

48. Dantec Service Manual of Counter Processor, 1986.

49. Yanta, W.J., Gates, D.F. and Brown, F.W., "The use of a Laser Doppler Velocimetee in Supersonic Flow", AIAA Paper No. 71-287, 1971.

50. Geskin, E., Li, H.Y. and Chen, W.L., "Investigation of Force Exerted by an Abrasive Waterjet on a Workpiece", Proceedings of 5th American Waterjet Conference, 1989.

51. Abramovich, G. N., The Theory of Turbulent Jets. Cambridge, U.S.A., M.I.T. Press, 1963, 663p.

52. Pai, S.I., Fluid Dynamics of Jets, Princeton, U.S.A., D. Van Nostrand Co., Inc., 1954.

53. Neter, J., Wasserman, W. and Whitmore, G.A., Applied Statistics, Allyn and Bacon, Inc., 1978.

54. Waugh, A.E., Elements of Statistical Method, McGraw-Hill Book Company, Inc., 1952.

55. Croxton, F. E., Cowden, D.J. and Klein, S., Applied General Statistics, Prentice-Hall, Inc., 1967.

56. Barnes, J. W., Statistical Analysis for Engineerings - A Computer-Based Approach, Prentice-Hall, Inc.,1988.

57. Gawlinski, E., Timlin, J., Michels, D., Anbalagan, N. A. and Mihalisin, T., TempleGraph 2.1 for Sun 3 or 4, Mihalisin Associates, 1988.

58. Galecki, G. and Mazurkiewicz, M., "Hydroabrasive Cutting Head- Energy Transfer Efficiency", Proceedings of 4th U.S. Water Jet Conference, 1987.

Fig. A1: Frequency Distribution of Velocities of Sapphire Waterjet; d_n=0.3556mm; d_m=6.35mm

Fig. A2: Frequency Distribution of Velocities of Sapphire Waterjet; d_n=0.3556mm; d_o=12.7mm

Fig. A3: Frequency Distribution of Velocities of Sapphire Waterjet; d_n=0.3556mm; d_o=25.4mm

Fig. A4: Frequency Distribution of Velocities of Sapphire Waterjet; d_n=0.3556mm; d_o=38.1mm

Fig. A5: Frequency Distribution of Velocities of Sapphire Waterjet; d_n=0.3556mm; d_w=50.8mm

Fig. A6: Frequency Distribution of Velocities of Sapphire Waterjet; d_n=0.3556mm; d_w=63.5mm

Fig. A7: Frequency Distribution of Velocities of Carbide Waterjet; d_e=1.09mm; d_n=0.1778mm

Fig. A8: Frequency Distribution of Velocities of Carbide Waterjet; d_o=1.6mm; d_n=0.254mm

Fig. A9: Frequency Distribution of Velocities of Carbide Waterjet; d_o=1.09mm; d_n=0.254mm

Fig. A10: Frequency Distribution of Velocities of Carbide Waterjet; d_o=0.863mm; d_n=0.254mm

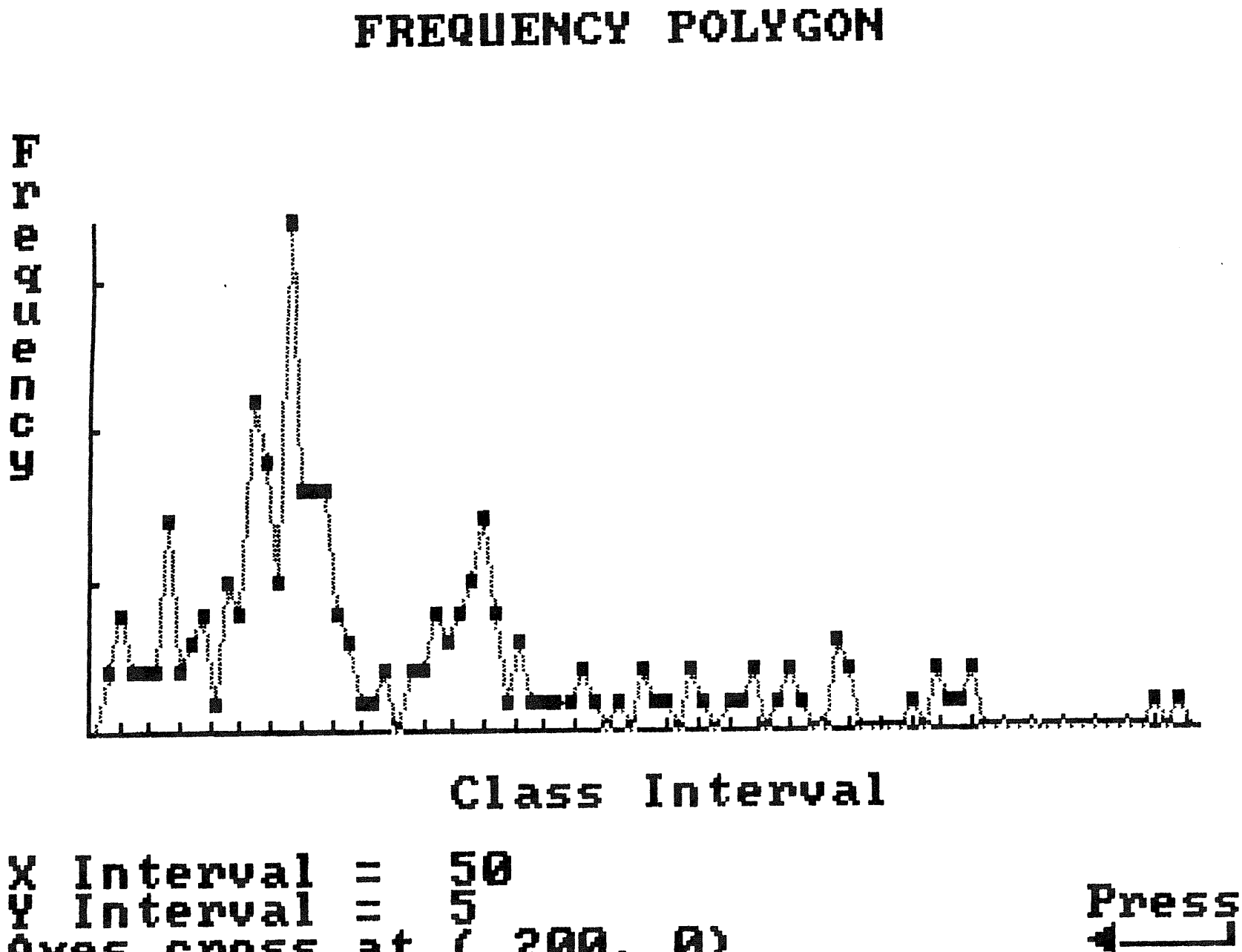

Fig. A11: Frequency Distribution of Velocities of Carbide Waterjet; d_e=0.863mm; d_n=0.254mm

Fig. A12: Frequency Distribution of Velocities of Entrained Particles in an AWJ; m_a=13 g/min; d_n=0.254mm d_c=0.863mm; d_a=220

Fig. A13: Frequency Distribution of Velocities of Entrained Particles in an AWJ; m_a=13 g/min; d_n=0.3048mm d_c=0.863mm; d_m=220

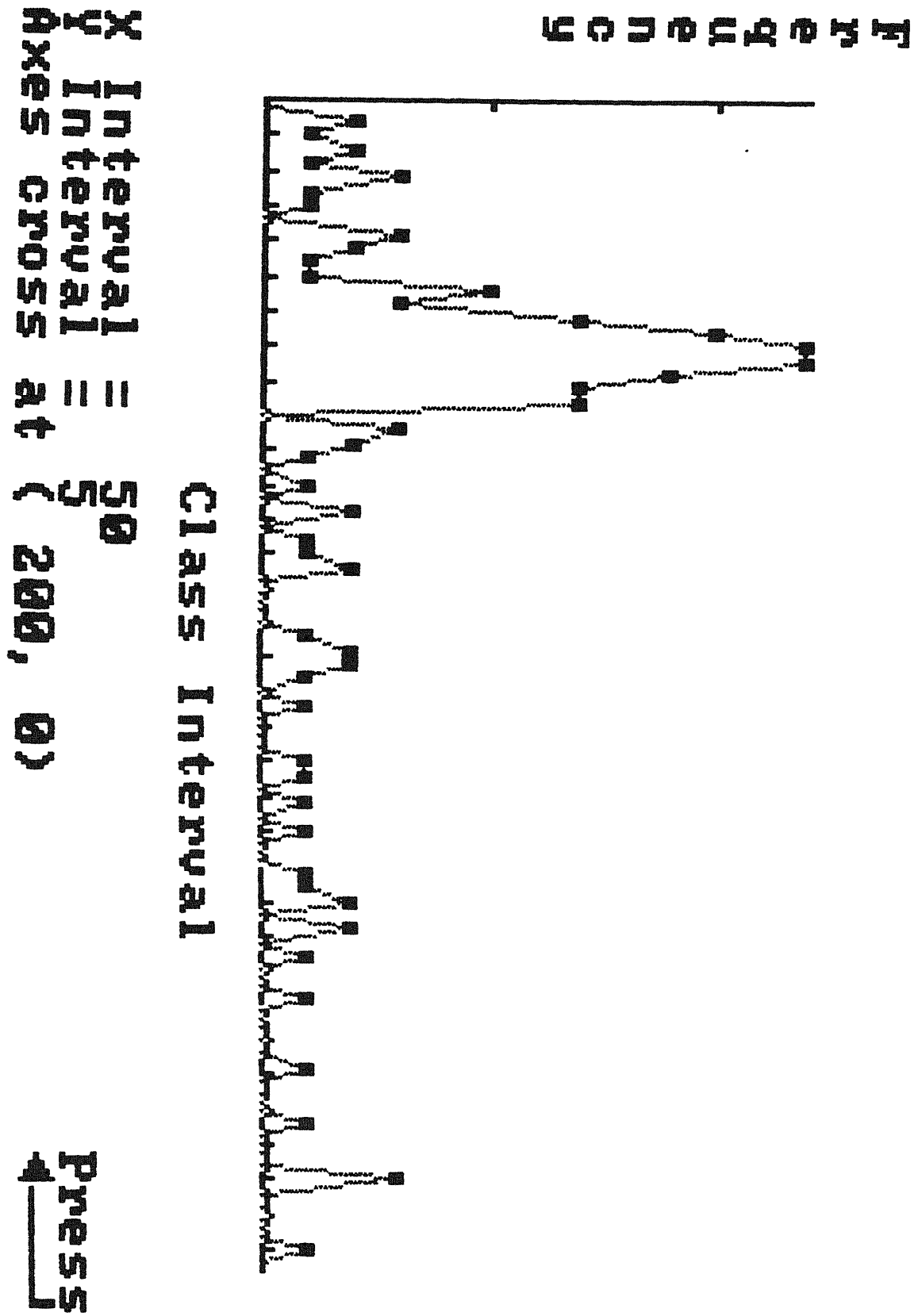

Fig. A14: Frequency Distribution of Velocities of Entrained Particles in an AWJ; m_a=68 g/min; d_n=0.254mm d_c=0.863mm; d_a=220